2015-12-01

Hand-portable Capillary Liquid Chromatography Instrumentation

Sonika Sharma
Brigham Young University

Hand-Portable Capillary Liquid Chromatography Instrumentation

Sonika Sharma

A dissertation submitted to the faculty of
Brigham Young University
in partial fulfillment of the requirements for the degree of

Doctor of Philosophy

Milton L. Lee, Chair
Paul B. Farnsworth
H. Dennis Tolley
Adam T. Woolley
David V. Dearden

Department of Chemistry and Biochemistry

Brigham Young University

December 2015

ABSTRACT

Hand-Portable Liquid Chromatography Instrumentation

Sonika Sharma
Department of Chemistry and Biochemistry, BYU
Doctor of Philosophy

This dissertation focuses on the development of hand-portable capillary liquid chromatography (LC) instrumentation. In this work, battery-operable nano-flow pumping systems (isocratic and gradient) were developed and integrated with portable UV-absorption detectors for capillary LC. The systems were reduced in size to acceptable weights and power usage for field operation. A major advantage of the pumps is that they do not employ a splitter, since they were specifically designed for capillary column use, thereby greatly reducing solvent consumption and waste generation. UV-absorption detectors were specifically designed and optimized for on-column detection to minimize extra-column band broadening. Initially, an isocratic nano-flow pumping system with a stop-flow injector was integrated with an on-column UV-absorption detector (254 nm). The pumping system gave excellent flow rate accuracy (<99.94%) and low percent injection carry-over (RSD 0.31%) suitable for quantitative analysis. Using sodium anthraquinone-2-sulfonate, the detector gave an LOD (S/N = 3) of 0.13 μM, which was 12 times lower than a commercial UV-absorption detector. Reversed-phase separations of a homologous series of alkyl benzenes was demonstrated.

Further miniaturization of UV-absorption detection was accomplished using a 260 nm deep UV LED. The detector was small in size and weighed only 85 g (without electronics). No optical reference was included due to the low drift in the signal. Two ball lenses, one of which was integrated with the LED, were used to increase light throughput through the capillary column. Stray light was minimized by the use of a band-pass filter and an adjustable slit. Signals down to the ppb level (nM) were easily detected with a short-term noise level of 4.4 μAU, confirming a low limit of detection and low noise. The detection limit for adenosine-5'-monophosphate was 230 times lower than any previously reported values. Isocratic separations of phenolic compounds were performed using a poly(ethylene glycol) diacrylate monolithic capillary column.

Finally, a novel nano-flow gradient generator integrated with a stop-flow injector was developed. Gradient performance was found to be excellent for gradient step accuracy (RSD < 1.2%, n = 4) and linear gradient reproducibility (RSD < 1.42%, n = 4). Separations of five phenols were demonstrated using the nano-flow gradient system. Efforts to develop a 405 nm laser diode-based UV-absorption detector for hemoglobin analysis were described.

Keywords: hand-portable, capillary liquid chromatography, nano-flow pumping system, UV-absorption detection

ACKNOWLEDGEMENTS

Words cannot express how grateful I am to Dr. Milton L. Lee for accepting me into his laboratory and mentoring me for the last five years. It has been a great pleasure for me to grow as a researcher under the guidance of such a successful scientist. All of these years, he has amazed me with his excellence, sincerity, work ethics, multi-tasking, generosity, integrity, and cogency, to name a few. His enthusiasm for life and strong dedication to his work has and will always inspire me. He has always been a great support for me and, without him, I would not have been able to come this far. He pushed me farther than I thought I could go. He made sure that I learned the best of everything. I am also thankful to Susan Lee for her hospitality all these years and letting us be part of her family. I am totally indebted to her and to Dr. Lee for taking care of me during my sickness last year.

I would like to thank all my committee members, Dr. Paul B. Farnsworth, Dr. H. Dennis Tolley, Dr. Adam T. Woolley and Dr. David V. Dearden, for their critical comments and valuable suggestions during my progress reports and preparation of papers. I am especially grateful to Dr. Farnsworth for being my spectroscopy mentor. His expertise and knowledge in spectroscopy has been an invaluable asset to me.

I am also sincerely thankful to Stanley Stearns, Alex Plistil, Robert Simpson, Hal Barnett and David Martin from VICI Valco Instruments for their collaboration and support during my projects. It has been a great experience working with them, and I am grateful for their friendship and understanding.

My projects involved considerable engineering work and I am grateful to Bart Whitehead and Therin Garrett for their help and patience, and for finishing my work on tight timelines. I appreciate all past and present members of Dr. Lee's group, especially Pankaj and Xiaofeng for

their helpful discussions and friendship. I believe I have worked with and under great minds, which has been a great experience.

Finally, I am especially thankful to all of my near and dear friends who stood by me in thick and thin and have gone out of their ways to support me during my PhD, even if we were countries apart. They are an important part of life, and I hope they know that. I am also grateful to my family for letting me come to the US for higher studies, and for providing support and encouragement during my studies.

TABLE OF CONTENTS

LIST OF ABBREVIATIONS

ACN	Acetonitrile
AU	Absorbance units
AMP	Adenosine-5'-monophosphate
AC	Alternating current
A/D	Analog-to-digital
A-h	Ampere-hour
CCD	Charge coupled device
CE	Capillary electrophoresis
DAQ	Data acquisition device
DMPA	2,2-Dimethoxy-2-phenylacetophenone
2D LC	Two-dimensional liquid chromatography
DAD	Diode array detector
DLT	DL-tryptophan
DC	Direct current
2,4-DCP	2,4-Dichlorophenol
2,4-DNP	2,4-Dinitrophenol
EO	Electroosmotic
ECD	Electrochemical detector
EOF	Electroosmotic flow
ESI	Electrospray ionization
EC	Electrochemical
FWHM	Full width at half maximum

GC	Gas chromatography
GC-MS	Gas chromatography-mass spectrometry
Hg	Mercury
HPLC	High performance liquid chromatography
1,6-HDDMA	1,6-Hexanediol dimethacrylate
Hb	Hemoglobin
IC	Ion chromatography
i.d.	Internal diameter
LC	Liquid chromatography
LC-UV	Liquid chromatography-ultraviolet absorption detector
LED	Light emitting diode
LOD	Limit of detection
MS	Mass spectrometry
M	Molarity
NaOH	Sodium hydroxide
2-NP	2-Nitrophenol
4-NP	4-Nitrophenol
o.d.	Outer diameter
PDA	Photodiode array
PEEK	Polyether ether ketone
PEGDA	Poly(ethylene glycol) diacrylate
P-P	Peak-to-peak
P	Phenol

RC	Resistor-capacitor
RSD	Relative standard deviation
RMS	Root mean square
S/N	Signal-to-noise
SAS	Sodium anthraquinone-2-sulfonate
SS	Stainless steel
SG	Sample groove
SCD	Sickle cell disease
TPM	3-(Trimethoxysilyl)propyl methacrylate
UHPLC	Ultra-high pressure liquid chromatography
UV	Ultra-violet

LIST OF TABLES

LIST OF FIGURES

CHAPTER 1 BACKGROUND AND SIGNIFICANCE*

1.1 Introduction

The desire for immediate chemical analysis at the sampling point is one of the main driving forces for the development of hand-portable instruments. Analyzing samples at the point of collection rather than in the laboratory is useful in many applications, such as space missions, forensics, homeland security, environmental contamination, geological studies, clinical analysis, and archeological studies, to name a few. This is especially important when health is at risk, such as in case of an oil spill or explosion, and in remote monitoring of locations contaminated with hazardous materials, such as biowarfare agents and/or toxic gases [1]. An ever-increasing number of harmful pollutants in water and air requires instruments that allow high throughput analysis as well [2]. Preservation of sample integrity is critical in most of these applications, and immediate analysis after sampling would allow quick action to be taken during emergencies. In the absence of portable instruments, samples must be collected and transported back to the laboratory for analysis. Sample loss and degradation is unavoidable during transport and subsequent storage, which often compromises the results. This process delays necessary actions in situations involving serious health hazards, and is certainly not time-efficient or cost-effective. With hand-portable instruments, both time and resources would be saved. However, the true potential of portable instruments can only be realized if reduction in size does not compromise performance.

Optical instrumentation has dominated the portable analytical instrument market with the availability of portable Raman spectrometers [3, 4], Fourier transform infrared spectrometers [4], near infrared spectrometers [4] and X-ray fluorescence analyzers [5, 6]. These have been used in

*This chapter was largely reproduced from: Sharma, S.; Tolley, L.; Tolley, H. D.; Lee, M. L. *J. Chromatogr. A* **2015**, *1421*, 38-47.

forensic analysis [7], space missions, organic and inorganic mineral analysis, stone and wall painting analysis, homeland security applications [8], and food quality control [9, 10]. The popularity of optical instruments stems from their non-destructive nature and minimal sample preparation required before analysis. However, analysis of complex environmental and biological samples always requires separation [11], which is often performed using gas chromatography (GC), liquid chromatography (LC), or ion chromatography (IC), with GC and LC being the most versatile and popular techniques.

LC is an important separation technique for environmental sample analysis, especially for non-volatile analytes such as pharmaceutical drugs, pesticides, phenols, etc. [12, 13]. A portable LC system would be useful for a number of such applications. It could also be easily integrated with a variety of portable detectors such as UV-absorption, fluorescence, electrochemical, and conductometric etc., increasing its potential applications. With a battery-operated, hand-portable LC, on-site analysis could be done, which would minimize the risk of sample loss and degradation. Furthermore, portable LC would offer an attractive benefit of reduced costs associated with waste disposal, sample storage and transportation [14].

Great effort has been made to miniaturize GC for field analysis, and several person-portable GC-MS systems are now commercially available [15-17]. GC is more amenable to portability than LC because of the use of gaseous mobile phases, which can be easily transported using compact pressurized gas cartridges weighing only a few grams; in some cases, air can be used directly as carrier gas. A GC operator does not have to worry about toxic waste disposal in the field, whereas portable LC demands transportation and handling of solvents, and disposal of waste. Reducing the size and weight of LC pumps and bulky detectors has always been

challenging. Therefore, limited work has been done in the past on miniaturization of LC [14, 18-23].

There are two main challenges in making LC systems smaller: (1) minimizing solvent consumption and subsequent waste generation and (2) reducing size, weight and power requirements of the system. A split arrangement, both in mobile phase flow (pre-column) and sample injection, which is typically used with commercial capillary LC instruments, is unacceptable, considering the amount of waste generation and the loss of detection sensitivity when dealing with trace concentrations. Also, a chromatograph without a sensitive and compact detector would be of little value. Therefore, an LC system could only be qualified as portable if it fulfilled the following requirements:

(1) weighs approximately 7 kg and measures <1000 cubic inches (16,387 cm^3) [1];
(2) contains all necessary electronics, digital interface and software integrated into a single unit;
(3) is solar or battery-powered, allowing at least 8 h of operation;
(4) is easily operable with minimal supervision;
(5) is rugged enough to withstand changes in temperature and humidity [1, 24];
(6) needs short instrument warm-up time;
(7) uses low amounts of toxic organics [14] in compliance with green analytical chemistry principles [25];
(8) is customized for capillary column use with a non-splitting flow arrangement, non-splitting injector, and low extra-column volume to minimize dispersion;
(9) is integrated with a small detector that has excellent sensitivity; and

(10) is capable of binary gradient generation, competitive in performance to benchtop instruments.

Considering these requirements, it is obvious that some trade-offs must be made between portability and performance. If a portable LC could provide all of the advantages of a benchtop instrument in a compact size, current benchtop LC instruments would become obsolete. However, as long as portable LC can fulfill the requirements for field detection, or even provide preliminary results on-site to complement further comprehensive analysis in a laboratory, it has its place. Moreover, in addition to environmental and point-of-care analysis, a portable system could also be utilized in a laboratory setting for routine analysis, reducing overall analysis costs, saving workspace and providing rapid results with minimal consumables.

The purpose of this chapter is to outline the main developments in miniaturization of LC instrumentation to allow the assembly of a person portable system. There are several LC reviews, which deal exclusively with micro- and nano-column chromatography and column advancements; however, none has dealt with system portability. This chapter initially focuses on miniaturization of LC components (column, pump, injector and detector) followed by a description of the construction and performance of the relatively few integrated portable LC systems. Finally, developments made in portable IC and microchip LC are described.

1.2 Development of portable LC components

1.2.1 Columns

LC instrument miniaturization has been strongly tied to column miniaturization. To reduce mobile phase consumption and required volume of sample, column dimensions have gradually decreased first to microcolumns (0.5-1.5 mm i.d.) and then to capillaries (0.01-0.5 mm i.d.). Capillary columns are attractive for miniaturized systems due to their small size, high

efficiency and minimum sample and solvent consumption [11]. Capillary columns can reduce solvent consumption by 3 orders of magnitude as compared to conventional columns and, with resultant low sample dilution, detection sensitivity is better. The reduction in the flow rate with capillary columns also allows easy coupling of capillary LC with MS. However, as briefly described below, it took almost two decades of extensive research to fully exploit the true potential of capillary LC columns. Thus, early portable LC systems used conventional size packed columns due to their ease of availability. However, the trend is changing and, with recent advancements in, and commercial availability of smaller and smaller particle-packed and monolithic columns, capillary columns are being incorporated in portable systems.

Packed microcapillary columns were first introduced by Tsuda and Novotny [26] with 50-200 μm i.d. glass capillaries loosely packed with activated or surface modified alumina particles (10-100 μm dia.). Long columns (several meters) packed with large diameter particles (> 20 μm) required long separation times [27, 28], but this was the only option for obtaining high chromatographic efficiencies due to the lack of high performance small particles, high pressure pumps, and good column packing procedures. Slurry packing of fused silica capillaries under high pressures markedly improved the homogeneity, efficiency and reproducibility of packed capillary columns [29-37]. Reducing extra-column dispersion was an integral part of these research efforts.

Jorgenson's group reduced the internal diameter of packed capillary columns to 20 μm [36], and by the mid-90's, 12 μm i.d. capillary columns were reported [37]. However, small i.d. columns could not be packed efficiently due to non-uniform particle sizes and shapes, which caused aggregation even when using dilute slurries. A decrease in column diameter, however, did improve column efficiency because of the plug-like flow obtained.

The trend of reducing particle size continued with sub-2 micron (1.5 and 1 μm) non-porous particles used for very high efficiency columns (> 200,000 plates/m), leading to the development of ultra-high pressure liquid chromatography (UHPLC > 16,000 psi), as reported by Jorgenson's group [38, 39]. Pneumatic amplifier and syringe pumps were modified to provide pressures to over 100,000 psi. Fast separations (few minutes) could be performed using high flow rates due to improved mass transfer characteristics (reduced C term in the van Deemter equation) with small diameter particles [40, 41]. Heat dissipation is efficient in small i.d. capillaries (≤ 50 μm), minimizing the detrimental effects of thermal gradients on UHPLC column performance. The first commercial ultra-performance LC (UHPLC) instrument appeared in 2004.

The chromatographic efficiency of packed capillary columns was markedly improved recently by Wirth's group [42, 43]. Colloidal crystal packings formed from sub-micron silica spheres (470 nm diameter) were created inside the capillary column. Owing to their crystalline structure, these particles allow highly homogenous packing in the capillary, facilitating slip flow through the packed bed. With slip flow, band broadening is greatly reduced due to the narrow velocity distribution profile obtained. Reduced band broadening and fast mass transport through the colloidal particle bed improves peak resolution, separation speed and peak capacity compared to sub-2 micron particle packed commercial columns. A slip flow column gave a million plates per meter, which was 3.5 times higher than the plate numbers achieved with 1 μm nonporous particle packed columns. Plate heights as low as 15 nm were obtained, which is several orders of magnitude better than UHPLC columns [44].

Although particle packed columns provide high efficiencies and are commercially available, the permeability of the packed bed is low and small particles lead to high back-

pressures, requiring UHPLC instruments for fast separations. To address this trend, monoliths arose in the early 1990s to provide fast mass kinetics at low back pressures. Monolithic columns provide high permeability and, therefore, can be used at high velocities without significant increase in back pressure [45]. The capillary walls are pretreated so that the monolith clings to the wall, eliminating the need for frits and reducing wall effects. Monolith morphology can be easily controlled by changing the functional monomers, cross-linkers and porogen concentrations, as well as polymerization conditions [46], but must be optimized carefully to obtain high efficiencies [47, 48]. The surface chemistry of the monolith and, hence, column selectivity can be easily manipulated by choosing the proper functional monomers.

There are two types of monoliths: inorganic and organic. Although inorganic monoliths made from silica provide higher efficiencies than organic polymeric monoliths, they have a more limited pH range, and fabrication and optimization is more complicated. Organic polymer monoliths, on the other hand, provide easier fabrication and are stable within a wide pH range. Both types of monoliths provide high permeability due to the presence of highly interconnected low micron diameter through-pores in the structure that allow for less restricted mobile phase flow. The difference in their separation performance arises from the mesopore density in the structure, which in turn determines the surface area and retention characteristics. Silica monoliths possess several hundreds of m^2/g of surface area and are applicable for small molecule separations. Efficiencies of silica monolith capillary columns have reached ~200,000 plates/m [49].

In contrast, organic polymer monoliths generally do not have as desirable morphology as silica monoliths and do not achieve as high efficiencies for small molecule separations [50]. Most applications are for large biomolecule separations such as proteins or nucleic acids [51-55].

However, significant advancements have recently been made to improve the efficiency of organic polymer monoliths for separating small molecules. Frechet *et al.* copolymerized poly(butyl methacrylate-co-ethylene dimethacrylate) with a C60 fullerene monomer and obtained an efficiency of 120,000 plates/m (H_{min} = 8.3 μm, 0.33 mm/s) for benzene [56]. Aggarwal *et al.* reported a single monomer (polyethylene glycol diacrylate) based monolithic column [57], which gave an efficiency of 157,000 plates/m (H_{min} = 6.4 μm, 0.33 mm/s) for phenol [58]. Yang *et al.* nearly doubled the efficiency of polymeric monoliths by polymerizing a divinyl monomer (bisphenol A epoxy vinyl ester resin) with ethylene glycol dimethacrylate cross linker. A maximum efficiency of 235,790 plates/m (H_{min} = 4.24 μm, 4.01 mm/s) was reported for phenol at a back pressure of < 1500 psi [59]. While these efficiencies are excellent for monoliths, sub-micron particle packed columns typically perform better.

1.2.2 Pumping systems

There are several types of pumping systems available for LC, including electroosmotic, diaphragm, direct current piston, reciprocating and syringe pumps. Usually, the column dimensions and back pressures determine the type of pump to be used in portable LC [14]. It is important to choose a column size that will yield cost- and time-efficient separations, and to design LC instrumentation that can withstand pressures equivalent to conventional commercial instruments (> 4000 psi) so that columns of different efficiencies/characteristics can be used. An ideal portable pumping system should possess the following essential features: (1) lightweight and battery-operated, (2) wide flow rate range (nL to μL/min or mL/min), (3) high flow rate accuracy and precision (≤ 1%), (4) constant flow rate independent of back pressure, (5) high gradient reproducibility (≤ 1%) and flexibility, (6) easy operation and maintenance, and (7) low pulsation noise.

Miniaturization of LC instrumentation has followed LC column miniaturization. The advent of microbore and capillary columns demanded changes in conventional instruments to (1) provide accurate low nL/min flow rates with solvent gradients, (2) introduce nL injection volumes, and (3) reduce extra-column volumes and detector flow-cell volumes. Miniaturization of LC dates back to the late 1970s when Ishii *et al.* reported a microHPLC instrument for exponential gradient generation, and pointed out the advantages of miniaturization in the LC field [60]. Since then, gradient generators have attracted much research interest, and a number of approaches to obtain exponential/sigmoidal [27, 60-74], step [27, 75-78] and nearly-linear gradient profiles [79-81] have been published. However, these self-built gradient generators suffer from problems, such as system complexity, limited gradient shape and step choice, distorted gradient profile due to diffusion, irreproducible flow rate, significant gradient delay, and dependence of gradient shape on mixer volume, tubing size and flow rate.

Commercial instruments have often been modified in the past to obtain sub-mL/min flow rates by employing a pre-injector flow splitter with the desired split ratio maintained by a micro process controller and pressure transducer [82, 83]. However, the sizes of the pumps generally remained the same. Also, dead volumes in such systems are high, and the reproducibility in flow rate has been poor [84]. Few commercial nanoLC instruments provide low nanoliter flow rates with high accuracy using electronically-controlled advanced flow splitters [85, 86]; however, for a portable system, solvent consumption is a main concern, and any system employing flow splitting impairs system portability, regardless of how good it is. A non-splitting capillary gradient system is advantageous for field work owing to its microliters of solvent consumption and waste generation. Today, commercial nano LC systems are available that provide flow rates in the low nLs per min range from reciprocating, syringe or pneumatic amplifier pumps without

using splitters [85]. However, there has been little if any reduction in the physical size of these instruments. Additionally, clogging in the low volume detector cell, hard-to-locate micro leaks, and extra-column dispersion from connecting tubing, detector cell and injector challenge the robustness of nanoLC techniques. Thus, although nanoLC is a miniaturized form of conventional LC, such instruments are far from being practical for portable applications. These instruments were recently comprehensively reviewed [85, 86].

Scott *et al.* obtained low μL/min flow rates from a commercial instrument by modifying the pump actuation instead of using a splitter [87-89]. Zhou *et al.* developed a splitless gradient pumping system based on pistons driven by a high resolution linear actuator (0.3 nL/step) using a micro-stepper motor [84]. In this setup, the dual pistons eliminated flow rate errors and pulsations that can occur in commercial systems due to liquid compressibility and mechanical problems at low μL/min flow rates. While the non-splitting flow reduced waste generation in these systems, their physical sizes were not smaller.

Electroosmotic and diaphragm pumps are attractive, considering the fact that these are easy to miniaturize and are pulse-free. However, reproducible flow rates and gradients are key to obtaining reliable and reproducible retention time data in separations, and favor pressure-actuated flow since it is not affected by varying surface chemistries as encountered in electroosmotic flow [90]. Electroosmotic pumps are not reliable for gradient generation and high-pressure operation. Battery-operated electroosmotic-diaphragm pumps were used to dispense liquid through a micro-chip based particle packed column in a portable chromatograph [20]. The pumping system consisted of two cylindrical modules (4 cm dia. × 6.8 cm long) each consisting of two vertical compartments with deionized water in the top and mobile phase in the bottom (8 mL volume) compartment. These compartments were separated by a silicone rubber

diaphragm. A porous silica rod (3 mm dia. × 4 mm long) with platinum wire electrodes was connected on the bottom of a deionized water chamber on each pump. Upon application of voltage (0-60 V) to the electrodes, EO flow occurred through the silica rod, generating pressure on the diaphragm and dispensing mobile phase up to 10 μL/min. Although integration of a diaphragm in the pump design overcame EO pump incompatibility with organic mobile phases, the pump could still only produce pulse-free flow for a limited time (< 1.5 h) at pressures less than 145 psi. The flow rate reproducibility was not reported and gradient operation was obviously difficult. An electrochemical pump is a low power alternative to electroosmotic pumps; however, such pumps are only useful in microchip-based LC systems [91].

Advancements in electroosmotic (EO) pump performance have recently been reported for splitless gradient generation at nL/min flow by Liu's group [92-94]. Three EO pumps were connected in series to drive the gradient generated using a 10-port switching valve to a transfer capillary connected to a valve injector [92]. Diffusional mixing occurred in the transfer capillary. Later, a single EO pump was used to drive the gradient to the column using an auto sampler [93]. However, the operation of these EO pumping systems was not simple, and achievable gradient profiles were limited. Another gradient generator used two EO pumps to separately drive mobile phases of different strengths to a mixer, and the gradient was formed by ramping the voltages on the pumps [94]. The major advantages of these EO pumps are small size and dwell volume compared to commercial nanoLC instruments; however, EO pumps are not particularly suitable for field work due to stringent electrical power requirements, which makes it difficult to incorporate these pumps into a portable system, and flow rates are dependent on both pump and column back pressures. They are yet to be accepted in conventional LC work owing to complexities encountered in gradient generation and inability to maintain constant flow rate.

Other miniaturized pumping systems include small diaphragm pumps [95] and miniaturized gas pressurized cylinders [96]. Small diaphragm pumps cannot withstand high pressures (> 200 psi). This low upper pressure limit greatly restricts the choice of columns that can be employed for separation which, therefore, limits its practical chromatographic application. Nevertheless, these diaphragm pumps were employed in a low pressure LC system (up to 100 psi) for quality control applications in the biomedical field [95].

The flow rate and pressure of a direct current piston pump are controlled by the input voltage, theoretically providing simple and accurate flow control. A commercial low-pressure piston-based direct current pump (< 4 kg) was used in a portable LC [18]. The pump was equipped with a pump head, pulse dampener and a pressure gauge (< 1 kg). The pump could be operated using a 6 V battery. Although rated for 100 psi, the pump could not operate stably above 60 psi because of flow rate changes from changes in the back pressure from the column. Due to the very low pressure available, high efficiency columns could not be used. Unstable and limited practical flow rates made this pump type not suitable for portable LC operation.

Reciprocating pumps are robust and provide excellent gradients at high pressures. However, these pumps are bulky, create pulsations at low flow rates and are generally difficult to make small and battery-operable. A portable gradient LC system employed battery-operated dual piston pumps [19]. The pumps were integrated with a high pressure mixer without a pulse dampener. The maximum pressure rating for this system was 5000 psi with a flow rate range of 0.1 to 2.5 mL/min. No performance characterization of the pumping system was reported (i.e., flow rate accuracy and precision, and pulsation noise). A commercial portable LC system employed a battery-operated dual-piston reciprocating pump (10.5 × 10 × 18.5 cm) [23]. The isocratic pump weighed 2 kg with a pressure limit of 5800 psi, which could provide flow rates in

the range of 0.001 to 10 mL/min with an accuracy of ± 1% and a precision of ≤ 0.5%. Another commercial portable LC used battery-operated piston pumps with a flow rate range of 0.1 to 5 mL/min and pressure rating of 6000 psi [22]. The system had solvent recycling and priming/purging options. No further information was available as both of these commercial systems were discontinued.

Syringe piston pumps are widely used in low-flow LC instruments. These are highly reliable in terms of high pressure operation, stable flow rates and gradient reproducibility. Syringe pumps can easily fulfill the requirements of a portable pumping system. They eliminate the need for dual pistons for dispensing a single mobile phase, which greatly reduces the complexity of the system. They are also pulse free and amenable to reduction in size. One downside of syringe pumps is that they cannot be refilled during a run; however, this is not a problem as long as a run can be completed before a refill is needed, and the refill can be done rapidly.

A portable gradient LC system was reported two decades ago that utilized two displacement-type syringe metering pumps (2.5 mL volume capacity each) actuated by stepper motors, and connected to a pressure transducer and a static mixer [14]. One pump also served as the suction device for an automatic stop-flow injector needle integrated with the pumping system using a tightening device. The maximum pressure rating of this system was 1000 psi. It could provide flow rates in the 5 to 1000 µL/min range with high accuracy (± 1%) and precision (± 0.3%). This pump system was not battery-operated.

1.2.3 Injection systems

Injectors are generally small and have not required significant change for portable LC. However, certain details must be kept in mind while selecting an injector. Injectors should be

able to inject samples with high precision at low or high pressures and should not cause excessive flow disturbance. Small diameter tubing should be used to reduce band broadening. Also, dead volumes in injectors should be minimized or eliminated to reduce peak tailing and band broadening. Liquid injectors for LC can be divided into two categories based on whether or not the mobile phase flow is stopped during injection: continuous flow or stop flow. Continuous flow injectors allow uninterrupted flow through the column and were used in portable LCs [18-20, 22, 23]; however, they typically increased the dead-volume in the LC system. For stop flow injection, the pump flow is stopped while sample injection is made. Automated stop flow injectors allow high precision injections to be made and are free from manual errors. However, automation increases power consumption, and size and complexity of the system. This type of stop flow injector was used only in one previously described portable LC [14].

In capillary LC, the sample introduction system should minimize or eliminate the extra-column dispersion [84, 97]. Loop injectors are most commonly used. They allow introduction of different amounts of samples under pressurized conditions. Split injectors are also available; however, they often suffer from poor reproducibility. Studies have shown that stop-flow injection has a negligible effect on the separation efficiency and, hence, is attractive for capillary injections [98, 99].

1.2.4 Detectors

A portable LC must be integrated with a sensitive detector that is either universally applicable or selective for the target analyte(s). High sensitivity would be very useful in field work where trace quantities are present and sample pre-concentration is a challenge. A variety of detectors could be used in portable LC work, such as refractive index, fluorescence, electrochemical, chemiluminescence, conductivity, evaporative light-scattering, mass

spectrometry and UV-absorption. However, only electrochemical and UV-absorption detectors have been integrated with portable LCs.

The electrochemical detector (ECD) offers excellent selectivity and sensitivity as only oxidizable/reducible compounds can be detected. Also, it is easy to miniaturize and operate with a battery. This detector is very useful for identifying similar compounds or isomers with different electrochemical properties. Such a detector was used for selective detection of polycyclic aromatic amines in the presence of phenols and azaarenes [18]. The detector consisted of a glassy carbon working electrode and a silver/silver chloride reference electrode in a thin-layer transducer cell. The cell potential was controlled using a commercial amperometric detector. A strip-chart recorder traced the current signals. The detection limits were in the 2.4-33 ppb range for polycyclic aromatic amines. The noise level of the system was in the 0.10-0.12 nA range. However, the detector signal varied greatly with a change in flow rate and gradient. The signal was also highly sensitive to changes in temperature, pH and electrode contamination. These factors induce irreproducibility in the data and, hence, the detector is not a good choice for a portable instrument. A microfabricated ECD was employed for nM catechin detection in another portable LC [20]. The detector consisted of a single digitated working electrode with 24 microelectrodes (50 μm width × 200 μm gap) to increase detection sensitivity. The gold electrodes were etched at the end of a microfabricated column on a polystyrene substrate, minimizing dead volume between the column and detector. No information was provided concerning the detector noise level and drift.

LC is typically used to analyze non-volatile analytes, most of which contain chromophores which absorb UV light. UV-absorption detectors are nearly universal for LC work; however, they lack selectivity and sensitivity compared to fluorescence and

electrochemical detection. UV detectors are widely used in LC due to their flexibility, simplicity, quantitation capability, high sensitivity and ruggedness [21]. Beer's law, in which absorption is directly proportional to the path length of the flow cell and to the concentration of the analyte, governs UV absorption. A flow cell connected to the end of the column is most commonly used for detection in LC. The UV-absorption detector generally employs a low-pressure mercury lamp or deuterium lamp as a light source. Single wavelength UV detectors are popular due to their low cost, compactness and higher sensitivity compared to multi-wavelength detectors [100]. To compensate for intensity fluctuations of the light source and its resultant noise, a reference detector or dual-beam design has usually been used in absorbance detectors. When different sides of a pen-ray Hg lamp are used to compensate for source fluctuations and its resultant noise, noise levels are higher than systems where sample and reference beams are drawn from the same point in the source [101]. Filters or monochromators are commonly used to reduce stray light. To maximize light throughput in the small detection cell, several focusing elements (e.g., biconvex lenses and mirrors) were employed [102]. Absence of filters, slow recorders, and single-beam arrangements generally result in high system noise levels [102-104].

A dual beam multi-wavelength (190-360 nm) UV detector was used in an early portable LC [14]. The light from a deuterium lamp was focused using optical lenses onto a holographic grating, which was controlled by a stepper motor to change wavelengths. An electromagnetically driven oscillating convex mirror focused light from the grating onto reference and sample Z-shaped flow cells with 1.6 mm pathlength [105]. The detector could scan 8 wavelengths in one cycle with a time constant selectable from 0.06 to 10 s. The detector noise and drift level were less than 0.2 mAU and 0.1 mAU/h, respectively, for a time constant of 0.3 s. The wavelength accuracy and reproducibility were reported to be ±0.5 nm and ±0.005 nm, respectively. The

detection limits were in the 1.1-3.2 ppm range for inorganic ions, and 0.1-2.1 ppb range for polycyclic aromatic hydrocarbons in snow water extracts. The disadvantage of a multi-wavelength detector is that it increases the complexity, size, weight and noise of the system by introducing moving parts. Also, the operation of this system was more complicated than desired for a portable LC system.

A fixed wavelength detector is advantageous for field portability as it reduces the size and cost of the system [106] and is simpler to operate. Most importantly, the noise levels of fixed wavelength detectors are usually at least an order of magnitude lower than multi-wavelength detectors. An early portable system employed a fixed wavelength (254 nm or 280 nm) UV detector [19]. The light source or lamp could be changed in this detector to accommodate a variety of applications. No details were given about the detector design and performance except that the detection limits were 0.2 ppm for phenol and 0.015 ppm for anthracene at 280 nm and 254 nm, respectively. Another portable LC used a commercial fixed-wavelength (254 nm) Hg lamp UV detector with exchangeable flow cells. The detector noise and drift levels were 30 μAU and < 0.15 mAU/h, respectively. The detector weighed 1.5 kg with dimensions of 11.3 x 13.5 x 22.5 cm. The detection limit of the detector was reported to be < 60 μAU for a time constant of 1 s. The time constant of the detector could be selected from 0.05 to 5 s [23, 107].

Obviously, mass spectrometry (MS) would be the ultimate detector for portable LC due to its high selectivity and sensitivity. It is the only detector that can provide unbiased compound identification and structural information with low detection limits. However, integrating a portable MS with a portable LC is a major challenge due to the greatly increased vacuum pumping requirements compared to portable GC. Reported portable MS systems fabricated for use with LC are not truly portable (weight ~ 27 kg) [108, 109].

1.3 Integrated hand-portable systems

1.3.1 Portable LC

Table 1.1 summarizes information available for the hand-portable LCs reported so far. An isocratic LC-ECD system reported by Otagawa *et al.* in 1986 was used for the separation of coal tar sample components; however, resolution was poor, making quantitation difficult. No information was provided about the size, power requirements and weight of the system. The system applicability for field work was greatly limited by the attainable flow rate, extremely low pressure limit and electrochemical detection [18]. A portable gradient LC integrated with a multi-wavelength UV detector was reported by Baram in 1996 [14]. The performance of this system was similar to commercial instruments in all aspects. The gradient, variable sample injection, and multi-wavelength detection capabilities allowed a broad application range. Hence, separations of several environmental pollutants including phenols, pesticides, polynuclear aromatic hydrocarbons and phthalate esters were demonstrated along with fast separations (< 4 min) of polynitro explosives. Both direct and indirect UV detection were performed for real samples. It was also used for the separation of nitrophenacyl derivatives of free fatty acid standards and laboratory algal cultures [110]. However, the system was designed for mobile laboratories and, therefore, was not battery-operable. Also, the weight (14 kg) and size (31,800 cm^3) of this system was almost double of what is expected for a field-portable instrument, and it utilized conventional columns.

Tulchinsky and St Angelo reported a portable gradient LC integrated with a fixed wavelength UV detector in 1998 [19], which could operate for 8 h on a 12 V DC battery. The system was fully integrated into one unit, except for the liter-volume solvent bottles and computer.

Table 1.1 Hand-portable LC systems.

Portable LC references	Total weight (kg)	Dimensions (cm)	Pumping system (flow rate range)	Detector	Injector	Column
Ottagawa 1986 [18]	-	-	Direct-current piston, Isocratic (0.22 and 0.58 mL/min)	ECD	Continuous-flow (20 µL)	RP 10 µm particles (3 cm × 4.6 mm i.d.)
Baram 1996 [14]	14	53 × 20 × 30	Syringe piston, Gradient (5 to 1000 µL/min)	Multi-wavelength UV (190-360 nm)	Automatic stop-flow (1-100 µL)	RP 5 µm particles (6 - 8 cm × 2 mm i.d.)
Tulchinsky 1998 [19, 106]	9.5	41 × 25 × 23	Dual-piston, Gradient (0.1-2.5 mL/min)	Fixed wavelength UV (254 or 280 nm)	Continuous-flow (20 uL)	RP 5 µm particles (25 cm × 2 mm i.d. and 10 cm × 4.6 mm i.d.)
Commercial (obsolete) [22]	-	-	Dual-piston, Isocratic (0.1-5 mL/min)	Fixed wavelength UV (254 nm)	Continuous-flow (20 µL)	-
Commercial (Obsolete) [23]	3.5	12 × 19	Dual-piston, Isocratic (0.001-10 mL/min)	Fixed wavelength UV (254 nm)	Continuous-flow (20 µL)	-
Ishiida 2012 [20]	2	26 × 18 × 21	Electroosmotic-diaphragm, Gradient (up to 10 µL/min)	Microfabricated ECD	Continuous-flow (10 or 20 nL)	Micro-chip RP 3 µm particles (3 cm length x 0.8 mm i.d.)

.

The weight (9.5 kg) and size (23,000 cm^3) of the portable LC were smaller than previous instruments by employing a fixed wavelength detector. A phenol separation from lake water was demonstrated, along with a vitamin E chromatogram.

Ishida *et al.* reported a portable battery-operated electroosmotically pumped LC in 2012 [20]. The size (9828 cm^3) and the weight (2 kg) of the system were reduced markedly compared to previous configurations by using EO-diaphragm pumps, microfabricated-column and ECD. Isocratic separation of catechins was demonstrated; however, the separation time was very long (15 to 40 min) for a 3 cm column at 5 µL/min flow rate. Also, the system performance was limited by low pressure, inability to generate gradients, and use of electrochemical detection.

1.3.2 Portable IC

IC is a prominent technique for ion analysis, especially anions, due to its high selectivity and ability to separate multiple ions in a single run. As IC does not use harmful chemicals, it is also environmentally friendly. It is a relatively low pressure mode of LC which generally uses a conductometric detector. Hence, this technique is easier to miniaturize than conventional LC.

A commercially available portable single column (or non-suppressed) IC was used by Tsitouridou and Puxbaum for field analysis [111]. The IC consisted of a conductivity detector (0.5 µL volume), 100 µL volume injector, and a temperature controller for both column and detector. It had dimensions of 46 × 30 × 28 cm and weighed 10 kg. The IC was integrated with a pump and strip-chart recorder, and the whole system weighed 20 kg. Ionic compositions of field samples (fog water and atmospheric aerosols) were determined with detection limits in the 10-440 µg/mL range for inorganic (chloride, nitrite, nitrate, fluoride and sulfate) and organic (lactate, formate, acetate, propionate and butyrate) anions, and for cations (Na^+, K^+ and NH_4^+).

Conventional size ion exchange and ion exclusion columns (2-8 mm i.d.) were used for separations.

Another commercial portable IC was used by Tanaka *et al.* for simultaneous ion-exclusion-cation-exchange chromatography of both anions (chloride, nitrate and sulfate) and cations (Na^+, NH_4^+, K^+, Mg^{2+} and Ca^{2+}). The portable IC had an integrated conductivity detector, 100 μL volume injector and a pump with no temperature control. The system was battery-operated. Acid rain field samples were analyzed in the laboratory with detection limits in the 5-17 ppb range [112]. Selective determination of fluoride ions in surface and rain waters, and snow samples was also reported using a portable suppressed-ion chromatograph [113]. No further information was available for these systems.

Kiplagat *et al.* reported a very small non-suppressed IC for open tubular capillary columns using gravity-induced flow, hydrodynamic injection, and a small capacitance sensor, eliminating the need for LC pumps and injectors [96]. The system weighed 2.5 kg, including a laptop. Electrical power was required for the detector and data acquisition, and it could run for more than 8 h using laptop power. However, this configuration was limited by the practical flow rates and available low pressures (< 3 psi), and was not really suitable for field work. Nevertheless, on-site analysis of cations in water and snow samples was demonstrated using this system, with detection limits in the 1-8 μM range. A pressurized system based on miniaturized gas cartridges (100 psi max. pressure) was also built and connected to an injector for use with capillary columns. The system weighed < 1 kg without laptop and had dimensions of 25 × 15 × 8 cm.

Suppressed-ion chromatography increases detection sensitivity compared to non-suppressed and is preferable for field work. Boring *et al.* reported a fully integrated, battery-

operated portable suppressed-ion chromatograph for packed capillary columns (180 μm i.d.) [11]. The system weighed 10 kg and had dimensions of 28 × 43 × 15 cm. The IC consisted of a high-pressure syringe pump to deliver the eluent, an injector, a trap-column for impurities, and an electrodialytic NaOH generator capable of gradient generation. An air pressurized pump was used to pressure deliver donor sodium hydroxide solution to the generator and sulfuric acid solution to the suppressor, and a conductivity detector with specially designed flow cell was used for high sensitivity detection. Isocratic separations of anions were demonstrated with detection limits in the 30-250 nM range. Excellent gradient separation of 15 anions was also reported with a delay time of 1.5 min. This is the only portable IC system reported with gradient capability.

A fully automated, battery-operated portable isocratic suppressed-ion chromatograph (62 × 48 × 30 cm) was reported recently by Elkin, which could allow autonomous operation in the field for up to a month [114]. The system was fully integrated with all necessary components into one unit and weighed 13 kg, excluding batteries. The main components of the system included an eluent reflux device serving as both eluent generator and suppressor, a mini-pump for solvent delivery, an electrolytic eluent purifier to remove impurities from the eluent, an autosampling system for sample preconcentration and injection, a column and a small capacitively-coupled contactless conductivity detector. Field analysis of anions was demonstrated with detection limits in the 23-550 ng/mL range.

Portable ICs have been around for a number of years. Therefore, it is not surprising that they have achieved a higher level of integration than portable LCs and have been successfully applied in field analysis. However, the weight (10-13 kg) and size (18,000-90,000 cm^3) reductions of these ICs are not very impressive.

1.3.3 Microchip LC

Microchip LC could facilitate high separation efficiencies by integrating all LC components such as pump, injector, sample preconcentrator and detector into one device, thus, minimizing extra column dispersion. Microchip LC integrated with a nano-spray emitter could be easily coupled to MS to improve detection sensitivity. Microchips consume very small amounts of sample (pLs-nLs) and solvent [115]. Samples prone to cross contamination could be analyzed using disposable microLC devices [116]. However, little has been reported to date on the integration of miniaturized pumps, injector, column and detector on a single microchip device. Most of the microfabricated LC work has focused on integrating separation columns and MS emitters on a chip and, in recent years, on applications using commercial LC chips [115, 117, 118].

The first chip-based LC was fabricated in 1990 [119] based on a microfabricated GC design [120] by Manz *et al*. An open tubular column (6 μm × 2 μm × 150 mm) was machined in spiral form on a silicon wafer to avoid sharp corners. An open tubular column was used to provide fast separation in narrow-width channels at a lower back pressure than experienced with packed beds. A platinum-electrode based conductometric detector with a cell volume of 1.2 pL was fabricated on a Pyrex glass chip. The chip was interfaced with conventional valve injector and pumping system. No actual experiments were performed using the LC device; however, this work opened the possibility for LC miniaturization in a microchip format and presented its potential advantages.

Lazar and Karger reported an open microchannel EO pump capable of generating pressures up to 80 psi [121]. The pump consisted of 100 microchannels connected to a single large channel to prevent backflow. An EOF valve was used for sample injection. Flow rates up to

400 nL/min were obtained. Two of these pumps were connected together for gradient formation; however, this was difficult due to the absence of proper mixing channels. A slightly modified version of this pump and valve configuration was utilized for isocratic separation and MS detection of cancer biomarkers [122]. The microchip consisted of two EOF pumps each having 200 nanochannels (1.5-1.8 μm deep × 2 cm long), a double T injector, a preconcentrator, a 5 μm particle packed column (2 cm x 50 μm deep) and an ESI interfacing capillary. The EOF was slow (50-80 nL/min) due to backflow problems with the pump design and high organic content in the mobile phase. Also, the separation time was long (~ 40 min). Borowsky *et al.* developed a straight channel EO pump using 5 μm porous silica particles (50 nm pore size). The pump was integrated with an injector and a sol-gel stationary phase (2.6 cm effective length x 100 μm deep x 230 μm wide) on a single quartz microchip [123]. A detection window was also formed on-chip for UV detection. The porous silica particles provided enhanced EOF due to numerous interstitial spaces with high zeta potential properties, and the sol-gel stationary phase provided lower back pressure for smooth EOF operation. At an applied voltage of 4.5 kV and a flow rate of 28 nL/min, degradation products from two explosives were separated in less than 100 s. A minimum plate height (H_{min}) of 10.4 μm was obtained at an optimum voltage of 3.5 kV. Further separations of multiple explosives and degradation products were reported without achieving baseline resolution.

Electrochemical (EC) pumps are ideal for portable devices. In EC pumps, an expanding gas bubble generated by electrolysis or thermal heating of aqueous solutions drives fluid flow. EC pumps have low voltage requirement (~10 V) and can be easily incorporated into a microfabricated device without increasing system complexity. Most importantly, since the fluid driving force is external to the column, these pumps are compatible with organic mobile phases

and, hence, do not limit device applications. Two EC pumps for solvent pumping (20 μL total volume) and one EC pump for sample injection (5 μL volume) were etched on a silicon wafer to drive LC separations by Xie *et al*. The pumps were integrated with a 1.5 nL static mixer, a restrictor packed with particles to prevent backflow of the solvent into the reservoirs, a particle packed column and an electrospray emitter on a single device [124]. The gradient was generated by changing the current applied to the electrodes in each solvent reservoir. Although the gradient profile was neither perfect nor reproducible, the pumps still successfully delivered a changing mobile phase composition to the column at a flow rate of 80 nL/min. MS analysis of a tryptic digest of bovine serum albumin using this microchip containing a 3 μm particle packed column (1.2 cm × 50 μm i.d.) was competitive with a commercial column (15 cm × 75 μm i.d.). An added advantage of a reduced delay time of 15 s was also obtained compared to long delay (15 min) for a commercial instrument. However, the analysis time was long (1 h). Fuentes and Woolley reported an isocratic electrolysis-based EC pump integrated with pressure balanced injection and an open tubular column (2.5 cm long) for the fast separation of labeled amino acids (< 40 s) [125]. Bubble formation at the electrode caused high flow variations in runs greater than 2 min. However, the column efficiency was high (H_{min} = 7.5 μm) due to low dead-volume integration. The pump produced 86 nL/min flow rates against 100 psi pressure, and pL sample injections were possible.

Dutta and Ramsey reported a miniaturized hydraulic pump which pumped fluid through an open tubular separation channel (3.7 cm long x 30 μm wide x 5 μm deep) on applying an electric field [126]. Pressure flow (~23 psi) was generated by differential EOF in polyelectrolyte multilayer-coated and uncoated arms of the pumping channels. Using an optimized microfluidic

device, separation of coumarin dyes was demonstrated in less than 40 s with an H_{min} around 9 μm.

1.4 Conclusions and future directions

Miniaturization of LC has been driven mainly by a reduction in particle size and column diameter, which has led to significant mobile phase flow reduction. Early portable systems used conventional-size columns, which led to high solvent consumption; however, recent developments have shifted focus toward capillary and micro-chip based columns. Progress toward portable LC has been very slow, but development of a truly portable system does not seem to be very far in the future. This is due to the availability of capillary columns, several portable detectors, and recent developments in nano-flow syringe pumps. Standard commercial injectors have been used in portable systems without much modification. New, miniaturized UV absorption detectors seem ideal for integration into portable LC. However, using UV-absorption for detection, compound identification must be based primarily on retention times. Mass spectrometry is the detector of choice for the identification of unknown analytes; unfortunately, developing a miniaturized MS that can accept even nL/min flows of liquid is a formidable challenge.

Complete integration of portable LC into a single robust package with all necessary electronics and interfaces is yet to be done. Even after complete integration, challenges associated with the use of portable LC for field work are significant. LC systems and their operation are more complex than many other analytical techniques, which may pose problems for field operators. Temperature changes in the field are inevitable. Temperature control would be required not only for the column to maintain separation, but also for the pumping system and transfer lines, because evaporation or freezing of the solvent could occur readily. This may

increase the size and power requirements of the system. Clogging and contamination of solvent transfer lines, injectors and columns are also common, and may pose problems. Simple filtration of field samples is not difficult; however, pre-concentration of samples in the field would be inconvenient and would require additional equipment and supplies. Column re-equilibration would affect the analysis throughput; however, this can be reduced by the use of short columns, which equilibrate faster. For applications requiring long columns, equilibration times may be reduced by operating the system at higher flow rates, which would require higher pressures. Even with these challenges, the development of portable LC systems is inevitable, and they are expected to become widely applicable in the future for a variety of applications.

Very small particle packed columns are beneficial, but have not been used with portable LC. With the availability of portable UHPLC systems in the future, fast separations will be feasible using these columns, increasing sample throughput. Microfabrication technologies can provide extremely small LC columns, and this column format is expected to show considerable growth in the future. Microchip LC columns have been successfully integrated into commercial capillary LC systems; however, they have yet to be reported as a component in a portable LC.

Ion chromatographs have achieved a higher level of integration than portable LCs; however, size and weight reductions of IC have not been very impressive. Nevertheless, ion chromatography continues to expand into additional applications, including exotic space-exploration projects [127].

1.5 Dissertation overview

My research was focused on the development of a hand-portable liquid chromatographic instrument. Chapter 2 reports the design and performance evaluation of an isocratic LC instrument integrated with a fixed wavelength (254 nm) Hg lamp-based UV-absorption on-

column detector. The nano-flow pumping system was integrated with a fixed volume stop-flow injector. Despite having a non-split flow arrangement, accurate flow rates were obtained down to a few nL/min. A pen-ray® Hg lamp-based dual-beam detector (254 nm) was successfully miniaturized for on-column detection with detection limits 12 times better than a commercial detector. A dual-beam arrangement was employed to reduce flicker noise from the light source. Reversed-phase isocratic separations of a homologous series of alkyl benzenes were performed using the integrated system. In Chapter 3, a 260 nm LED-based UV-absorption detector was developed for on-capillary detection without a reference. The noise level of the detector was among the lowest ever attained with capillary detectors, and the detection limits were up to 2 orders of magnitude lower than any previously reported detector. Elimination of the reference cell reduced the complexity of the system. The LED detector was successfully integrated with the isocratic nano-flow pumping system for isocratic separations of phenols using a monolithic column.

Chapter 4 reports the performance evaluation of a splitless nano-flow gradient pumping system using the LED-based detector. Gradient performance was found to be excellent in terms of step and linear gradient reproducibility, and the separation of five phenols was demonstrated using the integrated system. Chapter 5 describes the construction and evaluation of a portable detector using a 405 nm laser. This detector was designed for high-sensitivity hemoglobinopathy detection. The noise level obtained with this detector was comparable to Hg-lamp based detector. In Chapter 6, suggestions are given for further development of the portable LC-UV system.

1.6 References

1. McMahon, G., Portable Instruments in Various Applications. In *Analytical Instrumentation*, John Wiley & Sons, Ltd: New Jersey, 2007; pp 199-216.

2. Gómez, M. J.; Gómez-Ramos, M. M.; Malato, O.; Mezcua, M.; Férnandez-Alba, A. R., *J. Chromatogr. A* **2010,** *1217*, 7038-7054.

3. Vandenabeele, P.; Edwards, H. G. M.; Jehlicka, J., *Chem. Soc. Rev.* **2014,** *43*, 2628-2649.

4. Hargreaves, M. D.; Green, R. L.; Jalenak, W.; Brown, C. D.; Gardner, C., Handheld Raman and FT-IR Spectrometers. In *Infrared and Raman Spectroscopy in Forensic Science*, John Wiley & Sons: New Jersey, 2012; pp 275-287.

5. Bosco, G. L., *TrAC, Trends Anal. Chem.* **2013,** *45*, 121-134.

6. Weindorf, D. C.; Bakr, N.; Zhu, Y., Donald, L. S., Ed. Academic Press: **2014**; 128, 1-45.

7. Vítek, P.; Ali, E. M. A.; Edwards, H. G. M.; Jehlička, J.; Cox, R.; Page, K., *Spectrochim. Acta A* **2012,** *86*, 320-327.

8. Mogilevsky, G.; Borland, L.; Brickhouse, M.; Fountain III, A. W., *Int. J. Spectrosc.* **2012,** *2012*, 12.

9. Cayuela, J. A.; Weiland, C., *Postharvest Biol. Tec.* **2010,** *58*, 113-120.

10. Sánchez, M.-T.; De la Haba, M.-J.; Pérez-Marín, D., *Comput. Electron. Agr.* **2013,** *92*, 66-74.

11. Boring, C. B.; Dasgupta, P. K.; Sjögren, A., *J. Chromatogr. A* **1998,** *804*, 45-54.

12. Smedts, B. R.; Baeyens, W.; De Bisschop, H. C., *Anal. Chim. Acta* **2003,** *495*, 239-247.

13. Chu, W.; Gao, N.; Yin, D.; Krasner, S. W.; Templeton, M. R., *J. Chromatogr. A* **2012,** *1235*, 178-181.

14. Baram, G. I., *J. Chromatogr. A* **1996,** *728*, 387-399.

15. Henry, C., *Anal. Chem.* **1997,** *69*, 195A-200A.

16. Contreras, J. A.; Murray, J. A.; Tolley, S. E.; Oliphant, J. L.; Tolley, H. D.; Lammert, S. A.; Lee, E. D.; Later, D. W.; Lee, M. L., *J. Am. Soc. Mass. Spectrom.* **2008,** *19*, 1425-1434.

17. Harris, C. M., *Anal. Chem.* **2002,** *74*, 585 A-589 A.

18. Otagawa, T.; Stetter, J. R.; Zaromb, S., *J. Chromatogr.* **1986,** *360*, 252-259.

19. Tulchinsky, V. M.; St Angelo, D. E., *Field Anal. Chem. Technol.* **1998,** *2*, 281-285.

20. Ishida, A.; Fujimoto, T.; Yokogawa, S.; Tani, H.; Tokeshi, M.; Yanagisawa, I., *16th International Conference on Miniaturized Systems for Chemistry and Life Sciences*, Okinawa, Japan, 2012, pp 1183-1185.

21. Sharma, S.; Plistil, A.; Simpson, R. S.; Liu, K.; Farnsworth, P. B.; Stearns, S. D.; Lee, M. L., *J. Chromatogr. A* **2014,** *1327*, 80-89.

22. http://www.srigc.com/2005catalog/cat92-95.htm.

23. http://www.iconsci.com/worldssmallesthplc.html.

24. Norgaard, J., *Environ. Protect. Mag.* **2005,** *16*, 32-35.

25. Gałuszka, A.; Migaszewski, Z.; Namieśnik, J., *TrAC, Trends Anal. Chem.* **2013,** *50*, 78-84.

26. Tsuda, T.; Novotny, M., *Anal. Chem.* **1978,** *50*, 271-275.

27. Hirata, Y.; Novotny, M., *J. Chromatogr. A* **1979,** *186*, 521-528.

28. Hirata, Y.; Novotny, M.; Tsuda, T.; Ishii, D., *Anal. Chem.* **1979,** *51*, 1807-1809.

29. Takeuchi, T.; Ishii, D., *J. Chromatogr. A* **1981,** *213*, 25-32.

30. Yang, F. J., *J. Chromatogr. A* **1982,** *236*, 265-277.

31. Takeuchi, T.; Ishii, D., *J. Chromatogr. A* **1982,** *238*, 409-418.

32. Borra, C.; Han, S. M.; Novotny, M., *J. Chromatogr. A* **1987,** *385*, 75-85.

33. Andreolini, F.; Borra, C.; Novotny, M., *Anal. Chem.* **1987,** *59*, 2428-2432.

34. Brooks, H. B.; Thrall, C.; Tehrani, J., *J. Chromatogr. A* **1987,** *385*, 55-64.

35. Karlsson, K. E.; Novotny, M., *Anal. Chem.* **1988,** *60*, 1662-1665.

36. Kennedy, R. T.; Jorgenson, J. W., *Anal. Chem.* **1989,** *61*, 1128-1135.

37. Hsieh, S.; Jorgenson, J. W., *Anal. Chem.* **1996,** *68*, 1212-1217.

38. MacNair, J. E.; Lewis, K. C.; Jorgenson, J. W., *Anal. Chem.* **1997,** *69*, 983-989.

39. MacNair, J. E.; Patel, K. D.; Jorgenson, J. W., *Anal. Chem.* **1999,** *71*, 700-708.

40. Lippert, J. A.; Xin, B.; Wu, N.; Lee, M. L., *J. Microcolumn Sep.* **1999,** *11*, 631-643.

41. Wu, N.; Collins, D. C.; Lippert, J. A.; Xiang, Y.; Lee, M. L., *J. Microcolumn Sep.* **2000,** *12*, 462-469.

42. Wei, B.; Rogers, B. J.; Wirth, M. J., *J. Am. Chem. Soc.* **2012,** *134*, 10780-10782.

43. Rogers, B. J.; Birdsall, R. E.; Wu, Z.; Wirth, M. J., *Anal. Chem.* **2013,** *85*, 6820-6825.

44. Wu, Z.; Wei, B.; Zhang, X.; Wirth, M. J., *Anal. Chem.* **2014,** *86*, 1592-1598.

45. Hjertén, S.; Liao, J.-L.; Zhang, R., *J. Chromatogr. A* **1989,** *473*, 273-275.

46. Svec, F.; Frechet, J. M. J., *Anal. Chem.* **1992,** *64*, 820-822.

47. Aggarwal, P.; Tolley, H. D.; Lee, M. L., *J. Chromatogr. A* **2012,** *1219*, 1-14.

48. Nischang, I., *J. Chromatogr. A* **2013,** *1287*, 39-58.

49. Hara, T.; Kobayashi, H.; Ikegami, T.; Nakanishi, K.; Tanaka, N., *Anal. Chem.* **2006,** *78*, 7632-7642.

50. Urban, J.; Svec, F.; Fréchet, J. M. J., *J. Chromatogr. A* **2010,** *1217*, 8212-8221.

51. Wang, Q. C.; Svec, F.; Frechet, J. M. J., *Anal. Chem.* **1993,** *65*, 2243-2248.

52. Petro, M.; Svec, F.; Gitsov, I.; Fréchet, J. M. J., *Anal. Chem.* **1996,** *68*, 315-321.

53. Premstaller, A.; Oberacher, H.; Huber, C. G., *Anal. Chem.* **2000,** *72*, 4386-4393.

54. Gu, B.; Chen, Z.; Thulin, C. D.; Lee, M. L., *Anal. Chem.* **2006,** *78*, 3509-3518.

55. Koeck, R.; Bakry, R.; Tessadri, R.; Bonn, G. K., *Analyst* **2013,** *138*, 5089-5098.

56. Chambers, S. D.; Holcombe, T. W.; Svec, F.; Fréchet, J. M., *Anal. Chem.* **2011,** *83*, 9478-9484.

57. Aggarwal, P.; Lawson, J. S.; Tolley, H. D.; Lee, M. L., *J. Chromatogr. A* **2014,** *1364*, 96-106.

58. Sharma, S.; Tolley, H. D.; Farnsworth, P. B.; Lee, M. L., *Anal. Chem.* **2015,** *87*, 1381-1386.

59. Niu, W.; Wang, L.; Bai, L.; Yang, G., *J. Chromatogr. A* **2013,** *1297*, 131-137.

60. Ishii, D.; Asai, K.; Hibi, K.; Jonokuchi, T.; Nagaya, M., *J. Chromatogr. A* **1977,** *144*, 157-168.

61. Takeuchi, T.; Ishii, D., *J. Chromatogr. A* **1982,** *253*, 41-47.

62. Karlsson, K. E.; Novotny, M., *J. High. Resolut. Chromatogr.* **1984,** *7*, 411-413.

63. Ishii, D.; Hashimoto, Y.; Asai, H.; Watanabe, K.; Takeuchi, T., *J. High. Resolut. Chromatogr.* **1985,** *8*, 543-546.

64. Slais, K.; Frei, R. W., *Anal. Chem.* **1987,** *59*, 376-379.

65. Šlais, K.; Preussler, V., *J. High. Resolut. Chromatogr.* **1987,** *10*, 82-85.

66. Davis, M.; Stahl, D.; Lee, T., *J. Am. Soc. Mass. Spectrom.* **1995,** *6*, 571-577.

67. Davis, M. T.; Stahl, D. C.; Hefta, S. A.; Lee, T. D., *Anal. Chem.* **1995,** *67*, 4549-4556.

68. MacNair, J. E.; Opiteck, G. J.; Jorgenson, J. W.; Moseley, M. A., *Rapid Commun. Mass Spectrom.* **1997,** *11*, 1279-1285.

69. Ducret, A.; Bartone, N.; Haynes, P. A.; Blanchard, A.; Aebersold, R., *Anal. Biochem.* **1998,** *265*, 129-138.

70. Zhang, Z.; Marshall, A. G., *J. High. Resolut. Chromatogr.* **1998,** *21*, 291-297.

71. Le Bihan, T.; Pinto, D.; Figeys, D., *Anal. Chem.* **2001,** *73*, 1307-1315.

72. Šesták, J.; Duša, F.; Moravcová, D.; Kahle, V., *J. Chromatogr. A* **2013,** *1276*, 26-32.

73. Čapka, L.; Večeřa, Z.; Mikuška, P.; Šesták, J.; Kahle, V.; Bumbová, A., *J. Chromatogr. A* **2015,** *1388*, 167-173.

74. Murata, K.; Mano, N.; Asakawa, N.; Ishihama, Y., *J. Chromatogr. A* **2006,** *1123*, 47-52.

75. Takeuchi, T.; Ishii, D., *J. Chromatogr. A* **1982,** *239*, 633-641.

76. Takeuchi, T.; Niwa, T.; Ishii, D., *J. Chromatogr. A* **1987,** *405*, 117-124.

77. Cappiello, A.; Famiglini, G.; Fiorucci, C.; Mangani, F.; Palma, P.; Siviero, A., *Anal. Chem.* **2003,** *75*, 1173-1179.

78. Siviero, A.; Bergna, M.; Famiglini, G.; Mantegazza, A.; Palma, P.; Cappiello, A., *Electrophoresis* **2012,** *33*, 575-582.

79. Natsume, T.; Yamauchi, Y.; Nakayama, H.; Shinkawa, T.; Yanagida, M.; Takahashi, N.; Isobe, T., *Anal. Chem.* **2002,** *74*, 4725-4733.

80. Deguchi, K.; Ito, S.; Yoshioka, S.; Ogata, I.; Takeda, A., *Anal. Chem.* **2004,** *76*, 1524-1528.

81. Ito, S.; Yoshioka, S.; Ogata, I.; Takeda, A.; Yamashita, E.; Deguchi, K., *J. Chromatogr. A* **2004,** *1051*, 19-23.

82. Van der Wal, S.; Yang, F. J., *J. High. Resolut. Chromatogr.* **1983,** *6*, 216-217.

83. Chervet, J.; Ursem, M.; Salzmann, J., *Anal. Chem.* **1996,** *68*, 1507-1512.

84. Zhou, X.; Furushima, N.; Terashima, C.; Tanaka, H.; Kurano, M., *J. Chromatogr. A* **2001,** *913*, 165-171.

85. Nazario, C. E. D.; Silva, M. R.; Franco, M. S.; Lanças, F. M., *J. Chromatogr. A* **2015,** *1421*, 18-37.

86. Šesták, J.; Moravcová, D.; Kahle, V., *J. Chromatogr. A* **2015,** *1421*, 2-17.

87. Scott, R. P. W.; Kucera, P., *J. Chromatogr. A* **1979,** *185*, 27-41.

88. Scott, R. P. W.; Kucera, P., *J. Chromatogr. A* **1979,** *169*, 51-72.

89. Scott, R. P. W.; Kucera, P.; Munroe, M., *J. Chromatogr. A* **1979,** *186*, 475-487.

90. Reichmuth, D. S.; Shepodd, T. J.; Kirby, B. J., *Anal. Chem.* **2005,** *77*, 2997-3000.

91. Munyan, J. W.; Fuentes, H. V.; Draper, M.; Kelly, R. T.; Woolley, A. T., *Lab on a Chip* **2003,** *3*, 217-220.

92. Gu, C.; Jia, Z.; Zhu, Z.; He, C.; Wang, W.; Morgan, A.; Lu, J. J.; Liu, S., *Anal. Chem.* **2012,** *84*, 9609-9614.

93. Chen, A.; Lynch, K. B.; Wang, X.; Lu, J. J.; Gu, C.; Liu, S., *Anal. Chim. Acta* **2014,** *844*, 90-98.

94. Zhou, L.; Lu, J. J.; Gu, C.; Liu, S., *Anal. Chem.* **2014,** *86*, 12214-12219.

95. http://www.sfc-fluidics.com/about-us/company-news/sfc-fluidics-creates-portable-handy-lc-using-its-rapid-prototyping-microfluidic-components/

96. Kiplagat, I. K.; Kubáň, P.; Pelcová, P.; Kubáň, V., *J. Chromatogr. A* **2010,** *1217*, 5116-5123.

97. Vissers, J. P. C.; de Ru, A. H.; Ursem, M.; Chervet, J.-P., *J. Chromatogr. A* **1996,** *746*, 1-7.

98. van Akker, E. B.; Bos, M.; van der Linden, W. E., *Anal. Chim. Acta* **1999,** *378*, 111-117.

99. Kubín, M.; Vozka, S., *J. Chromatogr. A* **1978,** *147*, 85-98.

100. Ishii, D.; Goto, M.; Takeuchi*, T., *J. Chromatogr. A* **1984,** *316*, 441-449.

101. Walbroehl, Y.; Jorgenson, J. W., *J. Chromatogr. A* **1984,** *315*, 135-143.

102. Kirkland, J. J., *Anal. Chem.* **1968,** *40*, 391-396.

103. Havaši, P.; Kaniansky, D., *J. Chromatogr. A* **1985,** *325*, 137-149.

104. Milano, M. J.; Lam, S.; Savonis, M.; Pautler, D. B.; Pav, J. W.; Grushka, E., *J. Chromatogr. A* **1978,** *149*, 599-614.

105. Baram, G. I.; Grachev, M. A.; Komarova, N. I.; Perelroyzen, M. P.; Bolvanov, Y. A.; Kuzmin, S. V.; Kargaltsev, V. V.; Kuper, E. A., *J. Chromatogr.* **1983,** *264*, 69-90.

106. Tulchinsky, V. M.; Glazunov, L. L.; Karev, V. V.; Morozova, E. R., Gottlieb, J.; Hötzl, H.; Huck, K.; Niessner, R., Eds. Springer Netherlands: **1997**, pp 367-370.

107. http://www.knauer.net/fileadmin/user_upload/produkte/files/Dokumente/detectors/smartline/brochures/b_e_dt_smartline_uv_detector_200.pdf.

108. Malcolm, A.; Wright, S.; Syms, R. R. A.; Moseley, R. W.; O'Prey, S.; Dash, N.; Pegus, A.; Crichton, E.; Hong, G.; Holmes, A. S.; Finlay, A.; Edwards, P.; Hamilton, S. E.; Welch, C. J., *Rapid Commun. Mass Spectrom.* **2011,** *25*, 3281-3288.

109. Wright, S.; Malcolm, A.; Wright, C.; O'Prey, S.; Crichton, E.; Dash, N.; Moseley, R. W.; Zaczek, W.; Edwards, P.; Fussell, R. J.; Syms, R. R. A., *Anal. Chem.* **2015,** *87*, 3115-3122.

110. Suscchik, N.; Gladyshev, M.; Kalachova, G.; Guseynova, V., *J. Chromatogr. A* **1995,** *695*, 223-228.

111. Tsitouridou, R.; Puxbaum, H., *Int. J. Environ. Anal. Chem.* **1987,** *31*, 11-22.

112. Tanaka, K.; Ohta, K.; Haddad, P. R.; Fritz, J. S.; Lee, K. P.; Hasebe, K.; Ieuji, A.; Miyanaga, A., *J. Chromatogr. A* **1999,** *850*, 311-317.

113. Kalyakina, O. P.; Dolgonosov, A. M., *J. Anal. Chem.* **2003,** *58*, 951-953.

114. Elkin, K. R., *J. Chromatogr. A* **2014,** *1352*, 38-45.

115. Ohla, S.; Belder, D., *Curr. Opin. Chem. Biol.* **2012,** *16*, 453-459.

116. Faure, K., *Electrophoresis* **2010,** *31*, 2499-2511.

117. Lin, S. L.; Bai, H. Y.; Lin, T. Y.; Fuh, M. R., *Electrophoresis* **2012,** *33*, 635-643.

118. Lin, S. L.; Lin, T. Y.; Fuh, M. R., *Electrophoresis* **2014,** *35*, 1275-1284.

119. Manz, A.; Miyahara, Y.; Miura, J.; Watanabe, Y.; Miyagi, H.; Sato, K., *Sens. Actuators B* **1990,** *1*, 249-255.

120. Terry, S. C.; Jerman, J. H.; Angell, J. B., *IEEE T. Electron Dev.* **1979,** *26*, 1880-1886.

121. Lazar, I. M.; Karger, B. L., *Anal. Chem.* **2002,** *74*, 6259-6268.

122. Lazar, I. M.; Trisiripisal, P.; Sarvaiya, H. A., *Anal. Chem.* **2006,** *78*, 5513-5524.

123. Borowsky, J. F.; Giordano, B. C.; Lu, Q.; Terray, A.; Collins, G. E., *Anal. Chem.* **2008,** *80*, 8287-8292.

124. Xie, J.; Miao, Y.; Shih, J.; Tai, Y.-C.; Lee, T. D., *Anal. Chem.* **2005,** *77*, 6947-6953.

125. Fuentes, H. V.; Woolley, A. T., *Lab Chip* **2007,** *7*, 1524-1531.

126. Dutta, D.; Ramsey, J. M., *Lab Chip* **2011,** *11*, 3081-3088.

127. Shelor, C. P.; Dasgupta, P. K.; Aubrey, A.; Davila, A. F.; Lee, M. C.; McKay, C. P.; Liu, Y.; Noell, A. C., *Astrobiology* **2014,** *14*, 577-588.

CHAPTER 2 INSTRUMENTATION FOR HAND-PORTABLE LIQUID CHROMATOGRAPHY*

2.1 Introduction

LC coupled with UV-absorption detection is a prominent analytical laboratory technique due to its broad applicability, high resolving power, and versatility. LC can separate analytes with widely different properties by utilizing different separation modes, such as ion exchange, reversed-phase, normal phase, hydrophilic interaction, hydrophobic interaction, and size exclusion. This versatile technique would be very useful for on-site analysis, since measurement immediately after the sample is collected avoids sample loss by degradation or interference by contamination that can occur during transport and storage. Also, actions to mitigate a chemical threat could be decided quickly on site [1]. Despite its popularity and wide use in the laboratory, LC has not been applied to any significant extent for field analysis. The main reasons for this are difficulties encountered in re-engineering the high pressure pumping system and most commonly used detectors (i.e., UV-absorption and mass spectrometry) to acceptable size, weight, robustness, and power usage, and difficulties associated with mobile phase use and disposal in the field [2].

With the advent of capillary LC, pumping systems were designed to provide flow rates in the nL to μL per min range. However, the sizes of the pumps generally remained the same, and a split-flow arrangement generated the same volume of solvent waste as pumps used for conventional packed columns. Also, dead volumes in such systems are high, and the reproducibility in flow rate has been poor [3]. Currently, pumps are commercially available that

---

*This chapter was largely reproduced from: Sharma, S.; Plistil, A.; Simpson, R. S.; Tolley, H. D.; Liu, K.; Farnsworth, P. B.; Stearns, S. D.; Lee, M. L. *J. Chromatogr. A* **2014**, *1327*, 80-89.

can provide sub-μL/min flow rates without a split-flow arrangement. Other miniaturized pumping systems include miniaturized gas pressurized cylinders [4] and electro-osmotic pumps [5]. However, these suffer from difficulties in generating gradients and poor flow rate reproducibility. Miniaturized diaphragm pumps are commercially available, but have the disadvantage of very low (<200 psi) maximum operating pressure [6]. This limits the chromatography columns that can be used. Direct current pumps have been used in portable LC; however, their flow rates were voltage dependent [7]. To meet the requirements of minimum power consumption and minimum toxic waste generation by a field-portable system without compromising performance, a miniaturized battery-operated piston pump with non-split flow arrangement is preferred.

Despite improvements in selectivity and sensitivity of other detection systems, such as mass spectrometry, the UV-absorption detector remains the most popular LC detector. Extra-column dispersion associated with the use of flow cells with capillary LC led to the development of on-column detection [8] and in-column detection [9]. This eliminates band-broadening problems from connecting tubes between the column and detector and, theoretically, should preserve separation efficiency and increase detection sensitivity [8]. However, perpendicular illumination of the capillary limits the detection path length to the internal diameter of the capillary [10] and decreases the effective path length [11], which increases the achievable LOD. This problem was addressed by efforts to increase the path length by using Z- and U-shaped cells [12-14], axial illumination [10], and multireflection cells [15]. These designs often suffer from disadvantages, such as complex design, high cost, high noise, poor separation efficiency, and poor chromatographic resolution and/or LOD [16]. Use of on- and in-column detection is also limited by the lack of availability of commercial LC columns with UV-transparent coatings.

Environmental samples containing contaminants such as pharmaceuticals, polycyclic aromatic hydrocarbons, pesticides, etc., in trace amounts (μg/mL to ng/mL), require detectors that have low short-term noise, since background noise controls the detection limits and quantitation reproducibility at low concentrations [17]. Also, it is important to focus the light properly on the internal diameter of the capillary to minimize the stray light [18]. Both short-term noise and stray light reduce the linear dynamic range of the detector. Stray light can be minimized by placing a slit in front of the capillary with a width equal to or smaller than the internal diameter of the capillary. However, an improperly placed slit decreases the amount of light passing through the capillary. Low light levels lead to poor signal-to-noise (S/N) ratio [18, 19]. Increasing the amount of light that passes through the capillary using optical fibers, ball lenses and properly focused optics can improve raw signal levels and the S/N ratio.

Another option to increase the S/N ratio is by signal averaging. Signal averaging has been explored in capillary electrophoresis (CE) detectors using a linear photodiode array (PDA) detector [20] and a charge coupled device (CCD) array detector [21]; however, reduction in noise level through averaging of the signals from a large number of detectors was not very effective. Another approach was recently published in which software averaging was employed to reduce the random noise in CE detection. A marked increase in S/N ratio was achieved [22]. This approach is applicable to all techniques in which data are recorded at rates lower than the maximum digitization rate of the computer interface. This technique is useful for a low-cost portable system because it can substitute for complex and non-ideal analog filters, and no extra hardware is needed for noise reduction.

A portable LC must have small components that can operate with battery power. In this chapter, an LC pumping system and UV-absorption detector (Figure 2.1) were reduced in size to

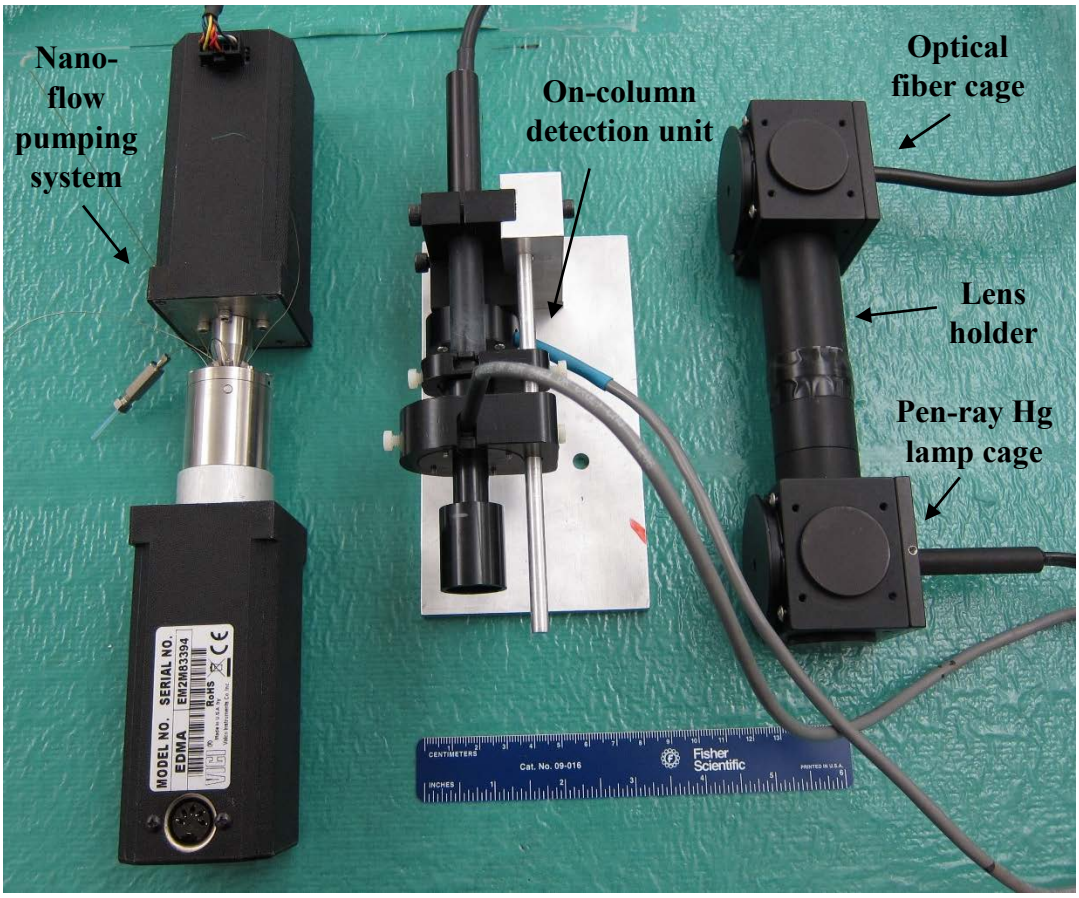

Figure 2.1 Photograph of the miniaturized LC components.

allow convenient use in the field. A nano-flow pump with stop-flow injector was used for mobile phase delivery and sample injection. A fixed wavelength detector (254 nm) was constructed, simplifying the detector hardware and reducing the cost and weight of the system. Separations using the isocratic instrument were demonstrated using a mixture of alkylbenzenes. The LC system was operated using regular line power in this work, although it was designed for battery operation.

2.2 Experimental section

2.2.1 Chemicals and reagents

Water, methanol, dodecanol, propylbenzene, butylbenzene, toluene, ethylbenzene, amylbenzene, uracil, sodium anthraquinone-2-sulfonate, 3-(trimethoxysilyl)propyl methacrylate (TPM, 98%), and 2,2-dimethoxy-2-phenylacetophenone (DMPA, 99%) were purchased from Sigma Aldrich (St Louis, MO, USA), and 1,6-hexanediol dimethacrylate (1,6-HDDMA) was a gift from Sartomer (Exton, PA, USA). Acetonitrile (ACN) was purchased from Fisher Scientific (Pittsburgh, PA, USA). All solvents and chemicals were HPLC or analytical reagent grade, and were used as received. HPLC water was filtered through a 0.22 μm membrane filter.

2.2.2 Instrumentation

Pump design and operation. An integrated battery-operated nano-flow pump and stop-flow injector (24 V DC) was constructed for nanoscale separations in collaboration with VICI Valco Instruments (Houston, TX, USA) (Figures 2.2 and 2.3). The major advantage of this system is that it does not employ a splitter, since it was designed specifically for capillary column use. It meets all requirements of a field-portable LC pumping system, i.e., light-weight, low mobile phase consumption and waste generation, and battery operation. The pump weighs only 1.4 kg (3 lbs) and can generate up to 110 MPa (16,000 psi) pressure.

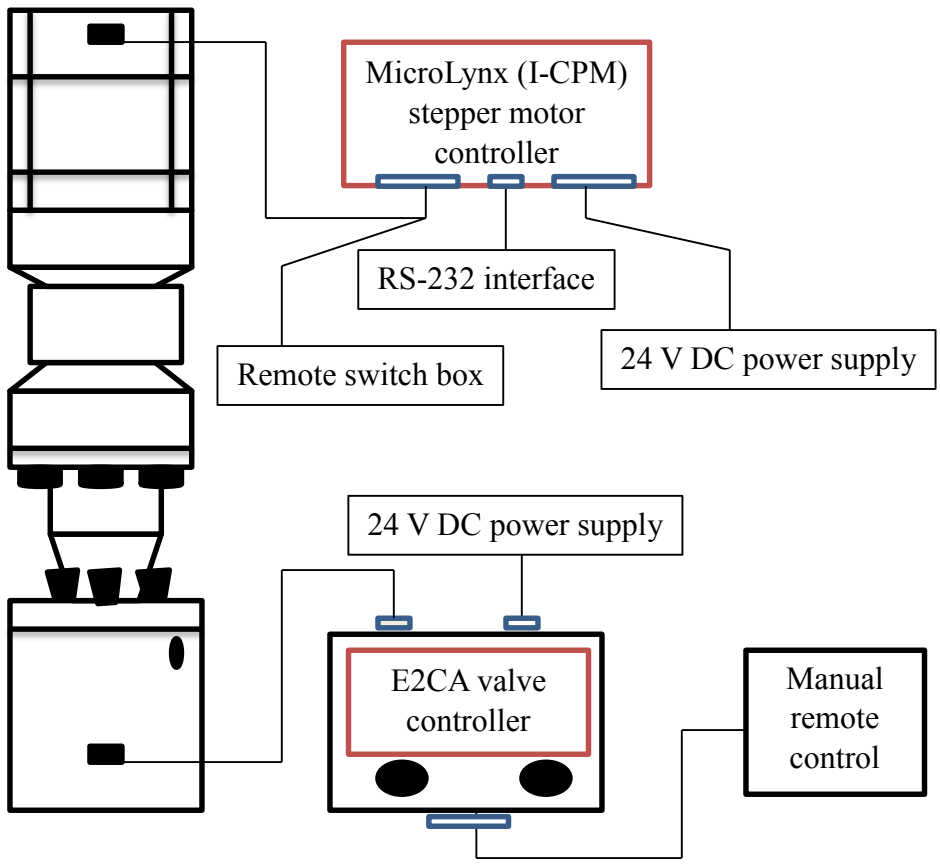

Figure 2.2 Schematic diagram of the nano-flow pumping system (i.e., nano-flow pump with stepper motor and high-pressure valve).

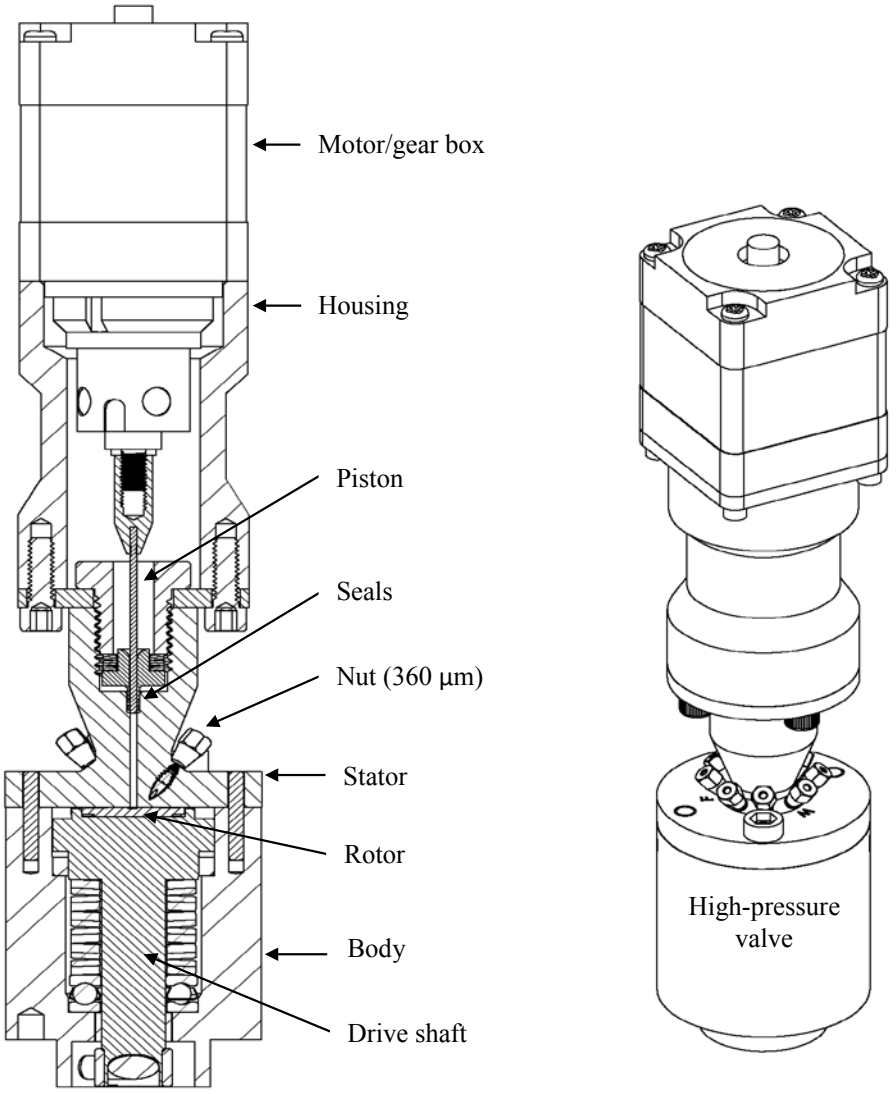

Figure 2.3 Cut-away drawing of the nano-flow pumping system (i.e. nano-flow pump with stepper motor and high-pressure valve).

The volume capacity of the pump is 24 μL, and a sample volume as low as 10 nL can be injected. In this work, I used a sample volume of 60 nL. During filling of both the pump and the sample loop, the mobile phase flow to the column is stopped; turning the valve to the inject position introduces both the sample and the mobile phase into the column. For column equilibration and/or bubble elimination from the system, mobile phase alone can be passed through the column if sample is not introduced into the sample loop. Pump re-filling takes less than 2 min. Since typical flow rates used in capillary columns (100-150 μm i.d.) range from 100-500 nL/min, an isocratic separation can be easily completed without the need to refill the pump. The maximum and minimum dispensing volumetric flow rates of the pump are 74.2 μL/min and 60 nL/min, respectively. This system uses 360 μm zero-dead-volume fittings. Both ends of the column can be connected to the nano-flow pump to maintain pressure during filling of the pump when the flow through the column is stopped, if desired. This would eliminate a delay period for column re-pressurization. However, in this work, the detection end of the capillary column was not connected back to the pump. The pump was controlled using Valco software, and the pump valve position (i.e., filling and dispensing) was changed using manual control.

The nano-flow pump contains eight inlet/outlet ports, each one for a specific purpose. The ports are spaced sequentially around the central axis (Figure 2.4), and serve the following functions: **F** allows the mobile phase to be withdrawn into the pump, the jumper loop (5 cm x 75 or 150 μm i.d. SS tubing, one end connected next to **F**) carries the mobile phase to the column during dispensing, **S** is the sample inlet, **W** is the sample waste, and **D** is the detector port. This last port can be used when both ends of the column are connected to the pump and detection is accomplished after the end of the column using a detector flow-cell.

The operation of the nano-flow pump is simple (Figure 2.4) and involves two major functions: pump filling and mobile phase dispensing. For pump filling, the valve must be in the filling position. A signal from the computer starts the needle piston retracting and drawing the solvent from the reservoir through a 15 cm x 200 μm i.d. stainless steel tube into the pump volume. At the same time and independent of pump filling, sample is introduced into the sample loop through a 5.08 cm x 75 μm i.d. capillary, which is connected to the **S** sample inlet port on the pump and to a zero-dead-volume connector at the other end, which in turn is connected to a short section of PEEK tubing into which a sampling syringe needle can be inserted. Sample loop filling (60 nL) can only be made while the valve is in the filling position.

For dispensing, the valve is switched to the dispensing position (i.e., the rotor rotates by 45°). The dispensing flow rate is controlled by the computer software. The needle piston starts dispensing on command by the computer, simultaneously driving the sample out of the sample loop and into the column. The mobile phase flows from the pump internal volume, through the jumper loop and sample loop, through the column and to the detector. The injection loop remains in the mobile phase flow path during dispensing, which facilitates cleaning for subsequent runs. The pump can be stopped anytime using a remote switch box.

Detector design and operation. The UV detector was based on a simple optical system (Figure 2.5). A pen-ray mercury lamp (bright line at 253.7 nm) from UVP (Upland, CA, USA) was used as a light source. This wavelength was chosen because it is used in most LC applications. Two plano-convex lenses (f = 50 mm, dia. = 1 in. fused silica) from Thorlabs (Newton, NJ, USA) were positioned such that their curved surfaces faced each other. This lens arrangement has been reported to give better light collimation and focusing than a single biconvex lens [23]. A line filter (25 mm x 3.5 mm, 254 nm) was positioned between the two

A. Filling position **B. Dispensing position**

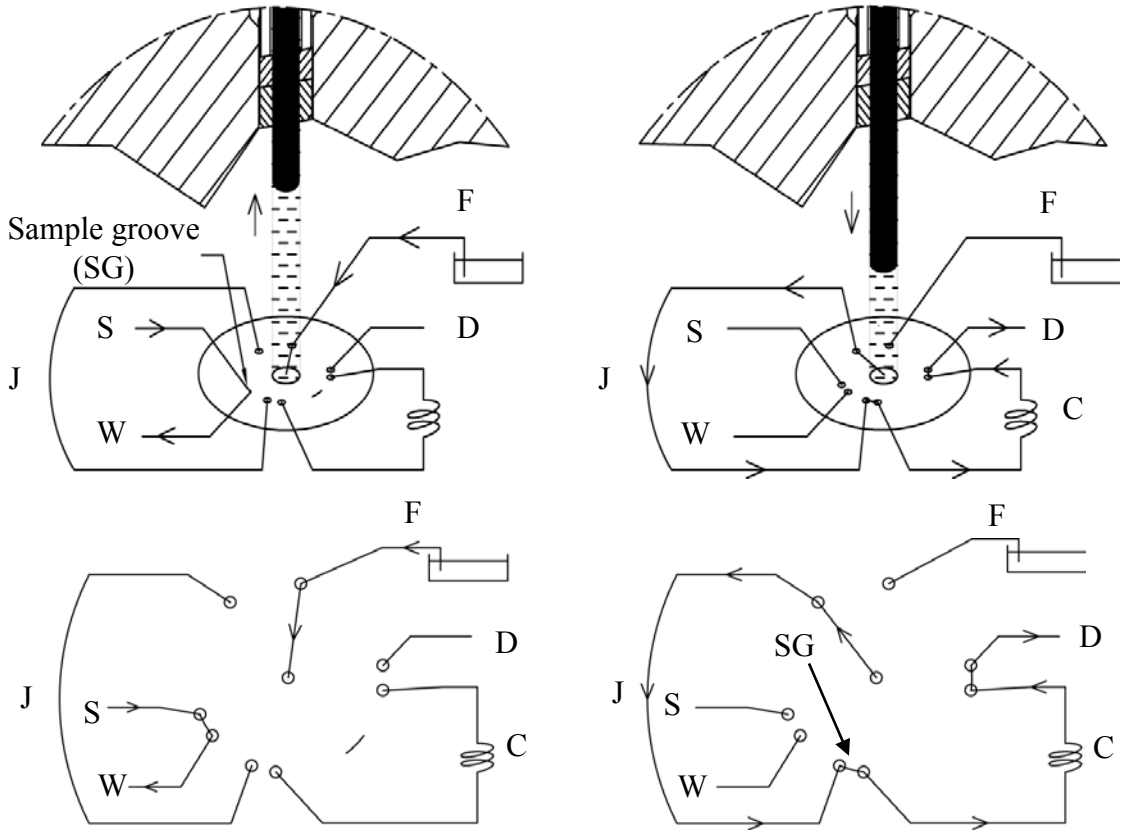

Figure 2.4 Operation of the nano-flow pumping system with stop-flow injector. (A) Rotor in filling position; needle moving from bottom to top; mobile phase being withdrawn from reservoir into pump volume; sample flowing from syringe through sample groove to waste; and no flow through jumper loop, column, or detector. (B) Rotor in dispensing position; needle moving from top to bottom; injection occurs at start of pumping; mobile phase flowing from pump volume through jumper loop, through sample groove, through column and to detector; and no flow from mobile phase reservoir, from sample syringe, or to waste.

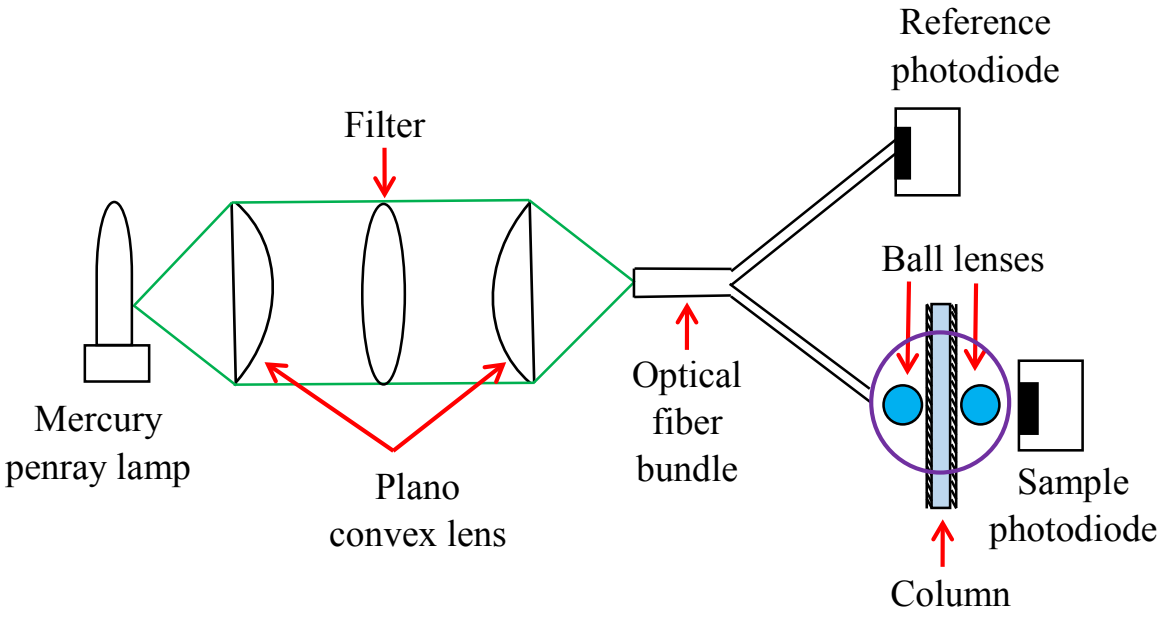

Figure 2.5 Schematic diagram of the UV-absorption detector.

lenses to minimize any stray light from other wavelengths. All of the lenses were housed inside a black threaded tube (Thorlabs) with the help of retaining rings. The positions of the lenses could be adjusted easily inside the tube using spanner wrenches (Thorlabs). The focused beam was collected by an optical fiber bundle. The lamp and optical fiber bundle were placed separately inside two black cages (Thorlabs) after making holes on the cage bottom. They were firmly secured in the upright position. The two cages were then threaded into the open ends of the black threaded tube mentioned above. This assembly was designed to eliminate any stray radiation coming from the surrounding light and from leakage of the source light. The bifurcated fiber bundle split the beam into sample and reference beams. Two identical silicon photodiodes (Hamamatsu) were employed as sample and reference detectors. The light from the two fiber sections fell on the respective photodiodes. Between the sample beam and silicon photodiode, a disc containing ball lenses (Edmund Optics, Barrington, NJ, USA) was employed for on-column detection. The bifurcated fiber bundle and disc containing ball lenses were obtained from a non-working model UV3000 detector originally from Thermo Separations (San Jose, CA, USA).

Ball lenses were used to focus light onto the center of the capillary, thereby increasing the light throughput. The split fiber bundle had apertures of different size and shape for sample and reference sides. They were circular in shape and 1 mm in diameter on the sample side, and rectangular in shape and 3 mm in length on the reference side. Using an oscilloscope, it was observed that the light intensity on the reference side was very high compared to the sample side. Therefore, to decrease the reference beam intensity and the difference between reference and sample beam intensities, a metal cap containing a 1-mm circular hole at its center was employed at the end of the beam splitter on the reference side. The output currents from the sample and reference photodiodes were converted to voltages with an operational amplifier circuit.

A USB 6009 (14 bit, 48 KS/s) interface was used to record voltage data with a computer. The voltage data were converted into absorbance values using a self-written LabView program. RC filters (time constant of 0.2 s) were employed for both signals (reference and sample) to reduce the high frequency noise. A small fan was also initially employed inside the electronics box to cool the power supply. The lamp and photodiodes required 12 V DC power for operation. The electronics circuit boards were housed in a separate aluminum box and were home-built, except for lamp power circuits (UVP, Upland, CA, USA). The detector requires 0.394 A current. Using a 4 A-h 12 V DC battery, this detector could run for approximately 10 h.

Other instrumentation. Before the nano-flow pump was ready for testing, the new UV-absorbance detector was evaluated with a commercial ISCO 100 DM syringe pump (Teledyne ISCO, Lincoln, NE, USA), which is referred to later in this chapter as a "commercial" pump to distinguish it from the new nano-flow pump. Likewise, an Eksigent Nano 2D LC system (Dublin, CA, USA) with a Model UV3000 detector from Thermo Separations (San Jose, CA, USA), modified for on-column detection [24], was used to obtain data for comparison with the new detector; this system is referred to later as a "commercial" system/detector. LabView (2010 version) self-written software was used for data collection and processing when using the new detector, while data were handled with ChromQuest 2.5.1 software (ThermoQuest, San Jose, CA, USA) when using the commercial system/detector.

2.2.3 Monolithic column preparation

A UV-transparent 15.5 cm x 75 μm i.d. fused silica capillary (Polymicro Technologies, Phoenix, AZ, USA) was used for column fabrication. The capillary pretreatment procedure was previously described in detail [25], except that the etching step with NaOH was not performed in this study. The monomer mixture was prepared by sequentially adding photo initiator (DMPA,

1% of the monomer weight), monomer (1,6-hexanediol dimethacrylate) and porogens (dodecanol and methanol) in a 1-dram glass vial. The composition of the monomer mixture was 33.1% w/w monomer, 45.0% w/w methanol and 21.9% w/w dodecanol (% w/w was based on total polymerization mixture). The solution was vortexed and ultrasonicated to obtain a homogenous solution, and then introduced into the UV transparent pretreated capillary using capillary action. The filled capillary was then placed under a UV lamp (390±15 nm, 1000 W, TAMARACK Scientific, Corona, CA, USA) for 3.5 min for polymerization. The resultant monolith was washed with water and methanol to remove unreacted monomer and porogens.

2.2.4 System evaluation

Reproducibility in flow rate and injection. Considering the low flow rates of the new pumping system, volumetric measurements were not feasible. Instead, an Eksigent calibration capillary (Dublin, CA, USA) was used to determine the reproducibility of the pump at different flow rates (0.005 - 0.102 µL/s or 300 nL - 6.12 µL/ min) on different days. The calibration capillary has four 1-µL markings. The time taken by the solvent to flow through each marking was recorded using a stop-watch, and the flow rate was calculated by dividing 1 µL by the time (s). The calculated and theoretical flow rates (µL/s) were compared, and the percent accuracy was reported. Stainless steel tubing (15 cm x 150 µm i.d.) was used to connect the pump outlet to the calibration capillary. Water and a mixture of acetonitrile/water (70:30 v/v) were used as solvents. Experiments were performed on two different days and a total of eight readings were recorded for each solvent. A flow rate variation within ±1% is generally considered acceptable for LC.

Injection carry-over was studied by recording signals obtained by first injecting uracil (0.33 mg/mL in ACN/water mixture, 70:30 v/v) on the column as described in the previous

section. Next, the injector was thoroughly cleaned and a blank injection (mobile phase) was made. A mixture of acetonitrile/water (70:30 v/v) was used as mobile phase at a flow rate of 900 nL/min. These experiments were repeated three times and the detector signals were recorded. For each experiment, the percent of the peak area in the blank divided by the peak area from an analyte signal, multiplied by 100%, was reported as the percent carry-over. Precision in injections was reported as RSD of peak area and peak height (n = 5).

Stray light assessment and improvement in the S/N ratio. Initial experiments with the new detector were performed using a commercial pump (see Section 2.2.2) with manual injector (60 nL volume) and flow rate of 10 μL/min before a splitting tee. A UV-transparent 150 μm i.d. hollow fused silica capillary (Polymicro Technologies, Phoenix, AZ, USA) was used for these experiments, and on-capillary detection was accomplished at 254 nm. HPLC grade water was used as mobile phase. The new detector developed in this work was compared to the performance of a commercial detector modified for on-column detection (see Section 2.2.2).

All solutions were prepared using HPLC grade water. For measuring detector response, uracil solutions (1 mg/mL) were made in HPLC grade water. Uracil was chosen because of its moderate absorptivity (approx. 7700) at 254 nm. Injections (60 nL) were made into the hollow capillary, analyte peaks were recorded and the S/N ratio was determined. Due to a high noise level, several changes were made to the detector as described in Section 2.2.2 to improve its performance. The effect of software averaging on detector noise was studied and the best averaging rate was determined at which marked improvement in the S/N ratio was obtained. Noise spectra from both sample and reference channels were recorded to check the performance of the RC filters. A 150 μm i.d. capillary was filled with black ink by capillary action. This

capillary was inserted into the capillary holder and the average absorbance was recorded to assess the stray light in the system.

Linearity and LOD. The linearity of the system and the LOD were determined using sodium anthraquinone-2-sulfonate solutions. Peak heights and areas were measured and their log values were plotted against log concentration. The concentrations used for the plot ranged from 3.2 μM to 12.8 mM (0.001 to 4 mg/mL). Injection volumes of 60 nL were made into a hollow fused silica capillary (150 μm i.d.), and a flow rate of 600 nL/min (non-split) was generated by the nano-flow pump. Water was used as mobile phase, and a data rate of 10 Hz was employed. Using the nano-flow pump, 2 identical runs were made on each of two days and average readings of peak area and peak height (i.e., averages of 4 measurements of each) were recorded. These experiments were repeated using a commercial capillary LC system/detector (see Section 2.2.2). The mobile phase for these experiments was a mixture of water/acetonitrile (98:2 v/v). The data rate employed was 12 Hz. The root mean square (rms or short-term noise) of the detector was determined by purging the hollow fused silica capillary with HPLC grade water, and recording the baseline for several minutes; the standard deviation of the baseline was reported as the short-term noise.

Reversed-phase separations. Uracil was injected as an unretained marker on the monolithic column (15.5 cm x 75 μm i.d.) at different flow rates (60-600 nL/min) using acetonitrile/water (70:30 v/v) as mobile phase, and the total variance (σ^2_{total}) was calculated using the Foley-Dorsey equation [26]. This equation was selected here since it takes into account peak asymmetry for an unretained analyte and gives a true estimation of the "goodness" of the column bed structure.

$$\sigma^2_{total} = W^2_{0.1} / [1.764(B/A)^2 - 11.15\ (B/A) + 28] \quad (2.1)$$

where $W^2_{0.1}$ is the square of the width at 10% of the peak maximum and B and A are peak widths at 10% peak height from the tail to the peak center and from the front to the peak center, respectively. The number of theoretical plates and equivalent plate height were calculated from

$$N = (t_R / \sigma_{total})^2 \quad (2.2)$$

and

$$H = L / N \quad (2.3)$$

where N is the theoretical plate number, t_R is the retention time, σ^2_{total} is the total peak variance, and H is the minimum plate height. The column efficiency (H_{min}) was plotted against linear velocity (mm/s).

Reversed-phase isocratic separations were performed using uracil as unretained marker and five alkyl-substituted benzenes (toluene, ethylbenzene, propylbenzene, butylbenzene and amylbenzene). A mixture of acetonitrile and water (70:30 v/v) was used as mobile phase. All solutions were prepared using the mobile phase as solvent, and concentrations of uracil and alkyl benzenes were 0.17 mg/mL and 0.9% v/v, respectively. Separations (6 measurements each) were performed at 480 nL/min, and the retention time reproducibility was calculated. From these data, the number of theoretical plates was calculated from

$$N = 5.54(t_R / W_{0.5})^2 \quad (2.4)$$

where N is the theoretical plate number, t_R is the retention time, and $W_{0.5}$ is the peak width at half height.

2.3 Results and discussion

2.3.1 Flow rate reproducibility

Constant flow rate is essential in chromatography. This ensures reproducible retention times. Also, quantitation using UV-absorption detection is compromised if the pump generates inconsistent flow rates, since the peak characteristics are influenced by the flow rate [27]. Peak area and height decrease with an increase in flow rate. Using the nano-flow pump, a flow rate accuracy of > 99.94% was obtained with percent error ranging from 0.000007% to 0.061% in day-to-day experiments. These data reveal excellent flow rate reproducibility generated by the nano-flow pump. A comparison of theoretical flow rate versus calculated flow rate is shown in Table 2.1. A linear fit ($y = 1.0006x - 0.0002$) between theoretical flow rate and calculated average flow rate gave a correlation coefficient (R) of 0.9998. It is evident from the data that the pumping system generates accurate flow rates.

2.3.2 Injection repeatability

The injector should give high precision and low carry-over. This is important for quantitative analysis. For unknown samples, it is recommended to always inject low concentrations first, followed subsequently by higher concentrations to avoid problems with carry-over. Also, the injector should be thoroughly cleaned after each injection, even if the same concentration is to be injected. The data from this work showed that the nano-flow pump injector had very low carry-over (0.31%) and was very reliable for quantitative work. The RSD values for peak areas and peak heights for repetitive injections of uracil were calculated to be 1.87% and 1.41% ($n = 5$), respectively. In future work, the injector will be deactivated/coated to further improve its performance. Uracil was used as test analyte because a non-retained marker is commonly used to evaluate the injector performance in terms of dead volume.

Table 2.1 Comparison of theoretical and calculated flow rates using the new nano-flow pump.

Theoretical flow rate (µL/s)	Calculated flow rate (µL/s)[a]	Calculated flow rate (µL/s)[b]
0.005	0.0049 ± 0.00011	0.0048 ± 0.00003
0.009	0.0090 ± 0.00003	0.0086 ± 0.00006
0.013	0.0128 ± 0.00011	0.0125 ± 0.00013
0.017	0.0170 ± 0.00029	0.0167 ± 0.00034
0.051	0.0510 ± 0.00077	0.0509 ± 0.00039
0.102	0.1017 ± 0.00077	0.1020 ± 0.00079

[a] Average flow rate of eight readings obtained using water on two days ± standard deviation.
[b] Average flow rate of eight readings obtained using a mixture of acetonitrile/water (70:30 v/v) on two days ± standard deviation.

2.3.3 Improvement in detector S/N ratio

For triplicate injections of uracil solution (1 mg/mL) made on three different days, an S/N ratio of 6.37 ± 0.26 was obtained. High S/N ratio is required to achieve good precision in the data. Efforts were made to reduce the noise of the detector. All of the electronics were insulated and shielded to reduce electrical interference. The lamp electronics were initially cooled with a fan; however, this increased the noise level by a factor of 1.76. Therefore, the fan was removed. No negative effects was observed on detector performance in one and half years of use. The LabView program was modified to perform real-time averaging of the signals.

Experiments were performed in order to determine the averaging rate at which a marked decrease in the noise was observed without compromising the signal intensity. Uracil solution (1 mg/mL) and a hollow fused silica capillary (150 μm i.d.) were used. The modified software collected "n" samples every 0.1 s, and averaged them. The final data rate was 10 Hz in all experiments. With an increase in the number of averages per 0.1 s, it was observed that the noise decreased and the S/N ratio became larger. The S/N ratio was obtained by dividing the average peak height (obtained from at least three consecutive runs) by the standard deviation of the baseline (1 min data). All experiments were repeated on different days to check the day-to-day repeatability. Experiments were performed using digitization rates from 5 Hz to 24,000 Hz (n varied from 5 to 2400 data points). An increase in the S/N ratio was observed up to 1200 data points averaging, followed by a slight decrease at 2400 data points, as shown in Figure 2.6. Good repeatability (RSD 9.2%) at 12 kHz (N = 1200) and maximum S/N ratio (481.5) were obtained. This averaging method was selected for further experiments. With 2400 data points averaging, a decrease in the S/N ratio was observed due to a corresponding decrease in the signal intensity.

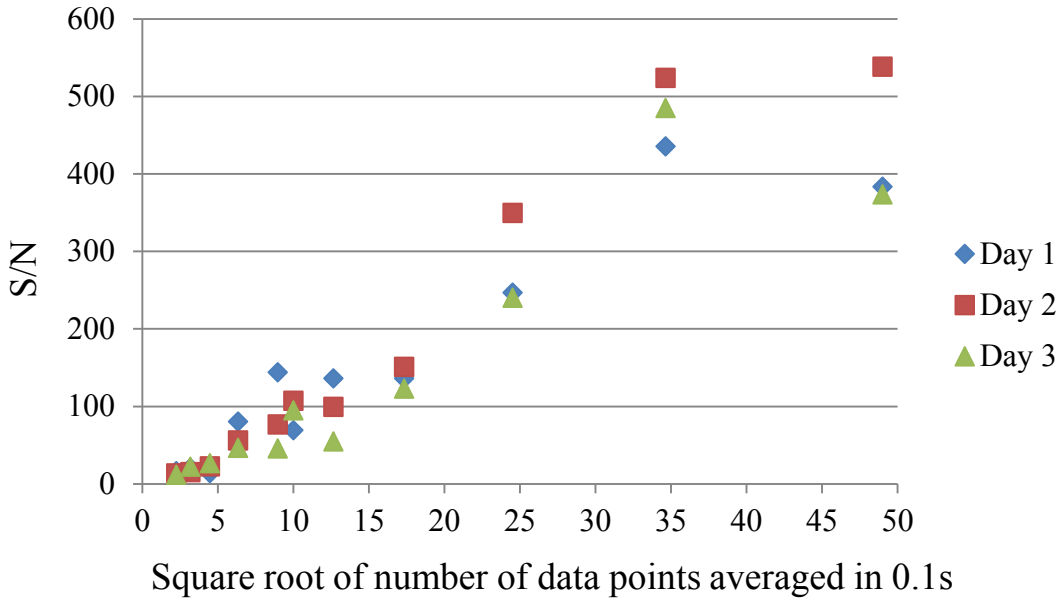

Figure 2.6 Plot of S/N ratio versus square root of the number of data points averaged per 0.1 s. The number of data points increased from 5 to 2400.

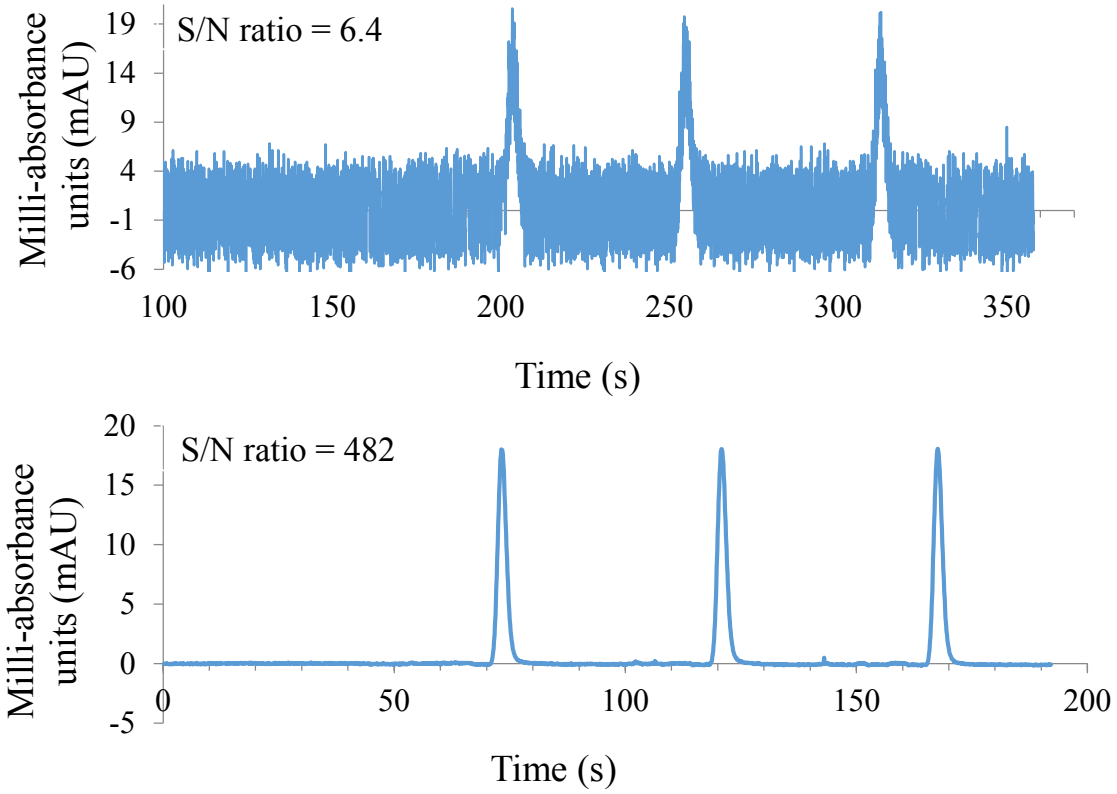

Figure 2.7 Comparison between signals obtained using 24 Hz data rate without averaging and 12 kHz rate with 1200 data point averaging. All peaks widths are approximately 6 s wide at the base.

Since the limit of detection of the system is dependent on the noise level, noise minimization was important in this work. Signals obtained without averaging (24 Hz data rate) were compared to signals obtained with 1200 data points per second averaging (10 Hz data rate after averaging). As shown in Figure 2.7, marked improvement in the S/N ratio was achieved with software averaging. The effect of averaging on the signal intensity was negligible. A low pass RC filter was expected to cut off the high frequency noise in the system. It was found using noise spectra that the RC filter did not work as expected. However, with software averaging, the noise level was markedly reduced.

2.3.4 Detector stray light

Stray light is the fraction of incident light that reaches the detector without passing through the sample. If all of the light passed through the sample, the transmittance observed would be the ideal transmittance. However, if a significant portion of the light reached the detector without passing through the sample, the observed transmittance would include the ideal transmittance plus transmitted stray light. This would cause negative deviations from ideal absorbance values. The effect of stray light on the system is to increase the LOD and decrease the maximum absorbance.

The transmittance can be calculated from

$$T = (I + I_s) / (I_o + I_s) \tag{2.5}$$

and

$$A = \log (1/T) \tag{2.6}$$

where T is the transmittance, I is the transmitted light intensity, I_s is the stray light, I_o is the incident light, and A is the absorbance.

When the capillary is filled with highly concentrated solution (e.g., black ink), the transmitted light should ideally be zero, and the percent of stray light can be calculated. Lowering the stray light in the system would increase the dynamic range of the detector. However, with on-column detection, eliminating stray light can come at the expense of light throughput [28]. The maximum absorbances of the new and commercial detectors were found to be 0.94 and 0.77 AU. This corresponds to stray light fractions of 11.5% and 16.8%, respectively. Considering the fact that no slits were employed in the new detector, acceptable stray light levels were achieved.

2.3.5 Detector linearity

Experiments were performed with sodium anthraquinone-2-sulfonate (3.2 μM to 12.9 mM, or 0.001 to 4 mg/mL), and log peak areas as well as log peak heights were plotted against log concentrations as shown in Figure 2.8. The linear regression equations and coefficients (R) for the new and commercial detectors are given in Table 2.2. The new detector was non-linear at concentrations higher than 6.4 mM (2 mg/mL) due to the presence of stray light as can be seen in Figure 2.8. For the new detector, RSDs for the peak areas ranged from 1.0% to 3.3% (day-to-day and batch-to-batch, respectively). The lowest concentration detected during the nano-flow pump experiments at an S/N ratio of 3 was 0.13 μM (7.8 fmol, or 40 ng/mL). From these data, it is evident that the new detector would be useful for high sensitivity detection in capillary columns. The performance of the detector could be further improved with a reduction in the stray light in the system. With the commercial system/detector, the lowest concentration detected was 1.6 μM (0.5 μg/mL). The difference in detection limits is most likely related to the difference in stray light levels of these two systems.

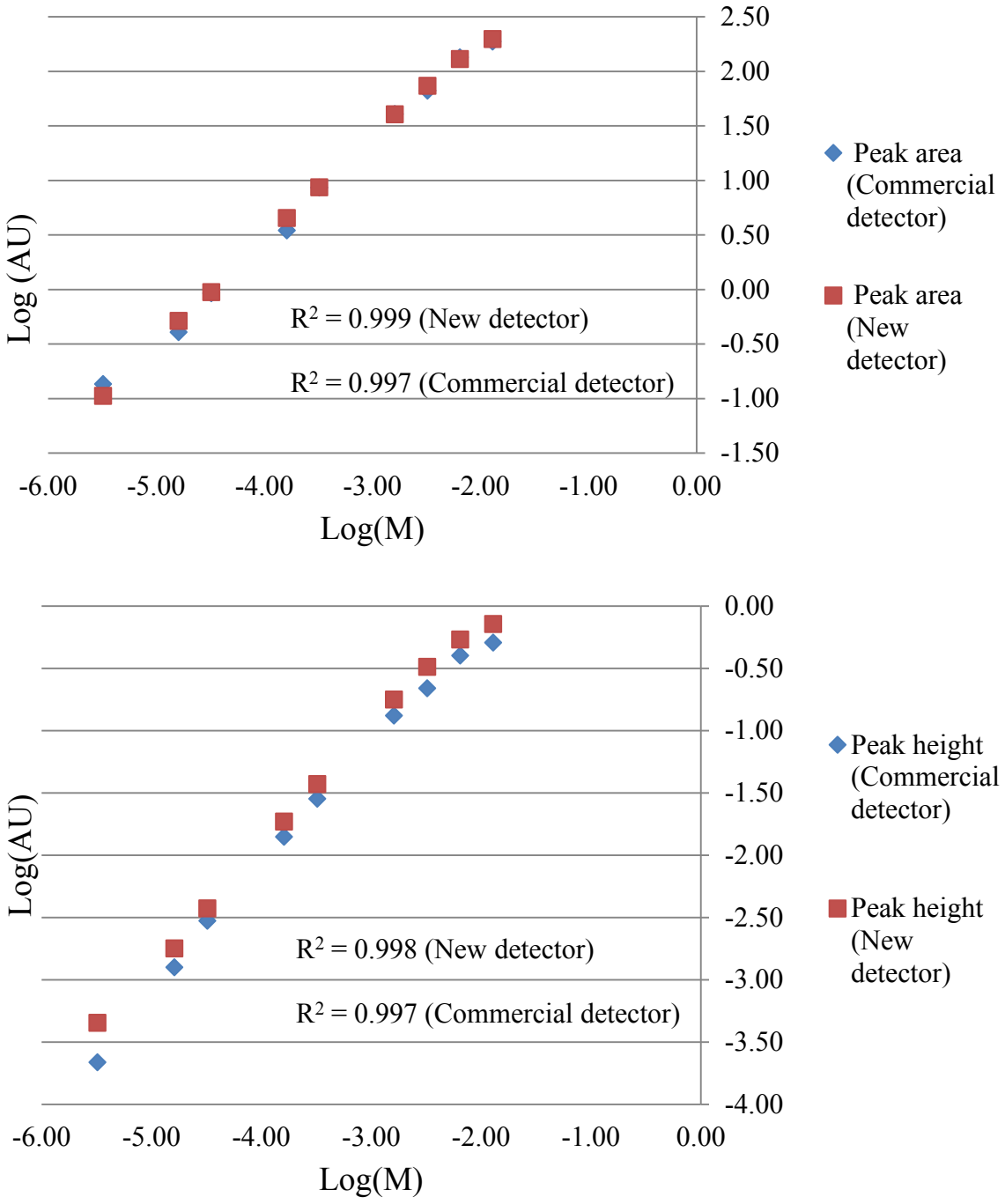

Figure 2.8 Plots of log of peak areas and peak heights (absorbance units) versus log of sodium anthraquinone-2-sulfonate concentration.

Initially, a commercial pump was used for detector evaluation experiments. The root mean square (rms) noise of the raw absorbance signals at 10 Hz data rate was found to be 4.4 x 10^{-3}. With 1200 data point averaging, the rms noise was reduced to 3.6 x 10^{-5}. In contrast, with the nano-flow pump, the rms noise was found to be even lower (1.6 x 10^{-5}). This indicates that the commercial pump significantly increased the detector noise. In both cases, the short-term noise was still comparable to commercially available detectors (~10^{-5} AU).

2.3.6 Reversed-phase separations

Extra-column volume can significantly affect the performance of a system by causing band-broadening. Major sources of extra-column broadening include the injector, improper connections, detector cell volume and connecting tubes. In this system, on-column detection was performed, which eliminated one extra-column broadening source. There was no connecting tube between the injector and column. Also, for an isocratic system, the peaks are less affected by the volume of mobile phase contained in the tubing between the solvent reservoir and injector. In the van Deemter curve (Figure 2.9), the minimum plate height was found to be 27.6 μm at a volumetric flow rate of 240 nL/min. For an unretained marker (i.e., uracil), the column generated 36,000 plates per meter at 240 nL/min. The peak asymmetry factor was found to be good (B/A = 1.04 to 1.28) in these experiments. Good resolution was obtained for reversed-phase separations (Figure 2.10) of a mixture of alkyl-substituted benzenes, even though the separations were performed at double the optimum flow rate, i.e., 480 nL/min. The retention time reproducibility for all analytes ranged from RSD 0.09 to 0.74% for n = 6. The retention times of the analytes were: uracil (5.6 ± 0.005 min), toluene (9.3 ± 0.03), ethylbenzene (10.3 ± 0.04), propylbenzene (11.9 ± 0.06), butylbenzene (14.4 ± 0.1) and amylbenzene (17.1 ± 0.1). The column efficiencies (N/m), retention factors and minimum plate heights (μm) (n = 3), respectively, for the retained

Table 2.2 Comparison of the new detector response linearity with a commercial system/detector.

	Concentration range	Peak area (AU)		Peak height (AU)	
		Regression Equation	**R^2**	**Regression Equation**	**R^2**
New detector	3.2 µM - 6.4 mM	y = 0.9416x + 4.2	0.999	y = 0.9559x + 1.8807	0.998
Commercial detector	3.2 µM - 6.4 mM	y = 0.9312x + 4.2	0.997	y = 0.9852x + 1.8356	0.997

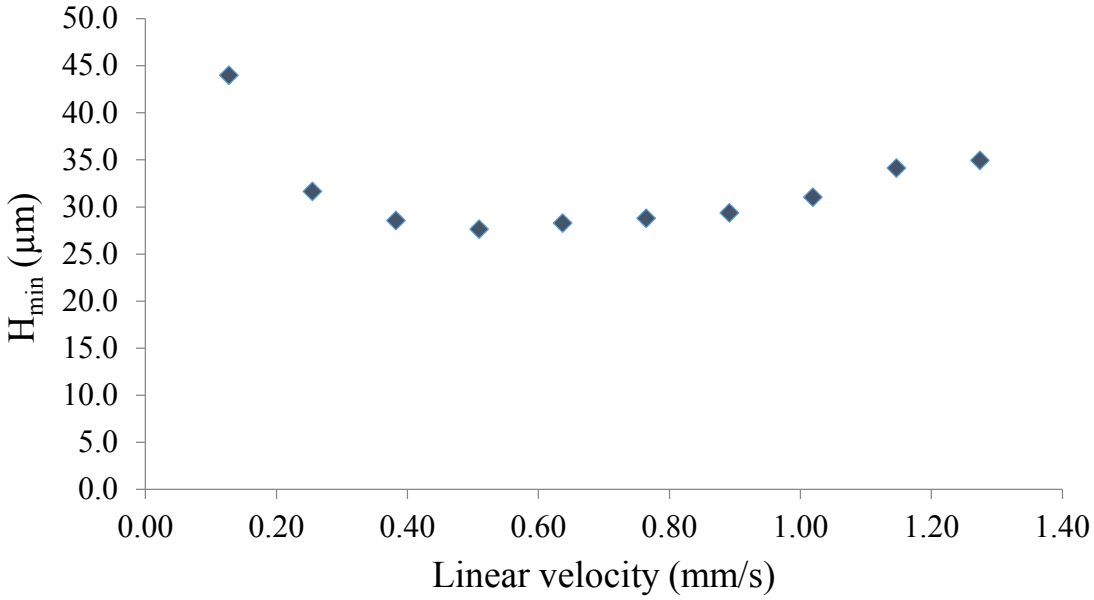

Figure 2.9 Van Deemter curve showing minimum plate height (µm) versus linear velocity (mm/s).

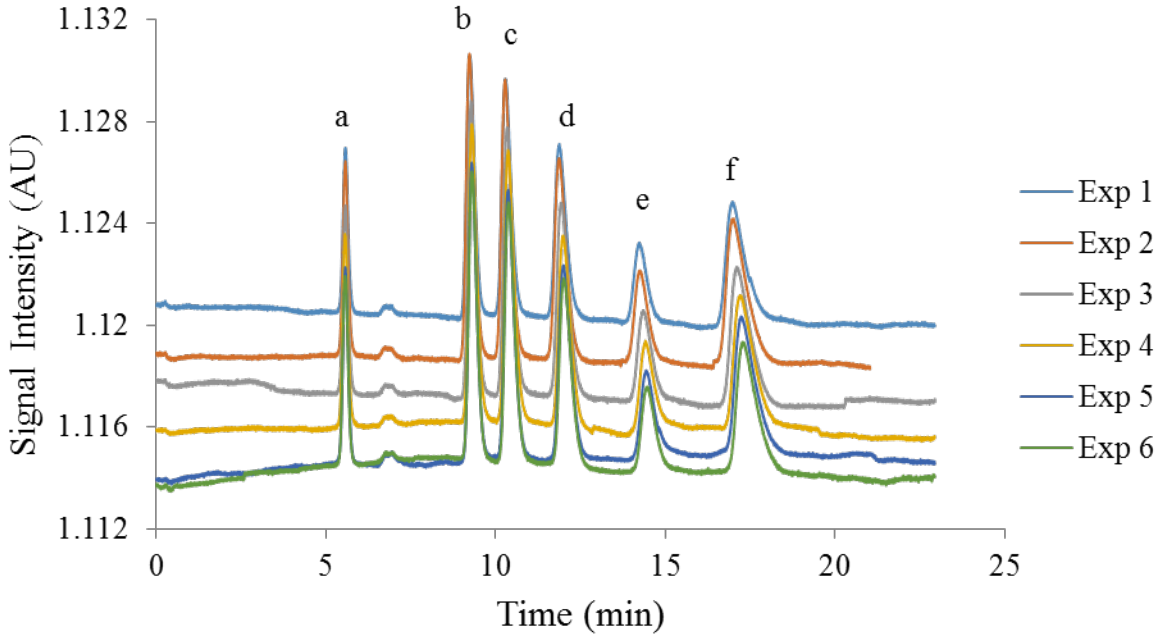

Figure 2.10 Separations performed with a 1,6-HDDMA monolithic capillary column (15.5 cm × 75 μm i.d.) at 254 nm using the new pumping system and new detector. Peak identifications (from left to right): (a) uracil, (b) toluene, (c) ethylbenzene, (d) propylbenzene, (e) butylbenzene and (f) amylbenzene.

compounds were: toluene (43,400, 0.7 and 23), ethylbenzene (40,600, 0.9 and 25), propylbenzene (36,800, 1.2 and 27), butylbenzene (38,400, 1.6 and 26), and amylbenzene (25,200, 2.1 and 40).

2.4 Conclusions

The overall performance of the portable LC components was found to be excellent. The nano-flow pumping system operation involved minimum mobile phase and waste generation. The pumping system showed excellent repeatability in terms of flow rate and retention time. The injection system provided high precision and low carry-over, which made it useful for quantitative analysis. Good linearity and sensitivity were achieved using the on-capillary UV-absorption detector and the nano-flow pumping system. With the nano-flow pump, short-term detector noise decreased. Good resolution and retention time repeatability were obtained in the reversed-phase separation of alkylbenzenes. The new, single wavelength UV-absorption detector was much smaller with lower power requirements compared to commercial instruments. Software averaging was found to be useful for noise reduction without compromising signal intensity, and the noise level was determined to be comparable to commercial detectors. Low stray light levels were achieved using the new detector. This detector can be easily modified to operate at other wavelengths merely by changing the lamp and filter. Since a single wavelength (254 nm) detector can detect the majority of the target analytes of interest, it is cost-effective for a field-portable system compared to a multi-wavelength detector.

Finally, it is important to mention that this chapter did not take into account the details and feasibility to perform operations such as representative sampling, sample preparation and preconcentration, in-field, since the focus of the chapter was only to evaluate the miniaturized LC components for eventual field-portable LC use.

2.5 References

1. Baram, G. I., *J. Chromatogr. A* **1996,** *728*, 387-399.
2. Boring, C. B.; Dasgupta, P. K.; Sjögren, A., *J. Chromatogr. A* **1998,** *804*, 45-54.
3. Zhou, X.; Furushima, N.; Terashima, C.; Tanaka, H.; Kurano, M., *J. Chromatogr. A* **2001,** *913*, 165-171.
4. Kiplagat, I. K.; Kubáň, P.; Pelcová, P.; Kubáň, V., *J. Chromatogr. A* **2010,** *1217*, 5116-5123.
5. Hargreaves, M. D.; Green, R. L.; Jalenak, W.; Brown, C. D.; Gardner, C., Handheld Raman and FT-IR Spectrometers. In *Infrared and Raman Spectroscopy in Forensic Science*, John Wiley & Sons: New Jersey, 2012; pp 275-287.
6. http://www.sfc-fluidics.com/about-us/company-news/sfc-fluidics-creates-portable-handy-lc-using-its-rapid-prototyping-microfluidic-components/.
7. Otagawa, T.; Stetter, J. R.; Zaromb, S., *J. Chromatogr.* **1986,** *360*, 252-259.
8. Yang, F. J., *J. Chromatogr. A* **1982,** *236*, 265-277.
9. Guthrie, E. J.; Jorgenson, J. W., *Anal. Chem.* **1984,** *56*, 483-486.
10. Xi, X.; Yeung, E. S., *Anal. Chem.* **1990,** *62*, 1580-1585.
11. Shintani, Y.; Hirako, K.; Motokawa, M.; Iwano, T.; Zhou, X.; Takano, Y.; Furuno, M.; Minakuchi, H.; Ueda, M., *Journal of chromatography. A* **2005,** *1073*, 17-23.
12. Chervet, J. P.; Van Soest, R. E. J.; Ursem, M., *J. Chromatogr. A* **1991,** *543*, 439-449.
13. Bruin, G. J. M.; Stegeman, G.; Van Asten, A. C.; Xu, X.; Kraak, J. C.; Poppe, H., *J. Chromatogr. A* **1991,** *559*, 163-181.
14. Moring, S. E.; Reel, R. T.; van Soest, R. E. J., *Anal. Chem.* **1993,** *65*, 3454-3459.
15. Wang, T.; Aiken, J. H.; Huie, C. W.; Hartwick, R. A., *Anal. Chem.* **1991,** *63*, 1372-1376.

16. Suhyeon, K.; Weonseop, K.; Jong, H. H., *J. Chromatogr. A* **1994,** *680*, 109-116.

17. Havaši, P.; Kaniansky, D., *J. Chromatogr. A* **1985,** *325*, 137-149.

18. Walbroehl, Y.; Jorgenson, J. W., *J. Chromatogr. A* **1984,** *315*, 135-143.

19. Liu, H.; Dasgupta, P. K.; Zheng, H. J., *Talanta* **1993,** *40*, 1331-1338.

20. Culbertson, C. T.; Jorgenson, J. W., *Anal. Chem.* **1998,** *70*, 2629-2638.

21. Bergström, E. T.; Goodall, D. M.; Pokrić, B.; Allinson, N. M., *Anal. Chem.* **1999,** *71*, 4376-4384.

22. Atcherley, C. W.; Vreeland, R. F.; Monroe, E. B.; Sanchez-Gomez, E.; Heien, M. L., *Anal. Chem.* **2013,** *85*, 7654-7658.

23. Farnsworth, P. B.; Smith, B. W.; Omenetto, N., *Spectrochim. Acta B* **1990,** *45*, 1151-1166.

24. Chen, S.; Lee, M. L., *Anal. Chem.* **2000,** *72*, 816-820.

25. Li, Y.; Tolley, H. D.; Lee, M. L., *J. Chromatogr. A* **2011,** *1218*, 1399-1408.

26. Usher, K. M.; Simmons, C. R.; Dorsey, J. G., *J. Chromatogr. A* **2008,** *1200*, 122-128.

27. Martin, M.; Blu, G.; Eon, C.; Guiochon, G., *J. Chromatogr. A* **1975,** *112*, 399-414.

28. Boring, C. B.; Dasgupta, P. K., *Anal. Chim. Acta* **1997,** *342*, 123-132.

CHAPTER 3 LED-BASED UV ABSORPTION DETECTOR WITH LOW DETECTION LIMITS FOR CAPILLARY LIQUID CHROMATOGRAPHY*

3.1 Introduction

Standard ultraviolet (UV) light sources, such as the mercury lamp, suffer from short lifespan, long warm-up time [1, 2] and unstable light output. New light sources have been proposed that are more stable and produce less noise compared to standard UV light sources. Among these, light-emitting diodes (LEDs) have gained interest due to their long life, high stability, bright output and low power requirement [3]. Additionally, they are small in size and more compact compared to standard light sources [4]. Considering the nearly monochromatic behavior of LEDs, a monochromator is not required [5]. An LED-based detector can be fabricated without using expensive optical lenses. All of these factors make LED-based UV-absorption detectors attractive for small, inexpensive instrumentation.

Since LEDs were introduced, several papers have been reported on the use of LED-based detectors for different applications [6]. These have been comprehensively reviewed [4, 7-10]. Commercially available deep UV LEDs (<300 nm) have become applicable for photometric detection [6]. For liquid chromatography (LC), the deep UV range is desirable since most compounds analyzed by LC exhibit absorption in that range [8]. A deep UV LED (255 nm) detector was first reported for LC in 2008 by Schmid *et al.* [6]. A single beam arrangement was used, in which light from the flat window LED was directly focused onto a flow-through cell (1 cm path-length, 8 μL volume) and detection was achieved using a photodiode. Hence, a simple detector design without optics was reported. However, the detector suffered from high noise,

*This chapter was largely reproduced from: Sharma, S.; Tolley, H. D.; Farnsworth, P. B.; Lee, M. L. *Anal. Chem.* **2015**, *87*, 1381-1386.

high detection limits and limited linearity. Although it was mentioned that emission bands at higher wavelengths than specified for the LED were eliminated by the use of special UV-photodiodes, the actual stray light level and subsequent improvement were not reported. The paper, however, mentioned an important characteristic of silicon photodiodes in that they are more sensitive at higher wavelengths than the deep UV, which is evident from a photodiode sensitivity plot. Therefore, any light emission from an LED at wavelengths higher than the deep UV will lead to significant stray light in the system, which should be minimized.

A 255 nm LED for on-column detection in capillary electrophoresis (CE) was reported by Krcmova *et al*. [5]. A hemispherical lens LED was used as a light source with a photomultiplier tube for on-capillary detection. The set-up suffered from a high level of stray light, which compromised the linear range and detection limits of the system. Bomastyk *et al.* reported referenced 255 nm and 280 nm LEDs in absorption detectors with a commercial flow-through cell assembly (1 cm path-length, 8 µL volume) for end-column detection. The detector gave comparable performance to a commercial diode array detector (DAD) [11]. Bui *et al.* reported a dual-beam deep UV LED-based absorption detector for narrow columns [12]. A ball lens window was used with the LED, which made more sense for capillary detection since it provided a narrow beam spot compared to a hemispherical lens. The design included a slit (100 µm), special UV photodiodes to reduce the stray light in the system, a low-pass filter and a constant current source. On-column detection was accomplished by connecting a fused silica capillary (250 µm i.d.) at the end of a narrow-bore column (1 mm i.d.). The detection limits were in the µM range.

A multi-wavelength (250 to 355 nm) deep UV LED detector was recently published by Kraiczek *et al.* for end-column detection [13]. The detector performance was reported to be

comparable to commercial detectors in the single wavelength mode, but worse in the multi-wavelength mode. Hauser *et al.* pioneered the multi-wavelength detection mode using visible LEDs [14].

Deep UV LED-based absorption detectors have shown great potential for miniaturization for field analysis. Further optimization of the detector design and reduction in the noise level can lead to better detection limits for small diameter columns. Since capillary columns have gained popularity in LC work, a detector is needed that can fulfill the detection requirements for such columns. The use of capillary columns puts stringent requirements on the detector. Since capillary columns allow only limited sample loading, and analytes are often present in trace concentrations in samples, the detector should allow highly sensitive detection with minimal dispersion. Preconcentration and/or pretreatment of sample at the sample site may be required. I recently developed an Hg pen-ray lamp-based detector for on-capillary detection (see Chapter 2), and good performance was achieved [15]. On-column detectors are preferable for capillary columns over flow cell based detectors. Commercial flow-cell based detectors introduce considerable dead volume for capillary columns. Also, low-volume flow cells (few nLs) are expensive and suffer from clogging problems due to salt deposition. However, since commercial capillary columns are usually fabricated using polyimide coated capillaries (opaque to UV light), a flow cell attached to the end of the column is typically used.

On-column detection when using capillary columns requires very accurate and narrow focusing of the light beam down to the internal diameter of the capillary. To eliminate stray light, slits equal to or less than the capillary internal diameter are commonly used. However, the use of a slit in front of the capillary also reduces the light throughput. A decrease in light intensity can decrease the S/N ratio of the detector [16]. Hence, trade-offs are required in choosing the

optimum slit widths. On-column detection is preferred for capillary columns, since narrow peak widths are obtained by eliminating extra-column band dispersion, and peak resolution is maintained. The short-term noise in the detector determines the detection limits and is generally reduced by integration, averaging, low-pass RC filters, etc. The LED output wavelength changes with changes in drive current and junction temperature. Therefore, LEDs should be driven by a constant current supply, and heating of the set-up should be avoided. The quasi-monochromaticity of the LED source contributes to stray light in the system, leading to detector non-linearity [17]. Provided the detection system is protected from any surrounding light, this effect can be effectively minimized by employing a filter in the system.

In this chapter, I constructed and evaluated a hand-portable 260 nm LED based UV absorption detector specifically for capillary LC on-column detection. The detector is very small, light-weight and has very low power consumption. The detector was integrated with a small nano-flow LC pumping system described earlier in Chapter 2.

3.2 Experimental section

3.2.1 Chemicals and reagents

All solvents and chemicals were HPLC or analytical reagent grade, and were used without filtration. Acetonitrile (ACN) was purchased from Fisher Scientific (Pittsburgh, PA, USA). Water, methanol, uracil, sodium anthraquinone-2-sulfonate (SAS), adenosine-5'-monophosphate (AMP), DL-tryptophan (DLT), 3-(trimethoxysilyl) propyl methacrylate (TPM, 98%), 2,2-dimethoxy-2-phenylacetophenone (DMPA, 99%), poly(ethylene glycol) diacrylate (PEGDA, $M_n \sim 700$), phenol, resorcinol, catechol and pyrogallol were purchased from Sigma-Aldrich (St. Louis, MO, USA). Dodecanol and decanol were purchased from Acros Organics

(NJ, USA). Decane was purchased from Spectrum Chemical (New Burnswick, NJ, USA). Tergitol 15-S-20 was purchased from Dow Chemical (Midland, MI, USA).

3.2.2 Instrumentation

A commercially available 260 nm deep UV LED with a ball lens (UVTOP255-BL-TO39) from Roithner Lasertechnik (Vienna, Austria) was used as a light source. The LED was mounted on a holder from Thorlabs (Newton, NJ, USA). The LED holder was threaded into a black lens tube (Thorlabs) and held tight with the help of retaining rings. A fused silica ball lens of 3 mm diameter from Edmund Optics (Barrington, NJ, USA) was mounted on a 3 mm ball lens disk from CVI Melles Griot (Rochester, NY, USA) and was placed at the LED focal point. The ball lens disk was centered on a home-made mount, which was threaded into the black lens tube containing the light source and the filter. A 260 nm bandpass filter (25 mm × 3.5 mm) with a FWHM of 20 nm from Semrock (Rochester, NY, USA) was positioned in between the LED and the ball lens in the black threaded tube. A silicon photodiode (S1226 - 5BQ) from Hamamatsu Photonics (Hamamatsu, Japan) was used as the detector. It was positioned on a diode holder (Thorlabs) with external threads. A black cap was built to thread into the diode holder. This cap had a V-shaped groove to hold the capillary in the center, a central hole to allow light passage, and grooves on opposite sides of the hole to hold the slits in place. A pair of razor blades was used to fabricate adjustable slits. The slits were placed on the opposite sides of the central hole in the cap covering the outer diameter of the capillary longitudinally. An operational amplifier acquired the current from the photodiode and converted it into voltage values. An analog-to-digital converter (USB 6009, 14 bit, 48 KS/s) from National Instruments Corporation (Austin, TX, USA) and a self-written LabView program was used to record the voltage output with a computer. All data were acquired at a 10 Hz data rate. The LED and silicon photodiode required

6 V and 12 V DC power, respectively, for operation. All electronics used in this work were home-built. The detector required 0.14 A current, and could run for approximately 70 h using a 10 A-h 12 V DC battery. However, in this work, regular line power was used with an AC to DC adapter.

The LED detector was tested with a nano-flow pumping system reported earlier [15]. The integrated stop-flow injector with an injection volume of 60 nL was used in these experiments, unless otherwise specified. A 150 μm i.d. x 365 μm o.d. Teflon-coated capillary was used in all experiments, unless otherwise specified. The absorbance values, where reported, were calculated by taking the $\log_{10}$ of the inverse of the transmittance values. The transmittance was calculated by dividing the sample signal by the reference signal obtained by recording the baseline.

3.2.3 Noise and stray light measurements

Detector noise was determined over 1-min measurements of baseline data. A hollow fused silica capillary was connected to the nano-flow pumping system and filled with water. The baseline was then recorded for approximately 1 min, and the peak-to-peak absorbance was calculated. This gave the peak-to-peak (p-p) noise. Short term noise (rms) was calculated as the standard deviation of the recorded baseline. For dark noise measurements, the LED was turned off and the dark noise was measured as the standard deviation in the baseline. To determine digitizer noise, the positive and negative terminals of the A/D converter were shorted. Detector drift was determined by flowing water through the capillary at 300 nL/min and recording the baseline for 1 h, followed by measuring the slope of the baseline. Software averaging (Chapter 2) was performed to reduce the noise level. Using a 150 μm i.d. capillary and 5.35 pmol injections of uracil in solution, the S/N ratio was determined at different averaging rates, and the best averaging rate was used for further work.

The effect of RC filters (time constants of 0.5 s and 1 s) on short-term noise was also studied with and without performing any averaging. A black ink-filled capillary was used for stray light assessment in the system. The stray light level was measured by dividing the voltage signal obtained for black-ink conditions by the voltage signal obtained with a water-filled capillary, multiplied by 100.

3.2.4 Detector linearity and detection limits

Solutions of different concentrations of sodium anthraquinone-2-sulfonate, adenosine-5-monophosphate, DL-tryptophan and phenol were made in HPLC grade water. Solutions were made to flow, under nitrogen pressure, through a capillary inserted into the detector. Baseline data were recorded before and after each concentration experiment by flowing water through the capillary. Baseline corrected maximum absorbance values (AU) were plotted against molar concentrations (M) to determine the linearity of the detector. Detection limits for flow-through experiments were reported as 3 times the standard deviation in the baseline. Log-log plots were used to determine the sensitivity of the detector. Calibration data for phenol were also obtained by making injections on a PEGDA monolithic column, and baseline corrected peak areas were plotted against concentrations. Elution conditions were as described in the next paragraph. Detection limits were determined as 3 times the standard deviation in the baseline area obtained from blank injections (n = 4) and calculated within the analyte peak zone.

Isocratic separations of phenols (i.e., phenol, catechol, resorcinol and pyrogallol) were performed using a PEGDA monolithic column (16.5 cm × 150 μm i.d.) using the integrated system. The capillary pretreatment procedure [15] and monolith fabrication were discussed in detail previously [18]. In short, the pretreated capillary was filled with monomer mixture and subjected to UV-initiated polymerization for 5 min. After polymerization, the monolithic column

was washed with methanol followed by water for at least 6 h to remove unreacted compounds. The monomer mixture composition was: DMPA (0.002 g), PEGDA 700 (0.2 g), dodecanol (0.15 g), decanol (0.15 g), decane (0.2 g) and tergitol 15-S-20 (0.3 g). The phenolic compounds were dissolved in HPLC water and the mobile phase was 80/20 % (v/v) acetonitrile/water mixture. Separations were performed at 350 nL/min.

3.2.5 Safety considerations

Phenols are toxic compounds, and proper personal protective equipment should be used when working with them. The UV output of the LED is potentially damaging to eyes, and protective eye wear should be used when the light source is not enclosed.

3.3 Results and discussion

3.3.1 Detector design

The deep UV LED-based absorption detector is much smaller than my earlier described Hg pen-ray lamp-based detector (Chpater 2). For on-capillary column detection, absorbance values are small, so noise reduction is the key to obtaining good detection limits. A bright light source increases the photocurrents used to calculate absorbances without proportional increase in noise. A single wavelength (260 nm) detector was fabricated instead of a multi-wavelength detector in order to reduce the cost and size of the detection system (Figure 3.1 and 3.2). Although the LED had an integrated fused silica ball lens (6.35 mm diameter), which focused the light beam down to a 1.5-2.0 mm spot at the focal point (15-20 mm), this was still too broad for the capillary dimensions (0.075 to 0.20 mm i.d.). Therefore, another fused silica ball lens (3 mm diameter) was placed at the focal point of the LED to obtain much better focusing of the light. A double ball lens arrangement was previously incorporated in a 280 nm LED-based fluorescence detector for CE [19].

Figure 3.1 Photograph of the deep-UV LED detector.

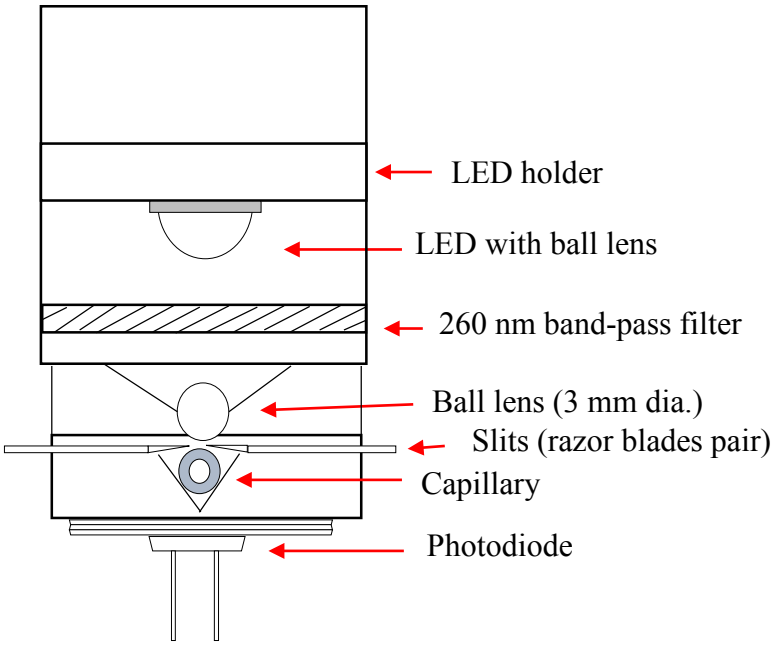

Figure 3.2 Schematic of the deep-UV LED detector.

The LED was claimed to emit light with a bandwidth of ± 5 nm; however, with a spectrometer, it was found that the LED emitted light at higher wavelengths as well. This contributed significantly to the stray light of the system. Therefore, a 260 nm bandpass filter with a FWHM of 20 nm was employed. The overlaid spectra in Figure 3.3 show the light output from the LED with and without the filter, confirming that the filter successfully eliminated the light from higher wavelengths. The LED position was optimized to obtain the best focus at the center of the capillary.

Due to the reported inherent stability of the LED, a reference cell was not included in the design. This eliminated the need for a beam splitter, which decreases the light throughput through the capillary. Since no other optical lenses except the ball lenses were used, complex alignment of optical elements and transmission losses from multiple surfaces were avoided.

3.3.2 Detector noise

The detector short-term rms noise was found to be 8 mV without the use of signal averaging and a low pass filter. The dark rms noise without averaging was calculated to be 7 mV. Software averaging reduced the dark rms noise level to 74 μV as shown in Figure 3.4. The dark voltage values were the same in lighted and dark rooms confirming that the capillary did not act as a light guide. Digitizer noise can contribute significantly to the minimum noise obtainable with a detector. The digitizer rms and p-p noise were found to be 2.4 mV and 7.7 mV, respectively. The effect of software averaging on the digitizer rms noise was studied as shown in Figure 3.4, and the minimum rms and p-p noise levels obtained were 15 μV and 95 μV, respectively. As can be seen from the data, dark current noise, which includes noise from the photodiode and amplifier, and digitizer noise both contributed to the total baseline noise, and both were effectively reduced using software averaging.

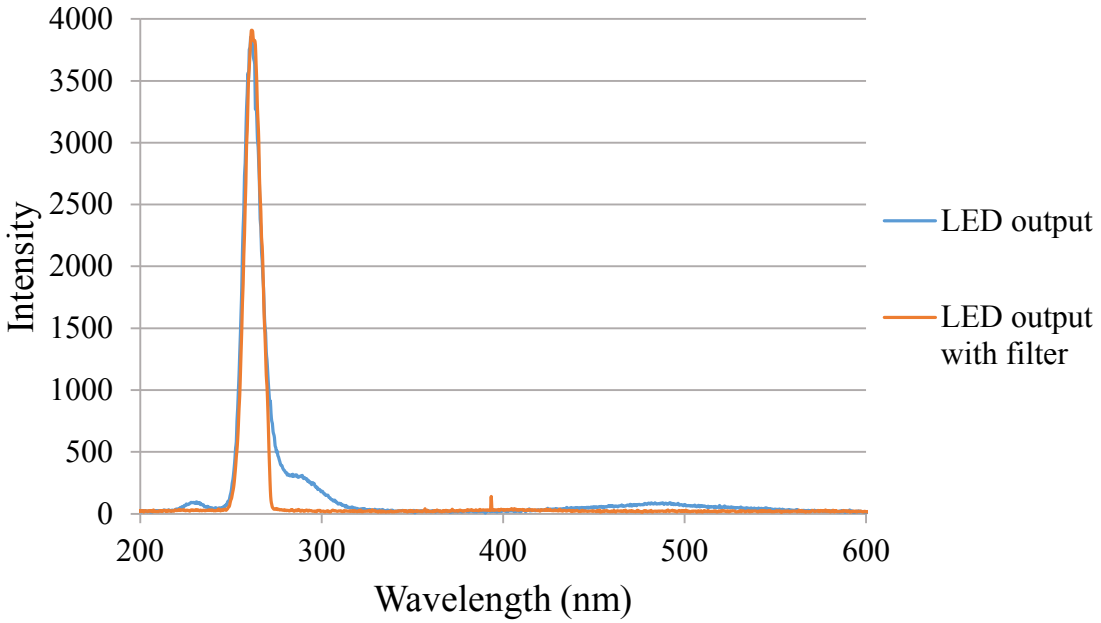

Figure 3.3 Overlaid spectra of light output with (orange) and without (blue) filter.

To further reduce the total noise level, the two low-pass filters (time constant = 0.5 s and 1 s) were applied to the input of the A/D converter. The unaveraged rms noise level dropped to 2.4 mV and 2.3 mV, respectively.

The effect of software averaging on the S/N ratio was also studied and, while it was found that the effect of averaging on the signal intensity for peak widths in my chromatogram was negligible, the rms noise level was markedly reduced to a level of 0.18 mV in the voltage corresponding to I_o (5.7 μAU) without the use of a filter. With a 0.5 s filter and 4200 data points per 0.1 s averaging, the rms noise further dropped to 0.14 mV (4.4 μAU). Thus, the LED detector rms noise was an order of magnitude lower ($\sim 10^{-6}$ AU) than my previous detector and other deep UV LED detectors ($\sim 10^{-5}$ AU). The detector drift was found to be very low (10^{-5} AU per h), which is negligible over a peak width and presents no problems for the duration of a typical chromatogram. As can be seen in Figure 3.4, the rms noise level decreased as the number of data points averaged per 0.1 s was increased from 100 to 2400; however, further decrease in the noise level after 2400 data points averaging was not significant. The S/N ratio for uracil increased from 14 (without averaging) to 408 (with 4200 data points averaging) as shown in Figure 3.5. Due to the reported and observed low drift and inherent light stability of the LED, a reference cell was not included, simplifying the detector design without compromising its performance. The photodiode signal through the capillary (an average of 70 μA) was three orders of magnitude higher than previous work (nA range) [13].

3.3.3 Stray light

Stray light causes negative deviations from true absorbance values. When the slit width was adjusted to be equal to the internal diameter of the capillary (i.e., 150 μm), the stray light level was measured to be 17 %. By visual inspection, it was found that a significant level of

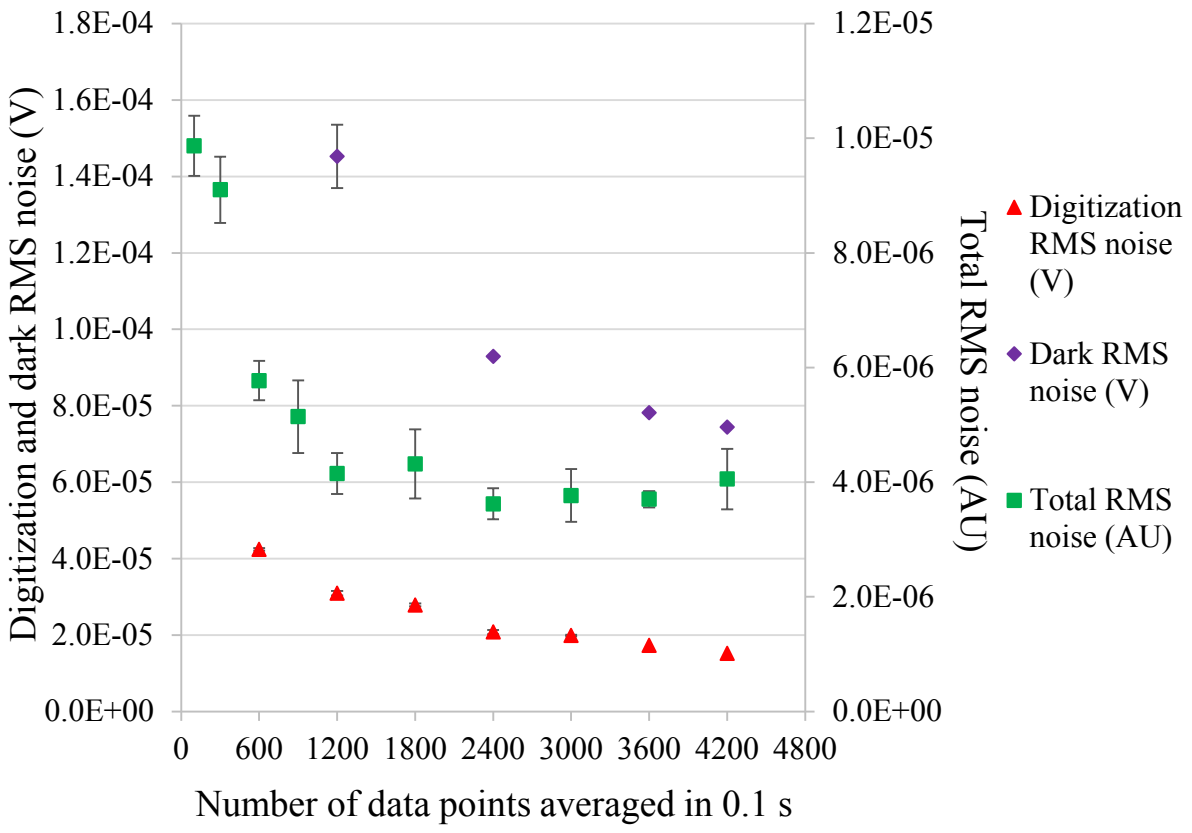

Figure 3.4 Effect of software averaging on digitization and dark rms noise without filter and on the total rms noise with 0.5 s filter.

A.

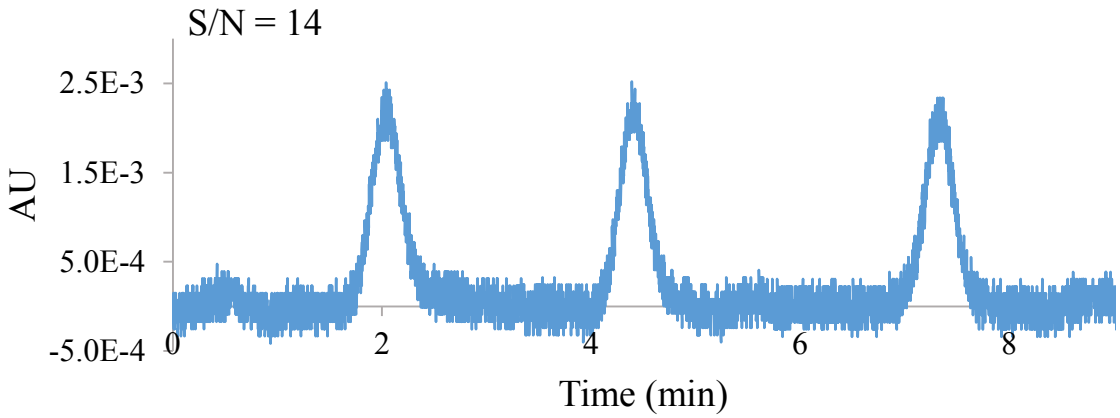

B.

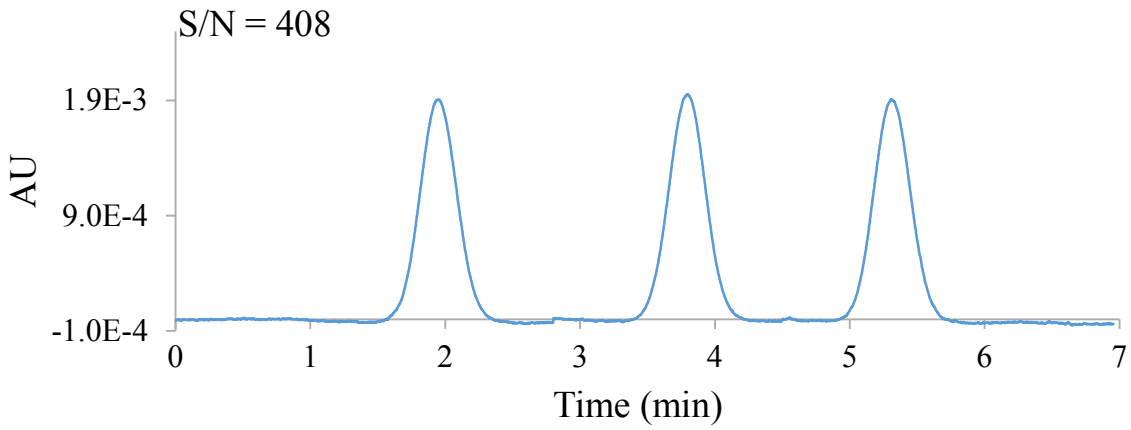

Figure 3.5 S/N ratio enhancement. Signals were obtained (A) without averaging and (B) with 4200 data points per 0.1 s averaging.

light reached the photodiode through the curved capillary wall. Therefore, the slit width was reduced to 100 μm, which reduced the stray light level markedly to 3.6%. A decrease in light intensity was compensated for by increasing the driving current on the LED (13.3 mA). Therefore, the output voltage signal intensity was not compromised at all by a reduction in the slit width. It is important to mention here that the LED was operated at only half of its maximum operating current. The maximum absorbance of the detector with the capillary was calculated to be 1.4 AU, which is higher than the value obtained with the Hg pen-ray lamp detector (0.94 AU) [16].

3.3.4 Linearity

The linearity of a UV absorption detector can be compromised by improper focusing of the light beam on the internal diameter of the capillary. Limits of detection depend on detector short-term noise and the test analyte molar absorptivity [20]. Selection of test analytes was based on molar absorptivities and relevant previous LED detector work. The detector gave a linear response up to the highest concentration tested, confirming that stray light was low in the system. The linear dynamic range was three orders of magnitude for all of the test analytes. The limit of detection at a S/N ratio of 3 was found experimentally to be 25 nM (7.6 ppb) or 1.5 fmol for SAS. This detection limit is 5 times lower than my previous pen-ray Hg lamp-based detector [16]. Considering that anthraquinone and anthracene exhibit similar molar absorptivities, this detection limit is also 200 times lower than the non-referenced single-wavelength flow cell-based detection limit reported earlier for the same pathlength [14]. The detection limits for AMP (88 nM or 31 ppb) would be 230 times lower for the same capillary dimensions (75 μm i.d.) than a non-referenced LED detector reported earlier [5]. For DLT, the detection limit at an S/N ratio of 3 was found to be 300 nM (60 ppb) or 18 fmol. This detection limit would be 60 times lower

than the referenced detector reported earlier for the same capillary dimensions (250 μm i.d.) [13]. Thus, the variations in detection limits for the various compounds is consistent with the variations in molar absorptivities at 260 nm. The detection limits for the detector are remarkable considering the fact that detection was performed on the capillary scale. The calibration data for SAS, AMP and DLT are listed in Table 3.1. The RSDs in peak areas (n = 3) for the three compounds ranged from 0.4-2.6%. These areas were calculated by injecting different concentrations of each compound three times into a hollow capillary using water as carrier fluid at 600 nL/min.

Since the detector is specifically designed for on-column detection, the detector performance was tested under LC conditions using phenol and compared with the flow-through experiments (Table 3.2). The detector linearity was excellent under both conditions, and the detection limits were found to be similar. Hence, the detector performance was not compromised, when used under actual LC conditions.

Application of the system was demonstrated using phenolic compounds as shown in Figure 3.6. Good resolution was obtained for all analytes in the isocratic mode. Baseline stability under LC experiments was remarkable, confirming the low drift exhibited by this detector. The retention times in min and peak widths in s (t_R /$w_{b1/2}$) of the compounds were found to be: phenol (11.8/10.4), catechol (13.0/13.4), resorcinol (14.0/12.8)and pyrogallol (14.9/16.6). The reproducibility of peak retention times ranged from 0.1-0.2% (n = 4). The column efficiencies (N/m) and minimum plate heights (μm) for the retained compounds were: phenol (157,000/6.4), catechol (113,000/8.8), resorcinol (145,000/6.9) and pyrogallol (97,000/10.4).

Table 3.1 Detector linearity data.

Analytes	Concentration range	Peak area (AU) Regression equation	R^2	Sensitivity[d]	LOD
SAS	24.6 nM – 50.4 µM	$y = 498.09x + 9 \times 10^{-6}$	>0.99[a]	0.99	25 nM
AMP	87.9 nM – 22.5 µM	$y = 185.44x + 5 \times 10^{-6}$	>0.99[b]	1.01	88 nM
DLT	299 nM – 0.61 mM	$y = 54.744x + 5 \times 10^{-6}$	>0.99[c]	0.99	300 nM

[a] For n = 12 ; [b] For n = 9; [c] For n = 12; [d] Sensitivity was obtained using log (AU) vs log (M) plots.

Table 3.2 Phenol linearity data.

Method	Concentration range	Peak area (AU) Regression equation	R^2	LOD
Flow-through	1.95 µM - 1.33 mM	$y = 1.43 \times 10^{1} x + 2 \times 10^{-5}$	>0.99	1.95 µM
On-column	1.70 µM - 1.33 mM	$y = 3.12 \times 10^{3} x + 1.2 \times 10^{-2}$	>0.99	1.96 µM

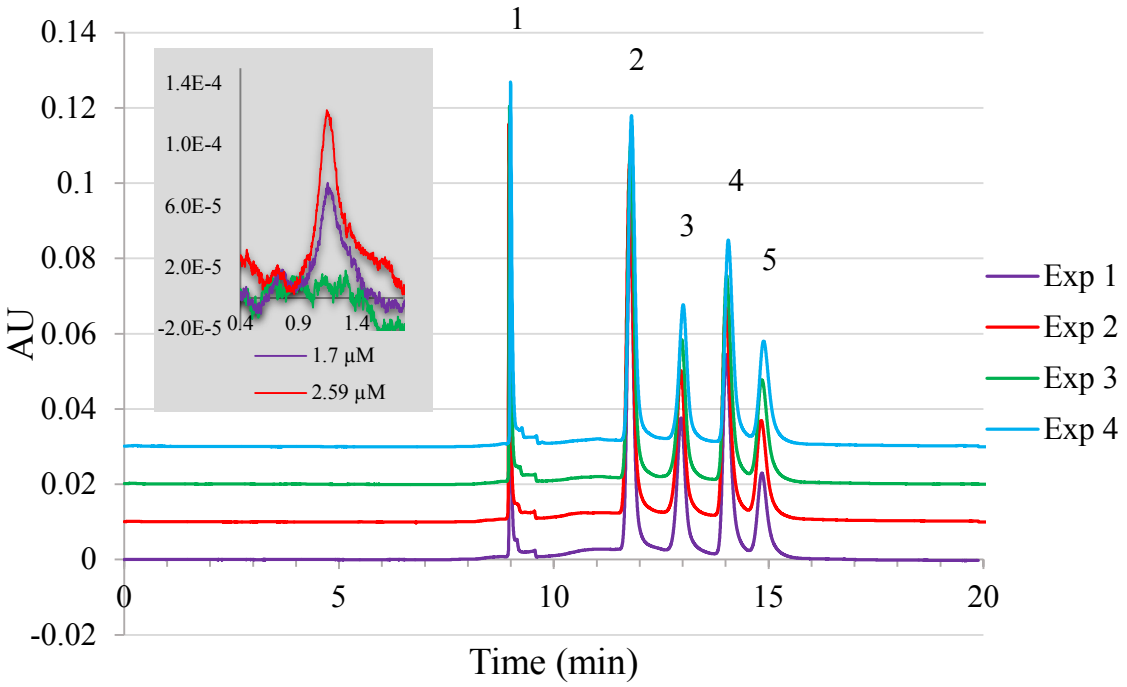

Figure 3.6 Separations using integrated nano-flow pumping system and LED-based detector (260 nm). Peak identifications: (1) Impurity in sample (2) phenol, (3) catechol, (4) resorcinol, and (5) pyrogallol. Baselines are offset for clarity. Small picture shows lower concentration phenol peaks.

3.4 Conclusions

A highly sensitive on-column detector was fabricated using a 260 nm deep UV LED that can detect in the ppb range. The noise level of the detector was remarkably reduced by the use of software averaging and a low pass filter, i.e., 3.4-4.4 μAU, which is among the lowest noise levels ever attained with absorption detectors designed for capillary work. The markedly low detection limits can be attributed to good light focusing, low stray light, and very low noise in the system. The overall performance of the detector is a significant improvement over published results from other deep-UV LED detectors. The detector was successfully integrated with an isocratic nano-flow pumping system for performing phenol separations.

3.5 References

1. Havaši, P.; Kaniansky, D. *J. Chromatogr. A* **1985**, *325*, 137-149.
2. Jones, K.; Malcolme-Lawes, D. J. *J. Chromatogr. A* **1988**, *441*, 387-393.
3. Dasgupta, P. K.; Bellamy, H.S.; Liu, H.; Lopez, J. L.; Loree, E. L.; Morris, K.; Petersen, K.; Mir, K. A. *Talanta* **1993**, *40*, 53-74.
4. Xiao, D.; Zhao, S.; Yuan, H.; Yang, X. *Electrophoresis* **2007**, *28*, 233-242.
5. Krcmova, L.; Stjernlof, A.; Mehlen, S.; Hauser, P. C.; Abele, S.; Paull, B.; Macka, M. *Analyst* **2009**, *134*, 2394-2396.
6. Schmid, S.; Macka, M.; Hauser, P. C. *Analyst* **2008**, *133*, 465-469.
7. Dasgupta, P. K.; Eom, I. Y.; Morris, K. J.; Li, J. *Anal. Chim. Acta* **2003**, *500,* 337-364.
8. Xiao, D.; Yan, L.; Yuan, H.; Zhao, S.; Yang, X.; Choi, M. F. *Electrophoresis* **2009**, *30*, 189-202.
9. Macka, M.; Piasecki, T; Dasgupta, P. K. *Annu. Rev. Anal. Chem.* **2014**, *7*, 183-207.
10. Bui, D. A.; Hauser, P. C. *Anal. Chim. Acta* **2015**, *853*, 46-58.

11. Bomastyk, B.; Petrovic, I.; Hauser, P. C. *J. Chromatogr. A* **2011**, *1218*, 3750-3756.

12. Bui, D. A.; Bomastyk, B.; Hauser, P. C. *J. Sep. Sci.* **2013**, *36*, 3152-3157.

13. Kraiczek, K. G.; Bonjour, R.; Salvade, Y.; Zengerle, R. *Anal. Chem.* **2014**, *86*, 1146-1152.

14. Hauser, P. C.; Rupasinghe, T. W. T.; Cates, N. E. *Talanta* **1995**, *42*, 605-612.

15. Sharma, S.; Plistil, A.; Simpson, R. S.; Liu, K.; Farnsworth, P. B.; Stearns, S. D.; Lee, M. L. *J. Chromatogr. A* **2014**, *1327*, 80-89.

16. Liu, H.; Dasgupta, P. K.; Zheng, H. J. *Talanta* **1993**, *40*, 1331-1338.

17. Macka, M.; Andersson, P.; Haddad, P. R. *Electrophoresis* **1996**, *17*, 1898-1905.

18. Aggarwal, P.; Lawson, J. S.; Tolley, H. D.; Lee, M. L. *J. Chromatogr. A* **2014**, *1364,* 96-106.

19. Sluszny, C.; He, Y.; Yeung, E. S. *Electrophoresis* **2005**, *26*, 4197-4203.

20. King, M.; Paull, B.; Haddad, P. R.; Macka, M. *Analyst* **2002**, *127*, 1564-1567.

CHAPTER 4 HAND-PORTABLE GRADIENT LIQUID CHROMATOGRAPHY PUMPING SYSTEM*

4.1 Introduction

The gradient LC mode is certainly more powerful than the isocratic mode for separating complex mixtures containing compounds with a range of polarities. Gradient capability is necessary to broaden the application range of a portable system. There have been few reports on portable gradient LC systems as described in Chapter 1; however, these systems used conventional columns. No capillary-based portable gradient system has been reported to date.

In this chapter, a small, potentially portable gradient nanoflow pumping system was developed for the first time and evaluated using an on-column LED-based UV detector reported in Chapter 3 [1]. The system was designed for capillary column use only. Gradient performance and separations are demonstrated using this new integrated nanoflow LC-UV system.

4.2 Experimental section

4.2.1 Chemicals and reagents

Water, methanol, 3-(trimethoxysilyl) propyl methacrylate (TPM, 98%), 2,2-dimethoxy-2-phenylacetophenone (DMPA, 99%), poly(ethylene glycol) diacrylate (PEGDA, $M_n \sim 700$), phenol (P), 2-nitrophenol (2-NP), 4-nitrophenol (4-NP), 2,4-dichlorophenol (2,4-DCP), 2,4-dinitrophenol (2,4-DNP), propyl paraben, isoproturon, monouron, phosphoric acid and diuron were purchased from Sigma-Aldrich (St. Louis, MO, USA). Dodecanol and decanol were purchased from Acros Organics (Morris Plains, NJ, USA). Decane was purchased from Spectrum Chemical (New Burnswick, NJ, USA). Tergitol 15-S-20 was purchased from Dow

*This chapter was largely reproduced from: Sharma, S.; Plistil, A.; Barnett, H. E.; Tolley, H. D.; Farnsworth, P. B.; Stearns, S. D.; Lee, M. L. *Anal. Chem.* **2015**, *87*, 10457-10461.

Chemical (Midland, MI, USA). Acetonitrile was purchased from Fisher Scientific (Pittsburg, PA, USA). All solvents and chemicals were HPLC or analytical grade.

4.2.2 Instrumentation

A new battery-operable capillary gradient nano-flow pumping system (31 × 18 × 14 cm) was constructed and evaluated in this study (Figures 4.1 and 4.2). The system weighs only 4 kg (9 lbs) and can hold up to 55 MPa (8000 psi) pressure. Each pump volume capacity is 32.5 μL. The stop-flow injector is a V-shaped groove in the rotor that injects a fixed volume of 60 nL; however, the groove can be engineered to deliver a smaller sample volume. All connections were made using zero dead-volume 360 μm fittings especially designed for capillary columns. The system is fully software controlled. The gradient system was fabricated from two electrically-driven needle piston-based nanoflow syringe pumps. The diameter of each piston is 1.5 mm, and they are driven with a resolution of 0.02 nL/microstep or 3 nL/step. The system contains two micro stepper motors (51,200 steps/revolution or 2,048,000 steps/inch) that control the movement of the needle pistons, a static mixing tee connected to a serpentine tube for solvent mixing, a high-pressure valve and a stop-flow injector. The dimensions of the mixing tube were 12.7 mm long and 0.254 mm internal diameter. No splitting was employed, thus reducing the solvent consumption for each analysis to a few microliters. The non-splitting flow arrangement also reduces sample discrimination, provides high separation reproducibility and minimizes waste generation. This system provides accurate non-splitting flow in nL to μL per min (i.e., 10 nL/min to 90 μL/min) with percent error less than 0.1%. Using a 10 A-h 24 V DC battery (weight ~ 2-3 kg), this system could be operated for up to 8 h. This system can be operated using a 24 V DC battery (power consumption of 40 W). However, in this work, the system was operated using a voltage.

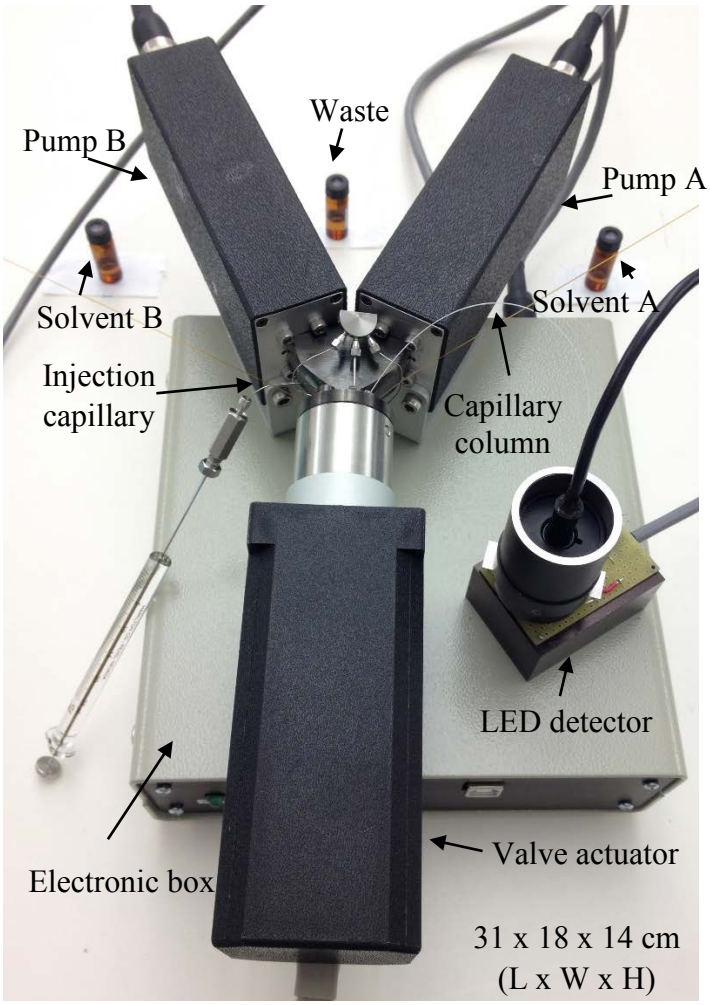

Figure 4.1 Photograph of the integrated gradient nanoflow pumping system with LED detector.

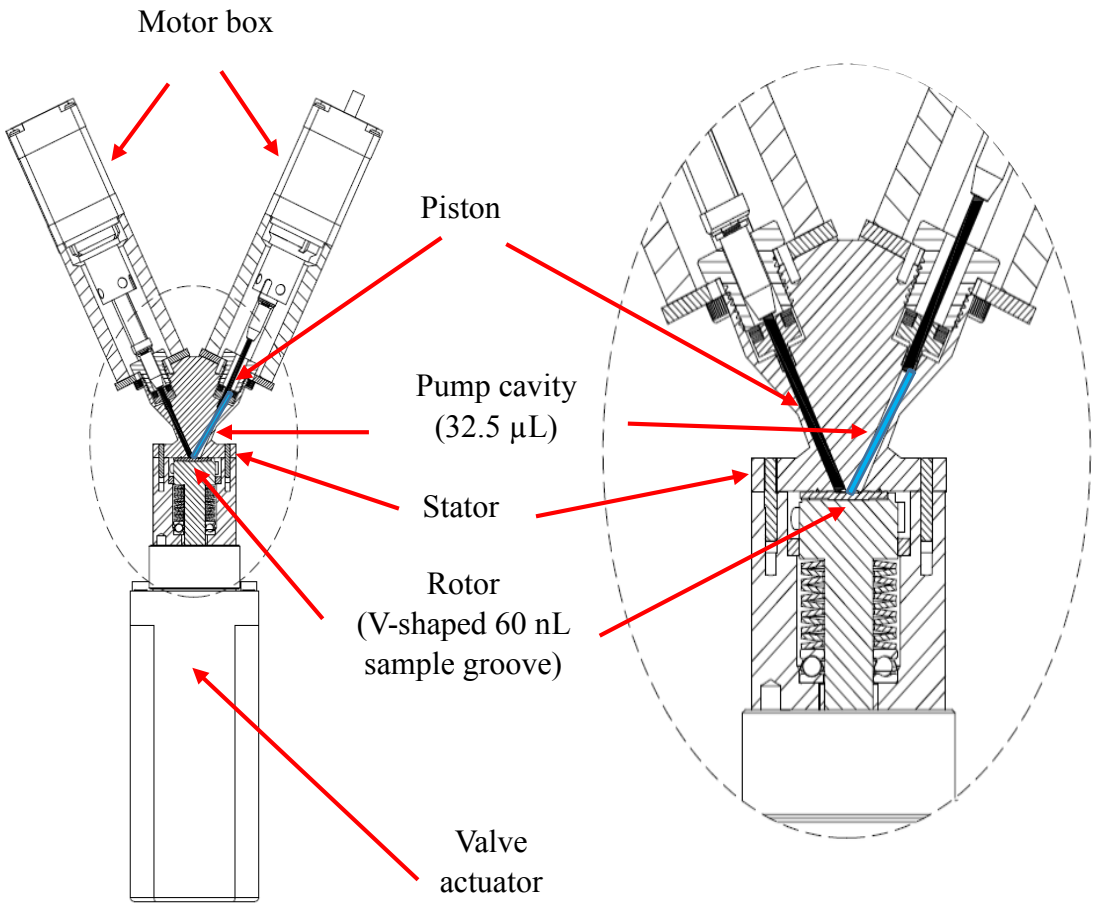

Figure 4.2 Schematic of the gradient nanoflow pumping system.

converter and regular 120 V AC power line. The pumping system was integrated with an on-column deep UV LED (260 nm) absorption detector described in Chapter 3 [1].

4.2.3 Column preparation

A UV-transparent fused silica capillary (150 μm i.d. x 365 μm o.d.) was used for preparing a polyethylene diacrylate (PEGDA) monolithic column. A monolithic column was chosen for this work because of easy in-house fabrication and ability to perform on-column detection. The capillary pretreatment and column fabrication procedures were described in detail elsewhere [2, 3]. Column preparation involves filling the pretreated capillary with a monomer mixture under nitrogen pressure up to a desired length, leaving an empty detection window for on-column detection and sealing both ends with rubber septa. This is followed by UV-initiated polymerization for 5 min and washing of the polymerized column first with methanol and then with water for sufficient time to remove unreacted monomers and porogens. The monomer mixture consisted of DMPA (0.002 g), PEGDA 700 (0.2 g), dodecanol (0.15 g), decanol (0.15 g), decane (0.2 g), and tergitol 15-S-20 (0.3 g).

4.2.4 Determination of dwell volume

To determine the dwell volume of this system, a UV transparent hollow fused silica capillary (150 μm i.d. x 10 cm) was connected to the column port on the pumping system. Pump A and pump B were filled with methanol and propyl paraben (9 μg/mL) in methanol, respectively. The gradient was programmed from 0% to 100% B in 10 min with an isocratic hold at 100% B for several minutes. To calculate the capillary dead volume, multiple injections (n = 4) of uracil were made and the average retention time was multiplied by the flow rate used (800 nL/min). The dwell volume of the system was calculated by subtracting the capillary dead volume from the gradient delay volume.

4.2.5 Gradient step accuracy and separations

First, the system was tested without the use of the separation column. For this, pumps A and B were filled with methanol and 9 µg/mL of propyl paraben in methanol, respectively. A hollow capillary (150 µm i.d. x 10 cm) was connected to the column port. For the step accuracy test, the system was programmed from 0% B to 10% B and then to 100% B. At each percentage, the UV absorption signal was recorded for several minutes. As the proportion of B solvent in the mobile phase increased with time, an increase in absorbance was recorded, with a maximum at 100% B. Absorbance obtained at each step was divided by the absorbance recorded at 100% B, which served as reference. Recordings were performed at different percentages (i.e., 10, 20,…90% B) and, at each step percentage, measurements were repeated at least four times to determine the precision of the results.

Chromatographic performance was evaluated under gradient programming conditions. For this, a mixture of pesticides (monouron, isoproturon and diuron) was separated four times on a PEGDA monolithic column (16.5 cm × 150 µm i.d.) using the same gradient (100% A to 100% B in 10 min, then isocratic elution with 100% B) at 350 nL/min flow rate. Solvent A was water and solvent B was acetonitrile. The retention time reproducibility was calculated for each compound. Five phenols considered to be pollutants were also separated.

4.3 Results and discussion

4.3.1 Pump operation

The gradient nanoflow pumping system has 10 ports (Figure 4.3); each port serves a different function as described in the following: *F* and *D* ports, on both pumps, allow the solvent to flow into and out of the pump, respectively; *S* is the sample injection port; *W* is the waste port; two *C* ports are used to connect the column at both ends to the pump to maintain pressure during

stop-flow injection; *DP* is the detector port which is used for off-column detection, and *M* is the port through which the mixed mobile phase flows into the internal sample loop and then to the column and detector.

The pump can be switched automatically between "load" and "dispense" positions. In the load position, the pumps are automatically filled with mobile phases A and B at a preset rate (90 µL/min) by suction using 15 cm x 150 or 200 µm i.d. SS tubing or polyimide-coated fused silica capillaries. Sample is injected manually, only in the load position, by inserting a 25 µL syringe into a short piece of PEEK tubing connected to a zero dead volume union. The union is connected to the S port using 5 cm x 75 µm i.d. SS tubing. Filling the pumps takes less than a minute. At the same time, the desired gradient is entered into the computer software. When the valve is switched to the dispense position, the sample groove (SG) moves between the M and C ports, and the pumps start delivering solvents at the programmed gradient flow rates to the capillary column. The second column port was not used in this study, since on-column detection was performed. The pump cavities and flow paths could be purged with solvent when desired. The valve could be changed automatically between load and dispense positions, allowing adequate purging. The pumps were filled at the rate of 30 µL/min and, in this study, dispensed at the rate of 60 µL/min during purging. A single gradient run including column re-equilibration consumed less than 32 µL (the total pump capacity was 74 µL); thus, a run was typically finished without having to refill the pumps.

4.3.2 Dwell volume

The dwell volume is the volume of the system from the mixing point to the head of the column. This volume delays gradient delivery to the column head [4]. Different systems have different dwell volumes, depending on the mixer and connecting tubing employed. It is

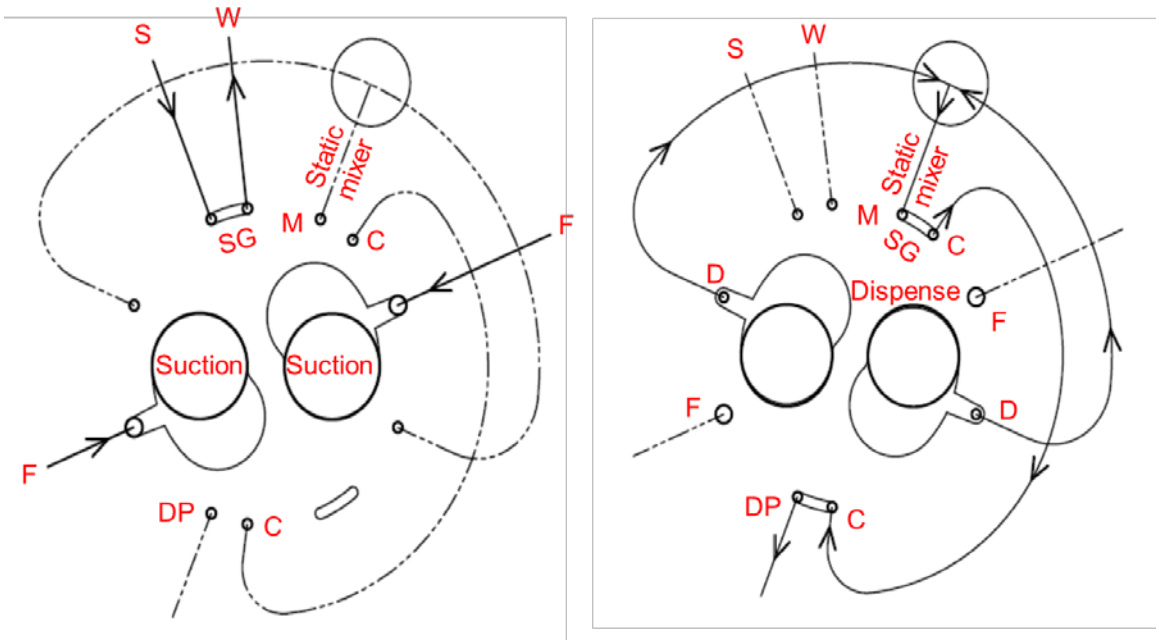

Figure 4.3 Operation schematics of the nanoflow LC system. Solid lines and broken lines represents "in use" and "on stand-by", respectively. Following are the functions of the ports: "F" is for pump filling, "C" is for column connection, "S" is for sample injection, "W" is for waste, "SG" is for the internal sample groove, "M" is for solvent mixing, and "DP" is for connection to an off-column detector.

important to know the dwell volume so that the gradient method can be easily transferred from one instrument to another, provided that all other conditions are the same. Propyl paraben was preferred over commonly used acetone as a gradient tracer because of its low volatility, which increased the reproducibility of the measurements. Methanol was used instead of water to minimize pump cavity contamination with the paraben UV absorber. As the % B was increased with time, a continuous increase in absorbance was traced, reaching a plateau at 100% B.

The point where a baseline change was perceived was chosen as the gradient start point. A zero dwell volume system would lead to immediate start of gradient delivery to the column and, hence, a change in baseline. Unfortunately, there is always a finite dwell volume present in any system. The actual dwell volume was calculated by subtracting the capillary dead volume from the gradient delay volume obtained from the graph. The capillary dead volume was calculated to be 1.75 μL (2.2 min x 0.8 μL/min). The dwell volume of this system was calculated to be 1.30 ± 0.007 μL. This dwell volume created a 4-min delay at the typical flow rate of 350 nL/min employed in this work. This volume can be further reduced by either shortening the mixing tube or using smaller i.d. tubing. This delay volume was much less than the delay volume of a commercial Dionex Ultimate 3000® capillary LC system (3.3 μL) used in our laboratory.

4.3.3 Gradient profile

It would be ideal to have a small portable capillary LC system that could provide chromatographic performance comparable to bench-top instruments. The stepper motor movement and proportioning efficiency control gradient accuracy and precision. The precision in the gradient translates into separation reproducibility. To obtain a reproducible gradient over time, it is necessary to maintain a constant gradient and flow rate. Irreproducible gradients lead to changes in analyte retention times and separation selectivities. Gradient mixer performance is

usually demonstrated by performing a step accuracy test. A set of experimental step errors was plotted against corresponding theoretical step percentage values as shown in Figure 4.4 (A). Deviations from the predicted values were less than 0.74%. A gradient step accuracy of +/- 1% is considered to be acceptable [5]; therefore, the pump performed very well in this test. To determine the precision in day-to-day experiments, experimental RSD values were calculated for the step percentages and plotted against the theoretical step percentages. As can be seen in Figure 4.4 (B), the RSD values (n = 4) were less than 1.2%, which is comparable to commercial instruments. Therefore, the gradient performance of this system was found to be excellent in terms of step accuracy and precision.

Under gradient conditions, peak retention time reproducibility is dependent on the gradient accuracy. As can be seen in Figure 4.5, retention time reproducibility for gradient runs of a pesticide mixture was high. RSD values were calculated to be less than 1.4%. These results verify that the pump is suitable for LC application. Phenols are widely used in the chemical industry and pose potential health hazards. Five phenols (P, 2-NP, 4-NP, 2,4-DCP, 2,4-DNP) were separated using the monolithic PEGDA column (13 cm × 150 μm i.d.) at 350 nL/min using water (A) and acetonitrile (B), each modified with 0.1% phosphoric acid as shown in Figure 4.6. The gradient was programmed from 30% to 75% B in 15 min. Baseline separation was achieved in less than 20 min with good peak shapes. The long delay in peak elution resulted from the dead volume created by the porous structure of the monolithic column.

4.4 Conclusions

Remarkable reduction in the size and power requirement of a gradient syringe pumping system was done without compromising the system performance. This new nanoflow gradient system was capable of reproducible gradient generation for LC applications at low nL/min flow

A.

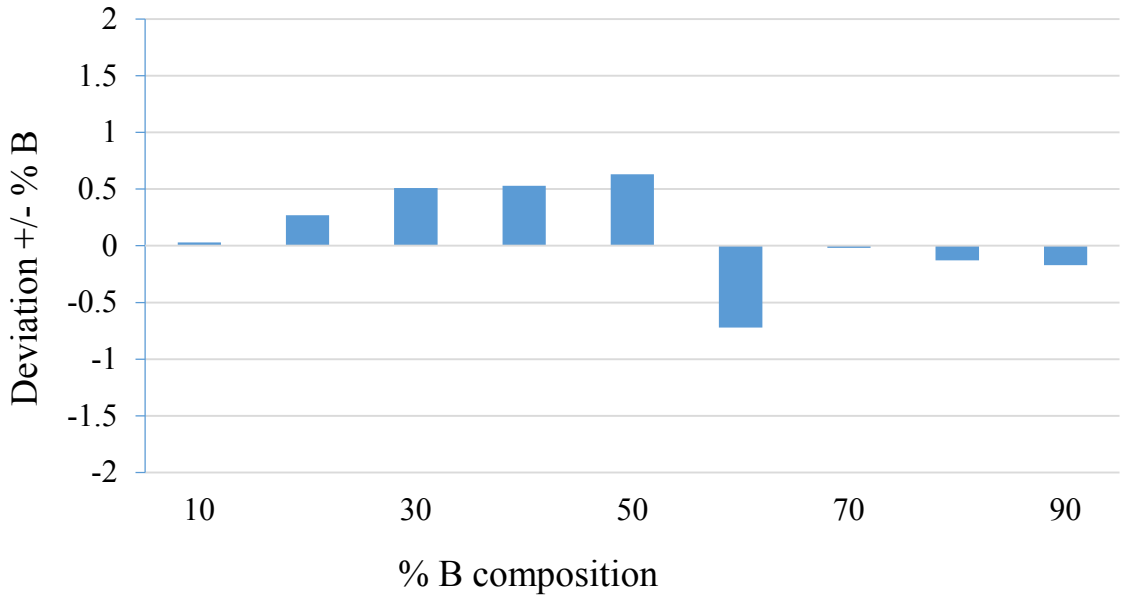

B.

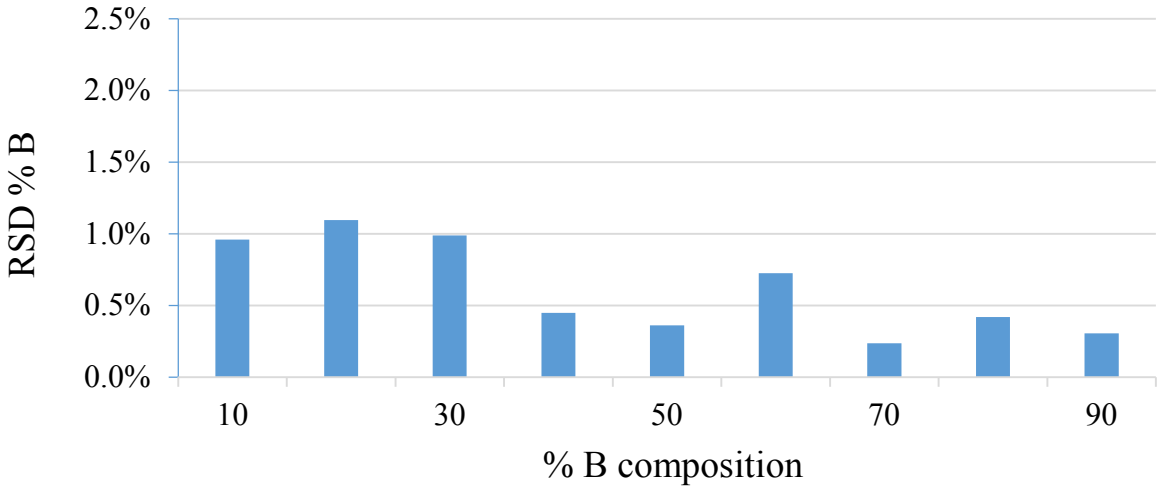

Figure 4.4 (A) Gradient step accuracy (+/- %B) and (B) precision in gradient step accuracy.

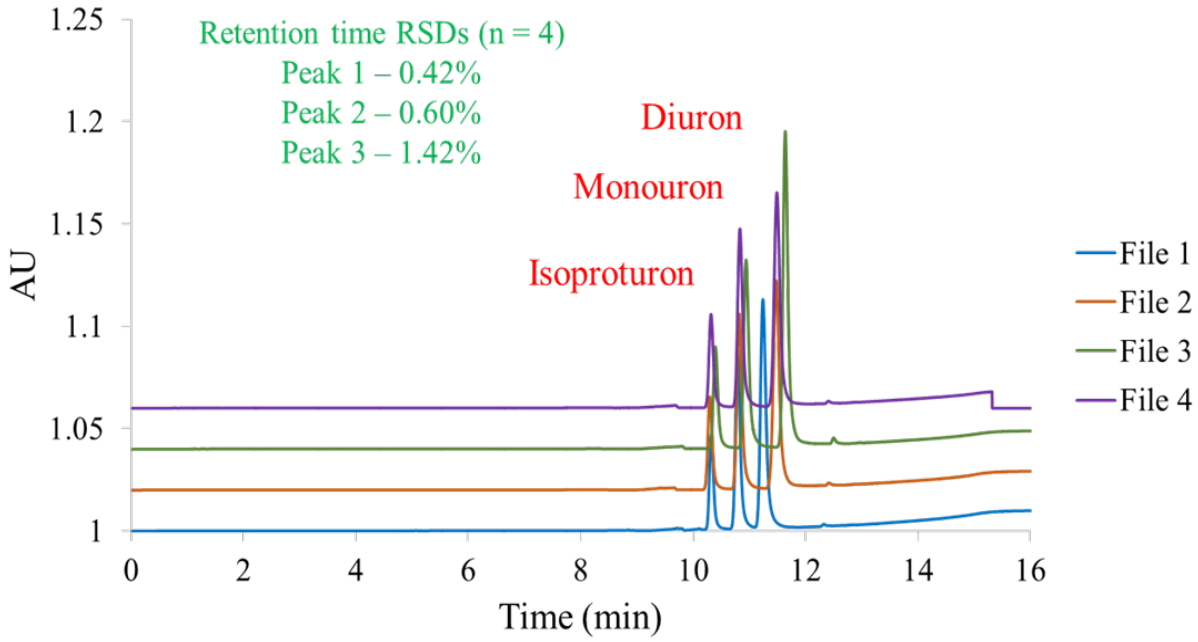

Figure 4.5 Reproducibility in gradient separations of a mixture of pesticides.

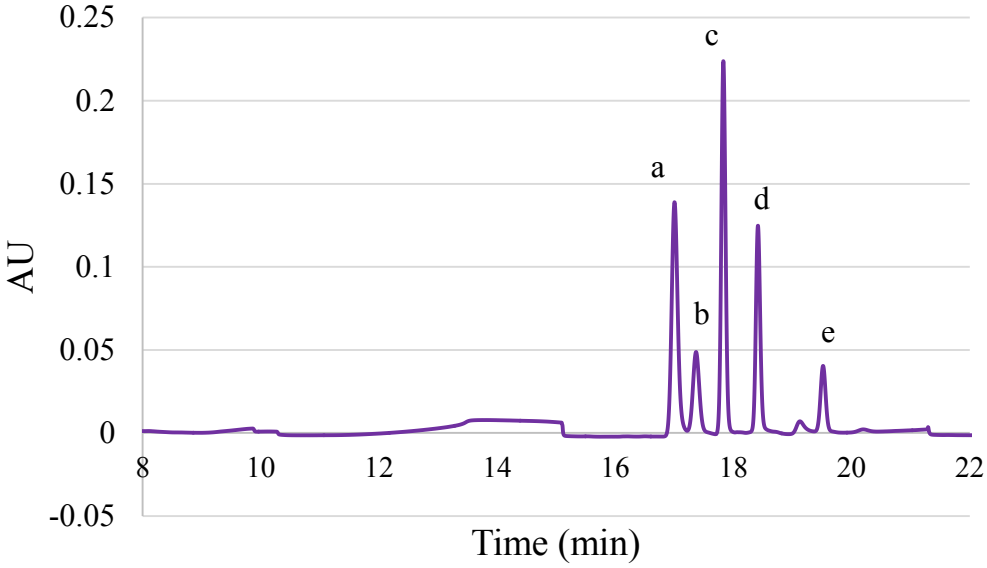

Figure 4.6 Gradient separation of a mixture of phenols. Peak identifications from left to right: (a) phenol, (b) 2-nitrophenol, (c) 4-nitrophenol, (d) 2,4-dichlorophenol, and (e) 2,4-dinitrophenol.

rates. The system was fully automated, eliminating operator error in gradient generation as is normally encountered in home-built low flow gradient generators. The system provided different gradient profiles as desired. Gradient separations of pesticides and phenols were successfully demonstrated using an on-column detector. This work reports the design and operation of a novel potentially portable nanoflow gradient LC system; further work must be done to combine the components into a compact and robust package for field use. Integration of LC-UV detector along with batteries and temperature control is expected to increase the weight of the instrument.

4.5 References

1. Sharma, S.; Tolley, H. D.; Farnsworth, P. B.; Lee, M. L. *Anal. Chem.* **2015**, *87*, 1381-1386.
2. Li, Y.; Tolley, H. D.; Lee, M. L. *J. Chromatogr. A* **2011**, *1218*, 1399-1408.
3. Aggarwal, P.; Lawson, J. S.; Tolley, H. D.; Lee, M. L. *J. Chromatogr. A* **2014**, 1364, 96−106.
4. Chen, H.; Horváth, C. *J. Chromatogr. A* **1995**, *705*, 3-20.
5. Kassaye, L.; Genete, G. *Intl. J. Chromatogr. Sci.* **2013**, *3*, 18-23.

CHAPTER 5 DESIGN OF A PORTABLE LASER DIODE-BASED UV-ABSORPTION DETECTOR FOR HEMOGLOBIN VARIANT ANALYSIS

5.1 Introduction

Liquid chromatography integrated with UV-absorption detection holds great potential for point-of-care analysis. A portable LC-UV system would be valuable in remote areas, where sample collection, preservation and transportation to distant laboratories significantly delay disease diagnosis. They also delay medical treatment or needed attention to the diseased. There are several commercially available point-of-care diagnostic tools for conditions such as diabetes and pregnancy.

Hemoglobinopathy encompasses genetic disorders caused by mutations in the hemoglobin globin genes. Hemoglobin variants, thus, created due to alterations in the globin chains are responsible for several medical conditions [1]. Although most of these mutations are asymptomatic, some variants are responsible for life-threatening diseases such as sickle cell anemia and β-thalassemia major and they mandate life-long treatment. Sickle cell disease (SCD) is the most prevalent hemoglobinopathy, especially in Africa, and the absence of proper medical care is responsible for the majority of deaths in the area. There is no universal cure for SCD, and early diagnosis in high-risk individuals helps in providing symptomatic treatment, which increases life expectancy. Earlier, electrophoresis techniques (i.e., cellulose acetate electrophoresis and citrate agar acid electrophoresis) were popular for hemoglobinopathy analysis; however, these techniques fail to separate common Hb variants [2-4]. They lack the required sensitivity and specificity, leading to false positive diagnosis. Isoelectric focusing provides better resolution; however, interpretation of data is time consuming and quantitation is difficult [2-4].

HPLC has gained popularity over the aforementioned traditional techniques due to its high sensitivity and ability to separate and quantify most Hb variants [5].

Hemoglobins have strong UV absorption around 405 nm wavelength and, hence, UV-absorption detectors have been widely used in Hb analysis [6]. To the best of my knowledge, no portable detectors have been developed specifically for hemoglobinopathy detection. In this work, a portable UV-absorption detector was designed and assembled based on a 405 nm laser diode module (Figures 5.1 and 5.2) that would allow field analysis of hemoglobinopathy.

5.2 Experimental section

5.2.1 Dual-channel laser-based detector

In this detector, a CPS405 collimated laser diode module from Thorlabs (Newton, NJ, USA) was used as the light source. The laser was held tight in the center of an SM05 lens tube (Thorlabs) using two sets of opposing screws machined perpendicular to each other in the sides of the tube. The light beam from the laser was directed to a non-polarizing beam splitter cube [BS025 (90:10, ratio of transmitted beam to reflected beam), Thorlabs], which was encased in a CM1-4ER compact cubic cage (Thorlabs) threaded with SM1A6FW adapters (Thorlabs) on four sides. The lens tube containing the laser was connected to the cubic cage using an adjustable coupler (SM05T10, Thorlabs). The transmitted laser beam was focused using an AC127-019-A-ML mounted achromatic lens (Thorlabs), which was threaded on the opposite side of the cubic cage (Figure 5.1).

The capillary center was positioned at 1.1 cm away from the outer edge of the mounted lens holder and was held perpendicular to the laser beam. The capillary holder was built in-house and consisted of two circular plates with a central hole machined to allow light to pass through the capillary and two semicircular grooves on opposite sides of the hole. Two short black tubes

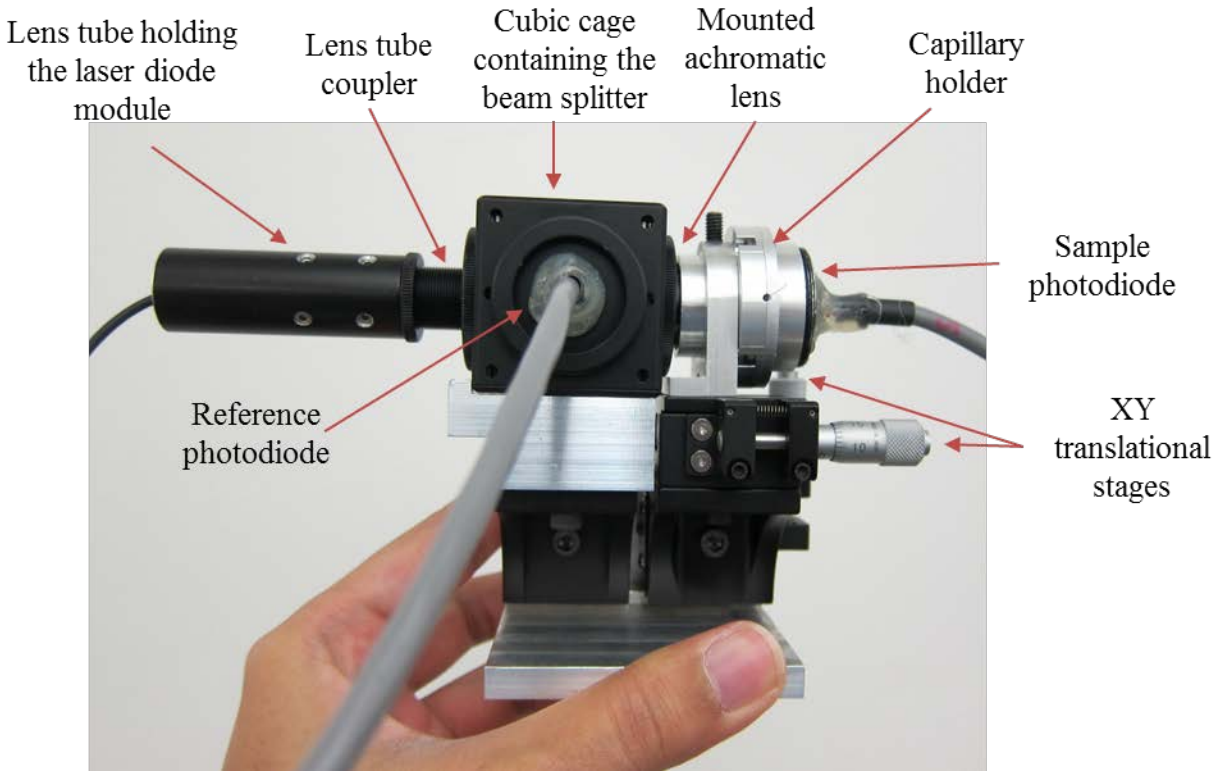

Figure 5.1 Photograph of the 405 nm laser-based on-column UV-absorption detector.

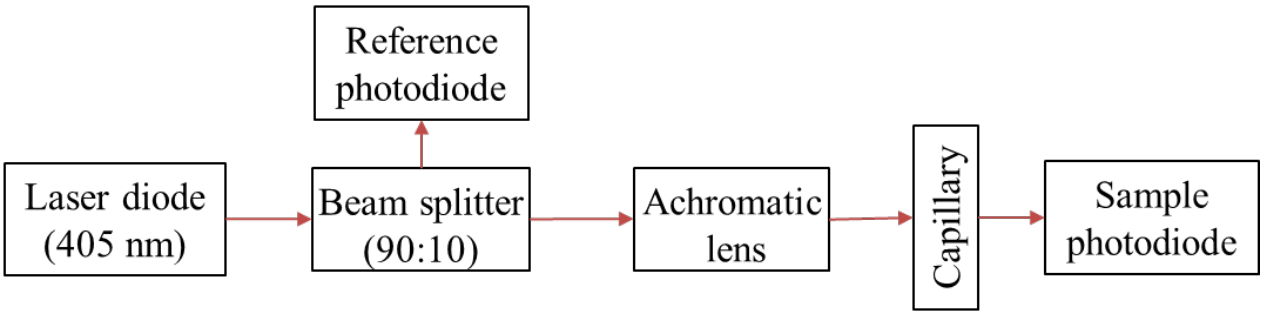

Figure 5.2 Schematic of the 405 nm laser-based on-column UV-absorption detector.

of approximately 360 µm i.d. were glued to the semicircular grooves on the circular plates, and the plates were attached together to hold the capillary in the center.

A S1LEDM holder (Thorlabs) was used to hold the sample photodiode (S1226-5BQ, TO-5) from Hamamatsu (Hamamatsu, Japan), and it was threaded into the capillary holder. This capillary and diode holder assembly was connected to two adjustable translation stages (MS1S, Thorlabs), which helped in centering the beam on the capillary by moving the capillary in the x and y directions with respect to the beam. The reference photodiode was mounted on an S05LEDM holder (Thorlabs) and directly connected to the cubic splitter cage, receiving 10% of the reflected laser beam. The laser was powered using a regulated power supply (LDS5, Thorlabs), and the photodiodes were powered by in-house built electronics. The current signals from the photodiodes were converted into voltage values using an operational amplifier circuit with a gain of 10k. A simultaneous sampling DAQ (NI PCI-6143) from National Instruments (Austin, TX, USA) was used to acquire signals. All data were acquired at a 10 Hz data rate using LabView software. The absorbance values were calculated using the software by taking the negative logarithm (base 10) of the sample signal divided by the reference signal. This detector could operate for at least 10 h using a 10 A h 12 V DC battery. UV-transparent 150 µm i.d. x 365 µm o.d. capillary from Polymicro Technologies was used for all experiments.

5.2.2 Noise level

A water-filled capillary was inserted into the detector to measure the noise level. The total noise level was determined by measuring the standard deviation (rms noise) on at least one minute of baseline data. The stray light was measured by dividing the signals obtained using a black ink filled capillary by the signals obtained using a water-filled capillary. Software averaging, as explained in Chapters 2 and 3, was used to reduce the noise levels.

5.3 Results and discussion

5.3.1 Dual-channel laser-based detector design

The detector was initially fabricated without a reference. However, high signal fluctuations mandated the inclusion of a reference channel. The light beam from the laser was elliptical in shape and the elongated beam had to be aligned along the capillary length to obtain the maximum light throughput. Using the adjustable laser coupler, this alignment was easily accomplished. It was found experimentally that the focal length of the achromatic lens was approximately 1.1 cm and, to obtain the proper focus onto the capillary, two linear translational stages were employed. Using these stages, the capillary could be moved up and down perpendicular to the laser beam, and towards and away from it up to 6 mm distance. Proper alignment of the capillary with respect to the beam was critical, and even slight misalignment led to the formation of interference fringes, which reduced the light throughput through the capillary. The capillary was properly aligned to obtain the best focus and minimum stray light before conducting any experiments.

The detector did not require slits to cut off stray light passing through the outer wall of the capillary due to a narrow focused spot obtained using the achromatic lens. Also, no optical filter was needed due to the monochromatic laser output.

The laser power was high compared to previous work using an LED (Chapter 3) and, hence, an operational amplifier was used with a gain of only 10k compared to a factor of a million used with my LED detector.

5.3.2 Detector noise and stray light

Initially, data were acquired using an NI USB 6002 DAQ (National Instruments); however, the device did not sample the sample and reference channels at the same time. This led

to increased noise in the system. Therefore, it was replaced with a simultaneous sampling device (PCI 6143). The rms total noise of the unaveraged signals was found to be 2.3 mAU with the simultaneous sampling device. With 2400 data points averaged per 0.1 s, the total noise level reduced to 30 μAU. This noise level was an order of magnitude lower compared to the noise level obtained with the USB 6002. With the dual beam arrangement, it was expected that the signal fluctuations and drift would be eliminated. However, even after inclusion of a reference channel and simultaneous sampling device, the signal fluctuations remained. Wavelength-dependent splitting by the beam splitter is expected to be the source of the problem. Stray light levels were insignificant (< 1.3%).

5.3 Conclusions

A 405 nm laser diode-based detector was designed and constructed for hemoglobin detection. A noise level equivalent to my Hg-lamp based detector was achieved; however, signal fluctuations were high, which compromised the detection limits. Studies are continuing to overcome this problem.

5.4 References

1. Traeger-Synodinos, J.; Harteveld, C. L. *Biomarkers Med.* **2014**, *8*, 119-131.
2. Ou, C.; Buffone, G. J.; Reimer, G. L., Alpert, A. J. *J. Chromatogr. A* **1983**, *266*, 197-205.
3. Ou, C.; Rognerud, C. L. *Clin. Chem.* **1993**, *39*, 820-824.
4. Ou, C.; Rognerud, C. L. *Clin. Chim. Acta* **2001**, *313*, 187-194.
5. Brennan, S. O. *Clin. Chem.* **2008**, *54*, 8-10.
6. Hanson, E. K.; Ballantyne, J. *PLoS One* **2010**, *5*, 1-11.

CHAPTER 6 CONCLUSIONS AND FUTURE DIRECTIONS

6.1 Conclusions

Various capillary-based portable LC-UV systems and components have been developed with performances that are either competitive with or surpass commercial instruments. A remarkable reduction in size and weight was achieved compared to commercial instruments without compromising LC performance. The performances of pen-ray® Hg lamp and LED on-column detectors were impressive considering the fact that their detection limits surpassed the best performance of flow cell-based detectors. With proper optimization, short path length is no longer a limitation to achieve high sensitivity from UV-absorption detectors. These systems should be useful for analysis in the laboratory and onsite, saving both time and resources.

6.2 Future directions

6.2.1 Hg lamp-based (254 nm) UV-absorption detector

While it would be hard to achieve the performance and size reduction of the LED-based detector with an Hg lamp detector because of the unfavorable characteristics of the Hg lamp as described in Chapters 2 and 3, there are certain design changes which could prove useful to improve this detector. Instead of using a fiber optics assembly for beam splitting as outlined in Chapter 2, a cubic beam splitter arrangement similar to the one employed in the laser-based detector described in Chapter 5 could be used. This would decrease the overall size and weight of the detector and should improve its performance.

6.2.2 LED-based (260 nm) UV-absorption detector

The LED-based UV-absorption detector has been, by far, the best detector developed for my portable capillary LC system. This detector holds great potential for high-sensitivity capillary LC work in the field as well as in the laboratory. This detector should also be less expensive

compared to other commercial fixed-wavelength detectors. I believe that there is little room for improvement in this design as far as detector performance is concerned. However, applications may be limited by the fact that it is designed for on-column detection requiring UV-transparent capillaries. These capillaries are not typically fabricated for commercial applications. Hence, inclusion of a fixed volume flow cell in the detector would expand its applications. Furthermore, a multi-wavelength LED-based detector should be developed, and has been attempted in the past as stated in Chapter 3; however, the complexity of the system and compromised detection limits are disadvantages.

It is important to mention here that the light source greatly impacts detector performance. If the light source performs differently from the one tested in this work, even with careful detector design replications, different detector results may be obtained. Hence, further steps may be required to improve performance from detector to detector.

6.2.3 Nano-flow pumping systems (isocratic and gradient)

These systems have performed competitively to commercial instruments in terms of flow rate and gradient reproducibility. Computer control of these systems is simple and user-friendly. Inclusion of flow and pressure sensors would provide useful information in real time; however, such features are usually not necessary.

6.2.4 UV detectors for hemoglobinopathy

Dual-channel laser-based (405 nm) UV-absorption detector. Other than the high fluctuations from the laser, the detector design appears to be quite good. The translation stages could be removed and the capillary position could be fixed with respect to the laser. High precision would be required since even a few μm misalignment would greatly reduce the light throughput through the capillary. A simultaneous sampling device seemed to be a quicker

solution to the high fluctuations in the detector; however, it was expensive. From consideration of the portability and affordability, it would be more practical to employ active filters in the detector design. Passive filter, as was used in the LED detector design, did not prove helpful in noise reduction in this detector or the LED detector as well.

The dual beam arrangement of this detector could be eliminated if highly stable lasers become commercially available in the future. If this happens, the lens tube holding the laser could be directly threaded into the mounted achromatic lens, eliminating the beam splitter and reference diode altogether. This design would reduce the size of the detector, and much lower LOD would be obtained due to less noise from the laser. This would also eliminate the need for an expensive simultaneous sampling device.

Single-channel LED-based (405 nm) UV-absorption detector. An alternative to the laser detector would be to develop a detector using a 405 nm LED. In preliminary work on such a detector, a 405 nm LED from Roithner LaserTechnik (Vienna, Austria) was selected as the light source. The design and construction of this detector was similar to the LED detector described in Chapter 3 with several variations. First, the 405 nm LED had an integrated ball glass lens (4 mm dia.) rather than a 6.35 mm dia. fused silica lens. Second, there was no need for an optical filter in this design as no stray light at other wavelengths were observed in the LED spectral output. Third, a ball lens of 6 mm dia. was needed for focusing the light onto the capillary because the LED gave a wider light spot. Finally, the distance between the LED, ball lens holder and capillary had to be adjusted for proper focusing. To adjust the distance between the ball lens holder and the capillary, two rods were machined on two sides of the ball lens holder, which allowed manual adjustment. This detector is smaller and simpler than the laser detector. The performance of the detector should be much better than the current laser detector.

6.2.5 Portable LC-UV system integration

While the systems described in this dissertation were greatly reduced in size, power consumption and solvent consumption, they have not been integrated into a single, self-contained, portable system. As outlined in the Conclusions section in Chapter 1, certain details require special attention. Temperature control is absolutely required for a field-portable LC. Solvent bottles and the capillary column would need to be firmly secured, but positioned so that these could be easily replaced by the user. Since sample preconcentration may often be unavoidable in the field, integration of a sample desorption device with the injector may prove useful for solid-phase extraction or solid-phase microextraction. With advancements in computer technologies, creating a user-friendly system with appropriate controls and graphic interface should not be a major problem. Data could also be wirelessly transferred to laptops for manual data analysis. Applications for such portable capillary LC-UV systems are expected to be numerous and varied.